POLITECNICO DI TORINO

Master of Science's Degree in Physics of Complex Systems

Master of Science's Degree Thesis

GAUSSIAN STATES MANIPULATION IN OPTOMECHANICAL SYSTEMS

Supervisors

Prof. FRANCESCO PIETRO MASSEL

Prof. VITTORIO PENNA

Candidate

LORENZO BINI

OCTOBER 2022

Summary

Quantum entanglement in optomechanical systems plays a vital role in the progress of quantum science and technology, such as exploring fundamental physics and quantum information processing. Although the physical laws of quantum mechanics do not specifically limit the size of objects that carry the entangled states, the experimental preparation and detection of quantum entanglement in the macro world still face great challenges. Fortunately, with the practical advances in recent years, several pioneering works have demonstrated non-local correlation and entanglement among mechanical oscillators or between electromagnetic fields mediated by a mechanical oscillator. In this perspective, we have summarized a part of the theoretical and experimental progress related to the macro entanglement states in optomechanical systems and the outlook on its future direction and potential applications.

Acknowledgements

To my family and my girlfriend, thank you. I love you.

Lorenzo

Contents

1 Introduction

Quantum optomechanics has its roots in the study of the mechanical action of light that goes back to the 19th century. More relevant to this century, it is an example of an emerging capability to engineer quantum systems de novo. Engineered quantum systems use modern fabrication techniques to enable the construction of macroscopic systems designed to exhibit novel quantum behavior in collective degrees of freedom. To fully understand the basics of quantum optomechanics, we must first understand how light, at both macro and microscopic levels, interacts with matter. The relationship of light to the mechanical motion of matter is a long and convoluted story in the Western philosophical tradition. The Greek atomists regarded light as particulate and all atoms could participate in the motion. In 55 B.C. the Roman epicurean poet Lucretius elegantly wrote in his *De Rerum Natura*: "The light and heat of the sun; these are composed of minute atoms which, when they are shoved off, lose no time in shooting right across the interspace of air in the direction imparted by the shove". In opposition to the Corporealists, Aristotle, Plato, and the Neoplatonists argued that light was incorporeal. How light could interact with matter, for example, in refraction, then required some explanation. It is often claimed that Kepler gave the first statement of the mechanical action of light in his explanation of why comet tails point away from the Sun [1]. Indeed, in discussing refraction Kepler viewed the action of light as mechanical, likening it to the action of a missile striking a panel.

The first unambiguous experimental demonstrations of the radiation-pressure force predicted by Maxwell were performed using a light mill configuration, in 1901 by Lebedew and Nichols & Hull [2, 3]. A careful analysis of these experiments was required to distinguish the phenomenon from thermal effects that had dominated earlier observations. The first indication of the quantum nature of light came in 1900 when Planck discovered he could account for the spectral distribution of thermal light by postulating that the energy of a simple harmonic oscillator was quantized. Further evidence was added by Einstein who showed in 1905 [4] that the photoelectric effect could be explained by the hypothesis that the energy of a light beam was distributed in discrete packets later known as photons.

As early as 1909, Einstein derived the statistics of the radiation-pressure force fluctuations acting on a movable mirror [5], including the frictional effects of the radiation force, and this analysis allowed him to reveal the dual wave-particle nature of blackbody radiation. Einstein also contributed to the understanding of the absorption and emission of light from atoms with his development of a phenomenological theory in 1917. This theory was later shown to be a natural consequence of the quantum theory of electromagnetic radiation.

Despite this early connection with the quantum theory, physical optics developed more or less independently of quantum theory. An early attempt to find quantum effects in an optical interference experiment by G.I. Taylor in 1909 gave a negative result. Taylor's experiment was an attempt to repeat Young's famous two-slit experiment with one photon incident on the slits. The classical explanation was based on the interference of electric field amplitudes, while the quantum version on the interference of probability amplitudes, and they both correctly explained the phenomenon.

Indeed, in Young's interference experiments, typically one does not distinguish between the predictions of the classical theory and the quantum theory. It is only in higher-order experiments, involving the interference of intensities, that differences between the predictions of classical and quantum theory arise. In these cases the probability amplitudes to detect a photon from two different fields interfere with a detector. The first experiment in intensity interferometry was the famous one of R. Hanbury Brown and R.Q. Twiss [6] in 1956, where they studied the correlation in the photocurrent fluctuations for two detectors. While these results may be derived from a classical and quantum theory, the quantum theory made additional unique predictions. This was

first elucidated by R.J. Glauber in his quantum formulation of optical coherence theory in 1963 [7], such that he was later jointly awarded the 2005 Physics Nobel Prize for this work.
Furthermore, in the 1970s Ashkin [8] demonstrated the fact that laser beams can be used to trap and control dielectric particles, which also included (feedback) cooling. This discovery later informed the development of optical tweezers, which has had a big impact in Biology. In the same spirit, following the non-conservative nature of the radiation-pressure force, the possibility to use this interaction for cooling atomic motion was first pointed out by Hänsch and Schawlow [9] and Wineland and Dehmelt [10], both in 1975. Laser cooling was subsequently realized experimentally in the 1980s (Stenholm, 1986 [11]) and has since become an extraordinarily important technique in Quantum Optics, for example, allowing cooling of ions to their motional ground state. Many applications have been enabled by laser cooling, e.g. by Metcalf and van der Straten in 1999 [12], including optical atomic clocks and precision measurements of position detection, which are essential for gravitational wave detectors such as LIGO or VIRGO.
Usually, interferometers worked by merging two or more sources of light to create an interference pattern, which can be measured and analyzed. The interference patterns contain information about the object or phenomenon being studied, and they are often used to make very small measurements that are not achievable any other way. This is why they are so powerful for detecting gravitational waves, in the case of LIGO's interferometers, for example, they are designed to measure a distance $1/10.000^{\text{th}}$ the width of a proton.
Back in the 1990s, several aspects of quantum optomechanical systems started to be explored theoretically. These include the squeezing of light, performed by Fabre et al. in 1994 [13], and Mancini & Tombesi in 1994 [14]. It was also pointed out that for extremely strong optomechanical coupling the resulting quantum non-linearities could give rise to non-classical and entangled states of the light field and the mechanics (Bose, Jacobs, and Knight, 1997 [15]; Mancini, Man'ko, and Tombesi, 1997 [16]). Furthermore, feedback cooling by radiation pressure was suggested by Mancini, Vitali, and Tombesi in 1998 [17]. Around the same time, in a parallel development, laser cooling was proposed as a method to cool the motion of atoms and molecules by Hechenblaikner et al. in 1998 [18], and Vuletic & Chu in 2000 [19].
On the experimental side, optical feedback cooling based on the radiation-pressure force was first demonstrated by Cohadon, Heidmann, and Pinard (1999) [20] for the vibrational modes of a macroscopic end mirror. This approach was later taken to much lower temperatures and, at the same time, to miniaturize the mechanical element. Producing high-quality optical Fabry-Pérot cavities below a certain scale, however, turned out to be very challenging. In this way, it became extremely important to model a theory of engineered quantum systems.
Engineered quantum systems represented, and represent, a new paradigm for the study of quantum physics. Despite the difficulty in reconciling quantum theory with our classical intuitions, it is a remarkably successful theory. However, quantum theory does not contain within it any law that forbids us from applying it to bigger things, even the entire universe in the case of quantum cosmology. The quantum-classical border is not co-located with the microscopic–macroscopic border. Until recently the possibility of quantum phenomena manifesting themselves in the ordinary everyday world of macroscopic physics could be safely confined to *gedanken* experiments. The last decade or so has finally changed this [21].
A key feature of the theory of engineered quantum systems is how the the quantum description is given. This is because, typically, one does not solve the Schrödinger equation for every atomic or molecular constituent of the macroscopic system. On the contrary, one begins with a classical description of the relevant macroscopic degrees of freedom and quantizes these collective degrees of freedom directly. This works if the macroscopic system can be so designed that the relevant collective degrees of freedom largely decouple from the microscopic degrees of freedom, which remain only as a source of noise and dissipation.

This approach was first pioneered in the field of superconductor circuits and championed by Tony Leggett in the 1980s [22]. He pointed out that the quantum theory of such circuits could begin with a direct quantization of the classical circuit equations. This approach was justified by the landmark experiment of Martinis, Devoret, and Clarke in 1987 [23]. For example, in quantum optomechanics, one often begins with the classical continuum mechanics, and then this continuum field is directly quantized. Essentially this is an *effective quantum field theory*.

Engineered quantum systems hold the promise of new technologies based on designing complex systems to exhibit functional quantum behavior. In the case of optomechanics, this might include a gain in sensitivity to external forces and fields. A fascinating possibility arises when the mechanical system becomes sufficiently large that gravitational interactions need to be included. This holds the promise of better determinations of the Newtonian gravitational constant and even the possibility of experimental evidence for how quantum theory and gravity might be reconciled.

On the other hand, with the development of the fabrication and measurement technology, this field has grown since the demonstration of optomechanical entanglement in a microwave optomechanical system [24]. The interaction of electromagnetic radiation with the motion of objects has an array of implications and manifestations, and further achievements have been reached since the proof-of-principle experiments that demonstrated the use of light to dampen the motion of relatively large mechanical oscillators [25]. For example, the quests to reach the quantum ground state of a mechanical oscillator, and to entangle two mechanical oscillators have all been completed. It is now time to look ahead at how optomechanical devices may be applied in forthcoming quantum technologies and as the basis for new experiments.

More advanced measurement technology makes people look forward to the entanglement between macroscopic objects. Encouragingly, a mechanical mode of a mirror with a weight of 10 kg has recently been cooled down close to its quantum ground state [26], which makes the boundary between quantum and classical much thinner. How big can an object observed in quantum mechanics phenomena be? This question awaits future scientific research. At present, experimental implementations are still eager to expand and upgrade because of the short time that optomechanical experiments are in the quantum regime. The technology of squeezed light and cryogenic refrigeration also becomes more mature nowadays, which is conducive to further experimental exploration, from the fundamental research of inseparability to quantum information technology.

As a versatile interface, a mechanical oscillator is able to interact coherently with various of quantum physical platforms. This makes mechanical oscillators suitable to interconnect different physical qubits in hybrid quantum network systems. Currently, microwave and light conversion has been studied in many physical systems, and optomechanics is one of the outstanding systems. The combination of this technique and the entanglement discussed here is significant. However, quantum teleportation is needed for the high-fidelity transfer of quantum states based on quantum repeaters.

Recently, the conversion of a microwave-frequency excitation of superconducting qubit into an optical photon has been achieved [27, 28], enhancing the prospects of hybrid quantum systems based on mechanical interfaces. The light-matter interface is valued in both long-distance quantum communication and distributed quantum computing. An essential step towards those quantum networks is the demonstration of optomechanical quantum teleportation [29] that achieves the full functionality of a single quantum repeater node. Last but not least, developing schemes to reduce the impact of thermal noise, will surely help to ease the experimental requirements and to reflect more practical value. It is worth noting that experiments in cryogenic environments will occupy the central position of experimental research of this field for an extended period in the future. In this way, maintaining quantum properties in a more ordinary environment will be the focus of the practical application in quantum optomechanics.

This thesis work is organized as follows: in Chapter 2 we will introduce the theoretical framework of Open Quantum Systems to develop the derivation of Quantum Langevin Equation (QLE). Chapter 3 is an overview of optical fields and their detection, concepts that are then interwoven together in Chapter 4 in which we focus on the entanglement measures, with an introduction of Bell's inequalities. In Chapters 5 and 6 we apply what we saw previously in the specific field of optomechanical systems, focusing on the interaction between light and matter, cooling of mechanical motion, amplification of input signals, and mechanical squeezing. Furthermore, in Chapter 7 we analyze in detail two-mode optomechanical systems, going to investigate entanglement properties between two cavity modes first and then between two mechanical modes. Finally, in Chapter 8, conclusions are drawn and an outlook is discussed. This work aims to introduce to the reader some of the modern developments in Quantum Optomechanics, from both an experimental and a theoretical standpoint, supplying a comprehensive treatment that incorporates the most recent advances and points the way toward future challenges.

2 Open Quantum System

The observation and experimental control of characteristic quantum properties of physical systems are often strongly hindered by the coupling of the system to a noisy environment. On the other hand, if you don't couple, you can't measure. In this way, the dynamical behavior of open quantum systems plays a key role in many applications of quantum mechanics, such as in quantum condensed matter theory, quantum transport, and quantum information. The unavoidable interaction of the quantum system with its surroundings generates system-environment correlations leading to an irretrievable loss of quantum coherence. In this sense, realistic quantum mechanical systems are open systems governed by some time development which describes all features of the dynamics such as relaxation to a thermal equilibrium, dissipation of energy, and, as mentioned, decay of quantum coherence and correlations (see [30, 31, 32]).
The dynamics of open quantum systems are therefore well established in the sense that all open systems' time evolution is described by a master equation, a first-order differential equation for the reduced density matrix of the open systems.
We could define an open quantum system as composed of two different subsystems: S (that will be the one under our analysis) and its bath (also called environment) B. So the total Hilbert space $S + B$ is given by the tensor product

$$\mathcal{H}_{\mathcal{SB}} = \mathcal{H}_{\mathcal{S}} \otimes \mathcal{H}_{\mathcal{B}}, \tag{2.1}$$

where $\mathcal{H}_{\mathcal{S}}$ and $\mathcal{H}_{\mathcal{B}}$ denote the Hilbert spaces of S and B, respectively. Pure states of the total system are represented by positive trace class operators ρ_{SB} on $\mathcal{H}_{\mathcal{SB}}$ with unit trace, satisfying $\rho_{SB} \geq 0$ and $\mathrm{tr}\rho_{SB} = 1$. In this way the systems, given a state of the total system, the corresponding states of subsystems S and B are obtained by partial traces over $\mathcal{H}_{\mathcal{S}}$ and $\mathcal{H}_{\mathcal{B}}$, respectively we have $\rho_S = \mathrm{tr}_B\rho_{SB}$ and $\rho_B = \mathrm{tr}_S\rho_{SB}$.
We suppose that the total system $S + B$ is closed (namely $\mathrm{tr}\rho^2_{\mathrm{SB}} = 1$) and governed by a Hamiltonian of the general form

$$H = H_S \otimes I_B + I_B \otimes H_B + H_I, \tag{2.2}$$

with H_S, H_B taking the role of the free Hamiltonian for the system and for the bath, while H_I takes simply into account the interaction between the two previous ones.
An important concept in the theory of open quantum systems is that of a dynamical map. To explain this concept we assume that the initial state of the total system is an uncorrelated tensor product state

$$\rho_{SB}(0) = \rho_S(0) \otimes \rho_B(0),$$

which leads to the following expression for the reduced open system state at any time $t \geq 0$:

$$\rho_S = \mathrm{tr}_B \left\{ U(t)\rho_S(0) \otimes \rho_B U^\dagger(t) \right\} \tag{2.3}$$

where the corresponding unitary time evolution operator is given by

$$U(t) = e^{-\frac{i}{\hbar}Ht}.$$

In this sense, if we consider a fixed initial environmental state $\rho_B(0)$ and any fixed time $t \geq 0$, Eq.(2.3) defines a linear map

$$\Phi_t : S(\mathcal{H}_{\mathcal{S}}) \to S(\mathcal{H}_{\mathcal{S}}) \tag{2.4}$$

on the open system's state space $S(\mathcal{H}_S)$ which maps any initial open system state $\rho_S(0)$ to the corresponding open system state $\rho_S(t)$ at time t:

$$\rho_S(0) \longmapsto \rho_S(t) = \Phi_t \rho_S(0).$$

Φ_t is called a quantum dynamical map, and it is easy to verify that it preserves the Hermiticity and that it is a positive map, i.e. it maps positive operators to positive operators. In this way, Φ_t maps physical states to physical states. A further important property of the dynamical map Φ_t is that it is not only positive but also completely positive. Without entering into technical details of this, that it is not the purpose of our work (we, therefore, leave the discussion to [33]), completely positivity is a stronger property of Φ that ensures not only all physical states of S are mapped into physical states of S, but also that all physical states of $S + R$, of a larger system described by ρ_S, are mapped to physical states of $S + R$. Broadly speaking, this fact assures that are involved only positive probabilities.
However, from now on, we will simply focus our attention on the mathematical derivation of the Quantum Langevin Equations (QLEs), which will give us the tools for understanding the system-bath interaction in open quantum systems. In this sense, we are going to follow what has been done in [34] and [35] for the analytical treatment of system-bath coupling, and also [36, 33, 37] for the QLEs derivation. We will also keep in mind that our discussion is aimed at the study of optomechanical systems, where QLEs are constantly derived and used to understand the dynamics of the problem (for example made by Giovannetti and Vitali [38]).

2.1 Derivation of Quantum Langevin Equations

In the previous section, we have seen the system-bath interaction. This kind of discussion is at the center of the investigation of quantum physics of noise. We will focus on analyzing the dynamics of an open quantum system, introducing the Langevin equations (QLEs) as a tool to model this type of system. It follows that the main idea will be to couple the system to a bath, often it will be a thermal state (but not necessarily), composed of an infinitely large number, within the thermodynamic limit, of harmonic oscillators (as shown in figure 1). For this reason, in Hamiltonian (2.2) the bath could be assumed to be a bosonic set of non-interacting particles. To derive the QLEs, the particles do not need to be bosons, since they can also be fermions. Obviously, for the purpose in which this work is applied, and for the systems under analysis, it is a necessary condition. With this in mind, let us recall the expressions, concerning the ladder operators, of the position and momentum (both for system and bath operators):

$$\begin{aligned} \hat{q} &= x_{zp}(c^\dagger + c) \\ \hat{p} &= i p_{zp}(c^\dagger - c) \\ \hat{q}_k &= x_{zp,k}(b_k^\dagger + b_k) \\ \hat{p}_k &= i p_{zp,k}(b_k^\dagger - b_k) \end{aligned} \tag{2.1.5}$$

with the zero-point motion and zero-point momentum of the harmonic oscillator written as

$$\begin{aligned} x_{zp} &= \sqrt{\frac{\hbar}{2m\omega}} \\ p_{zp} &= \sqrt{\frac{\hbar m\omega}{2}} \end{aligned}$$

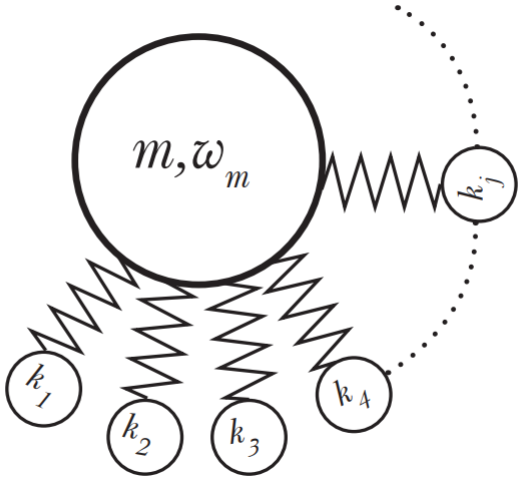

Figure 1: Schematic representation of the system-environment coupling. A quantum mechanical oscillator with mass m and resonance frequency ω_m is coupled to its environment. The coupling is obtain via springs with spring constant k_j, part of a large ensemble of environmental oscillators.

where m simply represents the mass of the k-th oscillator. Considering the following general expression for $\hat{H}_I$ in Eq.(2.2)

$$\hat{H}_I = \sum_k \left[\frac{\hat{p}_k^2}{2m_k} + \frac{g_k}{2}(\hat{q}_k - \hat{q})^2 \right] \tag{2.1.6}$$

where g_k is a parameter that measures the strength of the interaction with the k-th bath harmonic oscillator. Generally in quantum optics and optomechanics, to draw a meaningful distinction of system-bath interaction, the bath coupling rate is much smaller than other important system's rates. Therefore this is the reason why is commonly convenient to perform the so-called *Rotating Wave Approximation* (RWA) on the Hamiltonian of Eq.(2.1.6), i.e. to neglect the terms that do not conserve energy, and rewrite a new rotating wave QLE.
These non-energy conserving terms are the ones that create or destroy two quanta at the same time (also known as counterrotating terms), as they are strongly non-resonant, i.e. applying these terms to a state would change the total energy by a much larger amount than the coupling itself.
In this sense, plugging the former expressions of (2.1.5) into Eq.(2.1.6), neglecting the counter-rotating terms $cc, c^\dagger c^\dagger, b_k b_k$ and $b_k^\dagger b_k^\dagger$, we finally end up with the following

$$\hat{H}_{RWA} = \sum_k \left[\hbar\omega_k b_k^\dagger b_k + g_k \left(\hat{c}^\dagger \hat{b}_k + \hat{b}_k^\dagger \hat{c} \right) \right], \tag{2.1.7}$$

with the usual parameter g_i to estimate the strength of each coupling between system and bath, and $\hat{c}$ is one of several possible system operators which describes the interaction between system and bath. It is not necessary to specify what the operator $\hat{c}$ is but $\hat{b}_k$ is again supposed to be a bosonic operator. For sake of simplicity, we got rid of the zero-point energy terms of the bath as they simply bring additive contributions to our Hamiltonian, and from now on we also set $\hbar = 1$. Rotating Wave Approximation will prove to be particularly useful in future chapters,

such as Chapter 5 when we are going to derive the linearized optomechanical Hamiltonian, and we will see that most of the discussion in this work will be based on the results derived from this approximation.
At this point, we can add $\hat{H}_{RWA}$ to Eq.(2.2) to build up the full problem Hamiltonian

$$\hat{H} = \hat{H}_S + \sum_k \omega_k \hat{b}_k^\dagger \hat{b}_k + \sum_k g_k \left(\hat{c}^\dagger \hat{b}_k + \hat{b}_k^\dagger \hat{c} \right),$$

where $\hat{H}_S$ is the Hamiltonian of the system. Now, we can write down the Heisenberg equations of motion for another arbitrary system operator $\hat{a}$, one can imagine this as a bosonic annihilation operator that we will use throughout our discussion, and for the bath operator $\hat{b}_k$. In this way, the latter read

$$\dot{a}(t) = i[\mathcal{H}, a] = i[\mathcal{H}_{\text{sys}}, a] + i \sum_k g_k \left([c^\dagger, a] b_k + b_k^\dagger [c, a] \right) \tag{2.1.8}$$

$$\dot{b}_k(t) = i[\mathcal{H}, b] = -i\omega_k b_k - g_k c \tag{2.1.9}$$

Equation (2.1.9) can be solved with an initial condition $t = 0$, giving

$$b_k(t) = b_k(0) e^{-i\omega_k t} + -i g_k e^{-i\omega_k t} \int_0^t e^{i\omega_k t'} c(t') dt'$$

then we can plug this into equation (2.1.8) which leads to

$$\begin{aligned} \dot{a}(t) =& i[\mathcal{H}_{\text{sys}}, a] + i \sum_k g_k \left([c^\dagger, a] b_k(0) e^{-i\omega_k t} + b_k^\dagger(0) e^{i\omega_k t} [c, a] \right) \\ &+ \sum_k g_k^2 e^{-i\omega_k t} \left([c^\dagger, a] \int_0^t e^{i\omega_k t'} c(t') dt' - \left(\int_0^t e^{-i\omega_k t'} c(t') dt' \right) [c, a] \right) \end{aligned}$$

We have reached this point without any assumptions yet. If it is supposed that the system-bath interaction is independent of the frequency of a bath mode, one can make a significant simplification. This is called the *first Markov assumption* as it will lead to time-local dissipation. In this way let us suppose that $g_k^2 = \frac{\gamma}{2\pi} D$ where D is the modes density, i.e. $\omega_k = kD$, and γ is some dissipation constant stemming from the coupling with the bath. In the last term we can write $\sum_k e^{iD(t-t')k} = \frac{2\pi}{D} \delta(t - t')$ assuming infinite number of modes k. The resulting integral is somewhat problematic as it requires evaluation of the Dirac delta function at the integration limit. If we consider the Delta function to be the result of a limiting procedure in which, for instance, the variance of Gaussian distribution is taken to zero we have

$$\int_{t_0}^{t} dt' f(t') \delta(t - t') = \int_{t}^{t_1} dt' f(t') \delta(t - t') = \frac{1}{2} f(t)$$

when $t_0 < t < t_1$ and f is a smooth function. It is a reasonable interpretation in this case since it produces the same result even if we were integrating backwards in time. Finally, we end up with the QLE

$$\dot{a}(t) = i[\mathcal{H}_{\text{sys}}, a] - [a, c^\dagger] \left[\frac{\gamma}{2} c + \sqrt{\gamma} a_{\text{in}}(t) \right] + \left[\frac{\gamma}{2} c^\dagger + \sqrt{\gamma} a_{\text{in}}^\dagger(t) \right] [a, c] \tag{2.1.10}$$

in which the input mode is

$$a_{\text{in}} = -i\sqrt{\frac{D}{2\pi}}\sum_k b_k(0)e^{-i\omega_k t}. \tag{2.1.11}$$

The terms proportional to $\frac{1}{2}\gamma c$ and $\frac{1}{2}\gamma c^\dagger$ are in practice damping terms, and arise without any particular assumption on the thermal state of the reservoir. Furthermore, the simple example of $c = a$ gives

$$\dot{a} = -i\omega_0 a - \frac{\gamma}{2}a - \sqrt{\gamma}a_{\text{in}}(t),$$

with ω_0 being a proper system's frequency stemming from $\mathcal{H}_{\text{sys}}$. We notice that the damping is Markovian, i.e. the damping term depends only on the system operators evaluated at time t, and this arises from the *first Markov approximation*. On the other hand, the a_{in} operator is called input operator because the Heisenberg equations are solved forward in time, i.e. with some initial condition $b_k(0)$. Similarly one can solve the equation backwards in time which essentially changes only $\gamma \to -\gamma$ and $a_{\text{in}} \to a_{\text{out}}$. The output operator is defined similarly

$$a_{\text{out}} = -i\sqrt{\frac{D}{2\pi}}\sum_k b_k(0)e^{-i\omega_k t} \tag{2.1.12}$$

Carrying on the same procedure we arrive at the version of the Langevin equation written with respect to output operator

$$\dot{a}(t) = i[\mathcal{H}_{\text{sys}}, a] - [a, c^\dagger]\left[\frac{\gamma}{2}c + \sqrt{\gamma}a_{\text{out}}(t)\right] + \left[\frac{\gamma}{2}c^\dagger + \sqrt{\gamma}a_{\text{out}}^\dagger(t)\right][a, c] \tag{2.1.13}$$

The input and output are related by

$$a_{\text{out}} - a_{\text{in}} = \sqrt{\gamma}a(t) \tag{2.1.14}$$

from which the naming convention follows. This relations will be very useful in Chapter 5 where we will specify the actual form of our system Hamiltonian.

2.1.1 Input, output and causality

The previous equations (2.1.14) can be interpreted as a boundary condition, relating output, input, and internal modes. If the equation (2.1.10) is solved to give values of the system operators in terms of their past values and those of $a_{\text{in}}(t)$, then it is clear that $a(t)$ is independent of $a_{\text{in}}(t')$ for a certain time $t' > t$; i.e. the systems variables do not depend on the input variables in the future. This can be expressed as

$$[a(t), a_{\text{in}}(t')] = 0 \quad \text{if} \quad t' > t \tag{2.1.1.15}$$

but on the other hand is possible to show, using previous results, that also

$$[a(t), a_{\text{out}}(t')] = 0 \quad \text{if} \quad t' < t. \tag{2.1.1.16}$$

Now, if we define a step function $u(t)$

$$u(t) = \begin{cases} 1, & t > 0 \\ \frac{1}{2}, & t = 0 \\ 0, & t < 0 \end{cases}$$

using Eqs.(2.1.14) we can obtain

$$\begin{aligned}[a(t), a_{\text{in}}(t')] &= u(t-t')\sqrt{\gamma}[a(t), c(t')] \\ [a(t), a_{\text{out}}(t')] &= u(t'-t)\sqrt{\gamma}[a(t), c(t')].\end{aligned} \tag{2.1.1.17}$$

Having now a complete description of the system in terms of input-output, we notice that the commutation relations (2.1.1.17) provide us with an actual description of causality, meaning that only the future motion of the system is affected by the present input, and that only the future value of the output is affected by the present values of the system.
The obtained results in the previous paragraph are not yet stochastic results, since no assumptions have been made concerning the density operator of the bath. We will now develop the formalism [39] by defining *white noise* input as the idealised noisy input, similar to classical white noise.
The $a_{\text{in}}(t)$ field defined above will provide the input to our system described by $\mathcal{H}_{\text{sys}}$. Of course there will always be some quantum noise arising from the zero point fluctuations of the input, and depending on the input state, there may be additional noise, such thermal noise [34].
The input state, which corresponds closely to a classical white noise input, is not for the moment a thermal state, but one in which the input density operator ρ_{in} is such that

$$\text{Tr}\left\{\rho_{\text{in}} a_{\text{in}}^\dagger(t) a_{\text{in}}(t')\right\} \equiv \langle a_{\text{in}}^\dagger(t) a_{\text{in}}(t')\rangle = \bar{N}\delta(t-t') \tag{2.1.1.18}$$

$$\text{Tr}\left\{\rho_{\text{in}} a_{\text{in}}(t) a_{\text{in}}^\dagger(t')\right\} \equiv \langle a_{\text{in}}(t) a_{\text{in}}^\dagger(t')\rangle = (\bar{N}+1)\delta(t-t') \tag{2.1.1.19}$$

which in frequencies phase-space is

$$\begin{aligned}\langle a_{in}^\dagger(\omega) a_{in}(\omega')\rangle &= \bar{N}\delta(\omega-\omega') \\ \langle a_{in}(\omega) a_{in}^\dagger(\omega')\rangle &= (\bar{N}+1)\delta(\omega-\omega')\end{aligned} \tag{2.1.1.20}$$

This corresponds to a state in which the number of quanta per unit bandwidth is constant, and this is not the case in a thermal state, in which in (2.1.1.20) $\bar{N}$ would be replaced by $\bar{N}(\omega)$ given by

$$\bar{N}(\omega) = 1/[\exp(\hbar\omega/kT) - 1]$$

Thus, to an even larger extent than in classical stochastics, quantum white noise is an idealization, not actually attained in any real system.
Now, to define quantum stochastic integration, we define the quantum Wiener process by

$$B(t, t_0) = \int_{t_0}^{t} a_{\text{in}}(t')dt'$$

which allows us to write

$$\langle B^\dagger(t, t_0) B(t, t_0)\rangle = N(t - t_0) \tag{2.1.1.21}$$

$$\langle B(t, t_0) B^\dagger(t, t_0)\rangle = (N+1)(t - t_0) \tag{2.1.1.22}$$

$$[B(t, t_0) B^\dagger(t, t_0)] = t - t_0. \tag{2.1.1.23}$$

In addition we specify that the distribution of the density operator is

$$\rho(t, t_0) = (1 - e^{-\kappa})\exp\left[-\frac{\kappa B^\dagger(t, t_0) B(t, t_0)}{t - t_0}\right]$$

in which

$$N = \frac{1}{e^{\kappa} - 1}$$

and it is clear that any normal-ordered moment of order n in $B(t, t_0)$ and $B^{\dagger}(t, t_0)$ will be a constant times $(t - t_0)^{\frac{n}{2}}$, a crucial factor for manipulating stochastic differentials.

2.2 Power spectral density and Harmonic Oscillator dynamics within RWA

Before proceeding with our excursion into optomechanical systems it is first worthy recalling some analytical tools that will be particularly useful in future computations. For example, the input operator $a_{\mathrm{in}}(t)$ and its adjoint $a_{\mathrm{in}}^{\dagger}(t)$ obey the commutation relations

$$\begin{aligned} &[a_{\mathrm{in}}(t), a_{\mathrm{in}}^{\dagger}(t')] = \delta(t - t') \\ &[a_{\mathrm{in}}(t), a_{\mathrm{in}}(t')] = [a_{\mathrm{in}^{\dagger}}(t), a_{\mathrm{in}}^{\dagger}(t')] = 0 \end{aligned} \tag{2.2.1}$$

being $\delta(t)$ the Dirac delta function.
Recalling now the expression for the dimensionless bath position and momentum operators (we will use this type of notation throughout the entire work):

$$\begin{aligned} \hat{Q}_{\mathrm{in}} &= \frac{(a_{\mathrm{in}}^{\dagger} + a_{\mathrm{in}})}{\sqrt{2}} \\ \hat{P}_{\mathrm{in}} &= \frac{i(a_{\mathrm{in}}^{\dagger} - a_{\mathrm{in}})}{\sqrt{2}} \end{aligned} \tag{2.2.2}$$

from Eqs.(2.1.1.20) and (2.2.1) one can show that the same holds for the bath position and momentum

$$\begin{aligned} &[\hat{Q}_{\mathrm{in}}(t), \hat{P}_{\mathrm{in}}(t')] = i\delta(t - t') \\ &[\hat{Q}_{\mathrm{in}}(t), \hat{Q}_{\mathrm{in}}(t')] = [\hat{P}_{\mathrm{in}}(t), \hat{P}_{\mathrm{in}}(t')] = 0 \\ &\langle Q_{\mathrm{in}}(t) Q_{\mathrm{in}}(t') \rangle = \langle P_{\mathrm{in}}(t) P_{\mathrm{in}}(t') \rangle = \left(\bar{n} + \frac{1}{2} \right) \delta(t - t') \\ &\langle Q_{\mathrm{in}}(t) P_{\mathrm{in}}(t') \rangle = -\langle P_{\mathrm{in}}(t) Q_{\mathrm{in}}(t') \rangle = \frac{i}{2} \delta(t - t') \end{aligned} \tag{2.2.3}$$

where $\bar{n}$ is the average number of phonons stored in the mechanical resonator $\bar{n} = \langle b^{\dagger} b \rangle$. From these the corresponding frequency domain can be commutation and correlation relations could be obtained straightforwardly with the substitution $t \to \omega$ and $Q_{\mathrm{in}}(\omega) = \frac{(a_{\mathrm{in}}^{\dagger}(-\omega) + a_{\mathrm{in}}(\omega))}{\sqrt{2}}$, $P_{\mathrm{in}}(\omega) = \frac{i(a_{\mathrm{in}}^{\dagger}(-\omega) - a_{\mathrm{in}}(\omega))}{\sqrt{2}}$.
From what we have discussed above, we can now write down the expression for the power spectral densities for $Q_{\mathrm{in}}, P_{\mathrm{in}}$ within RWA. Knowing the definition for a general operator $\hat{\mathcal{O}}$, the expectation value reads

$$S_{\mathcal{O}\mathcal{O}}(\omega) \equiv \lim_{\tau \to \infty} \frac{1}{\tau} \left\langle \hat{\mathcal{O}}^{\dagger}(\omega) \hat{\mathcal{O}}(\omega) \right\rangle.$$

Then the Wiener-Khinchin theorem states that for an operator with stationary statistics

$$S_{\mathcal{O}\mathcal{O}}(\omega) = \int_{-\infty}^{\infty} d\tau e^{i\omega\tau} \left\langle \hat{\mathcal{O}}^\dagger(t+\tau)\hat{\mathcal{O}}(t) \right\rangle_{t=0} = \int_{-\infty}^{\infty} d\omega' \left\langle \hat{\mathcal{O}}^\dagger(-\omega)\hat{\mathcal{O}}(\omega') \right\rangle. \tag{2.2.4}$$

In this way, the power spectral densities[1] can be obtained

$$\begin{aligned} S_{Q_{\rm in}Q_{\rm in}}(\pm\omega) &= S_{P_{\rm in}P_{\rm in}}(\pm\omega) = \bar{n} + \frac{1}{2} \\ S_{Q_{\rm in}P_{\rm in}}(\pm\omega) &= -S_{P_{\rm in}Q_{\rm in}}(\pm\omega) = \frac{i}{2} \end{aligned} \tag{2.2.5}$$

where $S_{Q_{\rm in}(\pm\omega)P_{\rm in}}(\pm\omega)$ and $S_{P_{\rm in}(\pm\omega)Q_{\rm in}}(\pm\omega)$ are cross-spectral densities between the bath position and momentum operators.
These results have a more rooted physical meaning than one might think, in fact they reflect an uncertainty principle between bath position and momentum operator in the way

$$S_{Q_{in}Q_{in}}(\omega) S_{P_{in}P_{in}}(\omega) \geq \frac{1}{4}$$

which can be confirmed from Eq.(2.2.5) for a vacuum state with $\bar{n} = 0$.

2.3 Amplification Theory

To conclude this second Chapter we introduce the concept of an amplifier. It will be a concept that we will analyze in much more detail in Section 7.2, where we will rely on what has been done, for example, by Massel, Sillanpää, and collaborators [40] for the analysis of optomechanical systems that operate as amplifiers. To do so we should define what such devices are, and which is the theory behind their functionality.
In the most general way, an amplifier is any device that takes an input signal, carried by, in our case, a collection of bosonic modes (electromagnetic field), and processes the input to produce an output signal, also carried by a collection of bosonic modes. In this spirit, a linear amplifier is an amplifier whose output signal is linearly dependent on its input signal. Following Caves [41], we can now ask ourselves "How much noise does quantum mechanics require a linear amplifier to add to a signal it processes?". From a quantum point of view, an amplifier can be seen as a collection of non-interacting modes, each labeled by a parameter α and characterized by a frequency ω_α. It is commonly denoted $\mathcal{I}$ the set of (bosonic) input modes, and $\mathcal{O}$ the set of (bosonic) output modes. There is no necessary relationship between $\mathcal{I}$ and $\mathcal{O}$: they can have some modes in common or they can be completely disjoint. In the Heisenberg picture (used throughout the following), the creation and annihilation operators for mode α evolve from "in" operators $a_\alpha^\dagger, a_\alpha$, before the interaction, to "out" operators $b_\alpha^\dagger, b_\alpha$ after the interaction. Notice that each annihilation operator can be independently multiplied by a phase factor, i.e.

$$\begin{aligned} \tilde{a}_\alpha &= e^{-i\varphi_\alpha} a_\alpha \\ \tilde{b}_\alpha &= e^{-i\varphi_\alpha} b_\alpha \end{aligned}$$

without changing the commutation and anti-commutation relations. The operators $a_\alpha^\dagger a_\alpha$, $b_\alpha^\dagger b_\alpha$ are the number operators for mode α before and after the interaction.

[1] Notice that for a power spectral density of quantum variable it is not always true that $S_{\mathcal{O}\mathcal{O}}(\omega) = S_{\mathcal{O}\mathcal{O}}(-\omega)$ since $\hat{\mathcal{O}}(\omega)$ and $\hat{\mathcal{O}}(\omega')$ do not necessarily commute. On the other hand, for a classical variable the power spectral density is always frequency symmetric.

2.3.1 Linear Amplifier

In a linear amplifier the equations for the out operators take the general form;

$$b_\alpha = \sum_{\beta\in\mathcal{I}}(M_{\alpha,\beta}a_\beta + L_{\alpha,\beta}a_\beta^\dagger) + \mathcal{F}_\alpha, \qquad \alpha \in \mathcal{O} \tag{2.3.1}$$

where the $\mathcal{C}$-numbers $M_{\alpha,\beta}, L_{\alpha,\beta}$ depend only on the in operators of the internal modes; therefore, they commute with the $a_\beta, a_\beta^\dagger$ for $\beta \in \mathcal{I}$. The linearization procedure that yields to Eqs.(2.3.1) usually requires assumptions about the size of the input signal and the nature of the operating state. For further detail in this we recommend reading what was done in [41, 36, 37]. For our purpose of discussion we focus the attention on the operators $\mathcal{F}_\alpha$. They clearly are responsible for the amplifier's additive noise, i.e. the noise that the amplifier adds to the output signal, that cannot be neglected, regardless of the level of the input signal. Furthermore we'll see that the fluctuations in $\mathcal{F}_\alpha$, not the mean values, are of interest, and so nothing is lost by assuming $\langle\mathcal{F}_\alpha\rangle = 0$.
Equally clear is a connection between the amplifier's gain and the $\mathcal{C}$-numbers $M_{\alpha,\beta}, L_{\alpha,\beta}$. These numbers determine the gain, and their fluctuations produce fluctuations in the gain. Gain fluctuations introduce multiplicative noise into the output signal, i.e. noise which depends on the level of the input signal; such multiplicative noise inevitably degrades the amplifier's performance. As far as we are concerned, our interest is in limits on the performance of the best possible amplifiers, so we assume throughout the following that the fluctuations in $M_{\alpha,\beta}, L_{\alpha,\beta}$ are negligible. In this way, Eqs. (2.3.1) become the basic linear equations:

$$b_\alpha = \sum_{\beta\in\mathcal{I}}(M_{\alpha,\beta}a_\beta + L_{\alpha,\beta}a_\beta^\dagger) + \mathcal{F}_\alpha, \qquad \alpha \in \mathcal{O} \tag{2.3.2}$$

It is now easy to apply the requirement that the input-mode operators and the output-mode operators obey the bosonic commutation relations ($[a_\alpha, a_\beta^\dagger] = 0$ and $[a_\alpha, a_\beta^\dagger] = \delta_{\alpha,\beta}$). The resulting unitarity conditions are

$$0 = \sum_{\mu\in\mathcal{I}}(M_{\alpha,\mu}L_{\beta,\mu} + L_{\alpha,\mu}M_{\beta,\mu}) + [\mathcal{F}_\alpha, \mathcal{F}_\beta] \tag{2.3.3}$$

$$\delta_{\alpha,\beta} = \sum_{\mu\in\mathcal{I}}(M_{\alpha,\mu}M_{\beta,\mu}^* + L_{\alpha,\mu}L_{\beta,\mu}^*) + [\mathcal{F}_\alpha, \mathcal{F}_\beta^\dagger] \tag{2.3.4}$$

for every $\alpha, \beta \in \mathcal{O}$. Equations (2.3.2)-(2.3.4) are necessary conditions for a bosonic linear amplifier, and they are sufficient for the investigation of quantum limits. In order to do so, we better consider the so-called narrow band regime, in which the restriction to narrow-band amplifiers allow us to treat the input and output signals as being carried out by single modes. From this point of view, the input and output signals are nearly sinusoidal oscillations with frequencies ω_I, ω_O, both with bandwidth $\Delta\omega/2\pi \ll \omega_I/2\pi, \omega_O/2\pi$. In this situation for single-mode input and output, the linear evolution equations (2.3.2) become

$$b_O = Ma_I + La_I^\dagger + \mathcal{F} \tag{2.3.5}$$

and the unitary conditions collapse into

$$1 = |M|^2 - |L|^2 + [\mathcal{F}, \mathcal{F}^\dagger]. \tag{2.3.6}$$

Fortunately, for an investigation of quantum limits, the complexities buried in the noise term need not be exhumed, and the only important property of $\mathcal{F}^2$ is the unitarity condition (2.3.6), which places a lower limit on its fluctuation

$$|\Delta\mathcal{F}|^2 \geq \frac{1}{2}|1 - |M|^2 + |L|^2| \tag{2.3.7}$$

where we have exploited the fact that for any general Hermitian operator $\hat{A}$ the following hold:

$$|\Delta\hat{A}|^2 \geq \frac{1}{2}|\langle[\hat{A}, \hat{A}^\dagger]\rangle|$$

with the definition $|\Delta\hat{A}|^2 = \langle\hat{A}^2\rangle - \langle\hat{A}\rangle^2$ for Hermitian operators.
We can now investigate the consequences of the latter result. To do this, it is convenient to introduce the fundamental notion of phase sensitivity, defining first what is meant by a phase-insensitive amplifier. The property of a phase-insensitive linear amplifier is that when the input signal has phase-insensitive noise, the output, both in terms of the signal and the noise, shows no phase preference; the only effect of a phase shift of the input is an equivalent phase shift of the output. This idea is formalized by defining a phase-insensitive linear amplifier as one that satisfies two conditions.
Condition I.
The expression for $\langle b_O\rangle$ is invariant under any arbitrary phase transformations $\varphi = \varphi_I = \theta_O$ (*phase-preserving amplifier*) or $\varphi = \varphi_I = -\theta_O$ (*phase-conjugating amplifier*).
Condition II.
If the input signal has phase-insensitive noise, then the output signal also has phase-insensitive noise, namely

$$\langle b_O^2\rangle = \langle b_O\rangle^2 \quad \text{if} \quad \langle a_O^2\rangle = \langle a_O\rangle^2.$$

Condition I means that a phase shift of the input signal produces the same (phase-preserving) or the opposite (phase-conjugating) phase shift of the output signal, on the other hand, Condition II means that the noise added by the amplifier is distributed randomly in phase. An amplifier that fails to meet conditions I and II is called a phase-sensitive linear amplifier.
The consequences of these two conditions are that I implies

$$L = 0 \quad \text{if phase preserving}$$
$$M = 0 \quad \text{if phase conjugating,}$$

and II that

$$\langle\mathcal{F}^2\rangle = 0.$$

On the other hand, the output of a phase-sensitive linear amplifier depends effectively on the phase of the input. Nevertheless, from Eq.(2.3.5), one can define the mean gain of the amplifier as

$$G \equiv |M|^2 + |L|^2, \tag{2.3.8}$$

where we immediately see that obtained gain has no dependence on the noise term in this situation. This set two important conditions that we will keep in mind later, the first one is that only for a phase-preserved amplifier we have to add the noise term, and the second one that not in any amplifier it is impossible to disregard the term of quantum noise added from the measurement itself. The latter, as we have seen, could play an important role in the intrinsic nature of a phase-insensitive amplifier.

[2]We also point out that throughout this work we assumed that the noise is Gaussian, namely $\langle\mathcal{F}\rangle$, so that it can be characterized completely by its second moments.

3 Optical Fields: Coherent States and Detection

In this chapter correlation functions for the electromagnetic field are introduced, from which a definition of optical coherence may be formulated. Furthermore, we will give a characterization of coherent states, squeezed states, and optical field detection techniques, both homodyne and heterodyne, following the same type of analysis also done by Walls, Milburn, Bowen in [35, 42] and Zhang [43].
In 1926, Schrödinger first proposed the concept of what is now called "coherent states" [44] in connection with the classical states of the quantum harmonic oscillator. It is worth to note that the birth of the expressions of these states coincides with the birth of quantum mechanics, meaning the indispensability of one from the other.
In the early years of quantum mechanics the study of coherent states remained in a sort of "dormancy" period, only to be awakened by Glauber and Sudarshan in 1962-63 ([7, 45, 46]). In his two essential papers, in which the term coherent states was first coined, Glauber constructed the eigenstates of the annihilation operator of the harmonic oscillator to study the electromagnetic correlation functions, a subject of great importance in quantum optics. Roughly at the same time as Glauber and Sudarshan, Klauder in his work [47, 48], developed a set of continuous states in which the ideas of coherent states for arbitrary Lie groups were contained. In the same vein, but ten years after, the complete construction of coherent states, with various properties similar to the harmonic-oscillator, was achieved by Perelomov [49] and Gilmore [50] in 1972. The general aim of this development was to connect the coherent states intimately with the dynamical group for each physical problem.

3.1 Field Correlations and Optical Coherence

We begin our work by recalling the concept of field correlations, following the exhaustive analysis made by Glauber [7]. In this sense, the electromagnetic field, due to its intrinsic nature, may be regarded as a dynamical system with an infinite number of degrees of freedom. In the most accurate preparation of the state of a field usually, an indefinitely large number of parameters must be regarded as random variables. Our actual knowledge of the state of the field is fully specified by employing a density operator ρ (with its known properties) which is constructed as an average, over these random variables.
These considerations lead us to state that the quantity in which we are interested is of the form

$$\mathrm{tr}\,\{\rho\mathbf{E}_-(\mathbf{r},t)\mathbf{E}_+(\mathbf{r},t)\} \tag{3.1.1}$$

where $\mathbf{E}_-(\mathbf{r},t)$ and $\mathbf{E}_+(\mathbf{r},t)$ simply stem from the separation of the electric field operator $\mathbf{E}(\mathbf{r},t)$ into its positive and negative frequency parts (it's obvious that $\mathbf{E}(\mathbf{r},t) = \mathbf{E}_-(\mathbf{r},t) + \mathbf{E}_+(\mathbf{r},t)$). This separation is easily obtained when the operator is represented by a Fourier integral as

$$\mathbf{E}(\mathbf{r},t) = \int_{-\infty}^{\infty} d\omega \mathbf{e}(\omega,\mathbf{r})e^{i\omega t} \tag{3.1.2}$$

where the two separated parts will correspond to the regime integration $[0,\infty]$ and $[-\infty,0]$. Immediately following that the two parts, regarded separately, are not Hermitian operators and

$$\mathbf{E}_-(\mathbf{r},t) = \mathbf{E}_+^\dagger(\mathbf{r},t)$$

In the more general expression, the fields $\mathbf{E}_-, \mathbf{E}_+$ are evaluated at different space-time points. Expectation values of the latter type give us a measure of the correlations of the fields at separated positions and times. We shall define such a correlation function $G^{(1)}$ as

$$G^{(1)}(\mathbf{r}t,\mathbf{r}'t') = \mathrm{tr}\,\{\rho\mathbf{E}_-(\mathbf{r},t)\mathbf{E}_+(\mathbf{r}',t')\} \tag{3.1.3}$$

where these field correlations may be extended over considerable intervals of distance and time, and is essential to the idea of coherence, which we shall discuss later on. We can generalize the previous expression not only to quadratic correlations, but also to higher orders, for example by defining a correlation function to the second-order as

$$G^{(2)}(\mathbf{r}_1 t_1, \mathbf{r}_2 t_2; \mathbf{r}_3 t_3, \mathbf{r}_4 t_4) = \mathrm{tr}\left\{\rho \mathbf{E}_-(\mathbf{r}_1, t_1)\mathbf{E}_-(\mathbf{r}_2, t_2)\mathbf{E}_+(\mathbf{r}_3, t_3)\mathbf{E}_+(\mathbf{r}_4, t_4)\right\} \tag{3.1.4}$$

and consequently applying the same reasoning to n photons that we want to detect (we denote the pair coordinates $\mathbf{r}_j, t_j$ by x_j)

$$G^{(n)}(x_1, \ldots, x_n; x_{n+1}, \ldots, x_{2n}) = \mathrm{tr}\left\{\rho \mathbf{E}_-(x_1)\ldots\mathbf{E}_-(x_n)\mathbf{E}_+(x_{n+1})\ldots\mathbf{E}_+(x_{2n})\right\} \tag{3.1.5}$$

These correlations have several simple properties. The first is that if we interchange the arguments we obtain

$$G^{(n)}(x_{2n}, \ldots, x_{n+1}; x_n, \ldots, x_1) = \left[G^{(n)}(x_1, \ldots, x_n, x_{n+1}, \ldots, x_{2n})\right]^*$$

and secondly, they satisfy the same inequalities for our discussion, for example (we left the demonstration of these to [7]):

$$G^{(n)}(x_1, \ldots, x_n; x_n \ldots x_1) \geq 0$$

In this way, the simplest of the quadratic inequalities takes the form

$$G^{(1)}(x_1, x_1)G^{(2)}(x_2, x_2) \geq |G^{(1)}(x_1, x_2)|^2 \tag{3.1.6}$$

and the same holds for higher n-order correlations. One should notice that when the number of quanta present in the field is bounded, the sequence of functions $G^{(n)}$ terminates. Thus if the number of photons is smaller or equal than to a certain value N, the properties of $E^{(\pm)}$ as annihilation and creation operators show that $G^{(n)} = 0$ for any $n > N$.
On the other hand, if we would have restricted the character of ρ to describe only stationary fields (e.g $[\rho, \mathcal{H}] = 0$), then our first correlation $G^{(1)}$ would depend on the difference of two times $t - t'$.
In light of the above let us now consider the concept of coherence. As first coined by Glauber, this term in quantum optics is "used to denote a tendency of two values of the field at distantly separated points or greatly separated times to take on correlated values".
To discuss coherence in quantitative terms it is worthy to introduce normalized forms of the correlation functions. For example the first-order function

$$g^{(1)}(\mathbf{r}, t, \mathbf{r}', t') = \frac{G^{(1)}(\mathbf{r}t, \mathbf{r}'t')}{[G^{(1)}(\mathbf{r}t, \mathbf{r}t)G^{(1)}(\mathbf{r}'t', \mathbf{r}'t')]^{1/2}} \tag{3.1.7}$$

with $g^{(1)}$ that obeys the following inequality thanks to (3.1.6)

$$|g^{(1)}(\mathbf{r}, t, \mathbf{r}', t')| \leq 1 \tag{3.1.8}$$

of course for $\mathbf{r} = \mathbf{r}', t = t'$ we obtain $g^{(1)} \equiv 1$. Therefore the normalized forms for n-th order are defined as

$$g^{(n)}(x_1, \ldots, x_{2n}) = \frac{G^{(n)}(x_1 \ldots, x_{2n})}{\prod_{j=1}^{2n}[G^{(1)}(x_j, x_j)]^{1/2}} \tag{3.1.9}$$

(note that for $n \geq 1$ these functions are not in general restricted as $g^{(1)}$ in (3.1.8)).
Consequentially we can state that the condition for being a fully coherent field is rooted in the magnitude of the correlation functions, namely

$$|g^{(n)}(x_1, \ldots, x_{2n})| = 1 \qquad n = 1, 2, , 3 \ldots \tag{3.1.10}$$

However, this condition is not respected by all the fields that we normally define, or have defined, "coherent". We shall state as a necessary condition for first-order coherence that

$$|g^{(1)}(\mathbf{r}, t, \mathbf{r}', t')| = 1$$

or more generally for a field to be characterized by n-th order coherence we shall require

$$|g^{(j)}(\mathbf{r}, t, \mathbf{r}', t')| = 1 \qquad j \leq n$$

Of course, one can not expect that this relation holds exactly for all points in space and time. We shall therefore employ the n-th order coherence to mean that the first n coherence conditions are accurately satisfied over intervals as $x_1 = x_2 = x_3 = \cdots = x_{2n}$. It is only within such ranges, and therefore as an approximation, that we can speak of coherence at all.

3.2 Field coherent states

In the previous section we have seen how, in the most general way possible, the concepts of coherent field and optical coherence are defined. Our discussion now will have a slightly different emphasis on how the field coherent states can be constructed from the dynamical group of the system: the Heisenberg-Weyl group. As we are going to see, there are three equivalent ways to construct the coherent states for such a dynamical group. However, Glauber [7] showed that such states are enormously useful for describing the physics of quantum optics. Physically, they turn out to be eigenstates of the coherence (correlation) function of the electromagnetic field. Consequently, he named these states field coherent states.
According to Glauber [45], the field coherent states can be constructed starting from any of the following three mathematical definitions.

Definition 1: The coherent states $|\alpha\rangle$ are quantum states with a minimum-uncertainty relationship

$$(\Delta p)^2 (\Delta q)^2 = \frac{1}{4}$$

with the position and momentum operators defined as

$$\hat{q} = \frac{1}{\sqrt{2}}(a + a^\dagger)$$
$$\hat{p} = \frac{1}{i\sqrt{2}}(a - a^\dagger)$$

and generic variance and expectation value

$$(\Delta A)^2 \equiv \langle\alpha|(\hat{A} - \langle\hat{A}\rangle)^2|\alpha\rangle$$
$$\langle\hat{A}\rangle = \langle\alpha|\hat{A}|\alpha\rangle.$$

Definition 2: The coherent states $|\alpha\rangle$ are eigenstates of the harmonic-oscillator annihilation operator a,

$$a|\alpha\rangle = \alpha|\alpha\rangle$$

where α is a complex number.

Definition 3: The coherent states $|\alpha\rangle$ can be obtained by applying a displacement operator $D(\alpha)$ on the vacuum state of the harmonic oscillator,

$$|\alpha\rangle = D(\alpha)|0\rangle$$

where the displacement operator $D(\alpha)$ is defined as

$$D(\alpha) = \exp(\alpha a^\dagger - \alpha^* a).$$

We shall point out that the first definition does not provide a unique solution for $(\Delta p, \Delta q)$, as shown in Fig.2, where (a) represents the uncertainty circle for field coherent state (with $\Delta p = \Delta q = \frac{1}{2}$) and (b) the uncertainty ellipse for the so-called squeezed states, which will be discussed in detail in Sec. 3.2. Glauber's original approach was entirely motivated by the physical

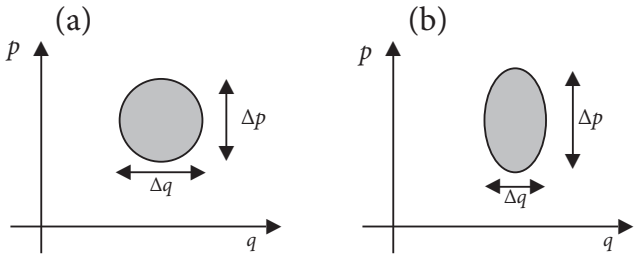

Figure 2: The uncertainty picture in the coherent states.

consideration of factorizing to all orders the electromagnetic field correlation functions.
To this end, he constructed the field coherent states by using the harmonic oscillator (HO) algebra. Nevertheless, we will analyze these three definitions, and how they can be met if we focus our attention on the case of HO. For this discussion in the future subsections, we will rely on what has been done from Penna in [51], following the steps that fit our analysis.

3.2.1 Minimum Uncertainty Coherent States

In quantum optics the simplest example from which the field coherent states are uniquely defined is precisely the harmonic oscillator. In this respect its Hamiltonian

$$H = \frac{p^2}{2m} + \omega^2 \frac{m}{2} q^2$$

is associated to the so-called *Schrödinger algebra*

$$\mathcal{A}_S = \{\mathbb{I}, q, p\}, \qquad [q, p] = i\hbar, \qquad [\mathbb{I}, q] = [\mathbb{I}, p] = 0$$

generated by $\mathbb{I}, q$, and p. In this sense, the commutators relevant to $\mathbb{I}, q, p$ contain the information determining its quantum character. As we know, the Heisenberg uncertainty principle states that

$$(\Delta q)^2 (\Delta p)^2 \geq \hbar/4$$

(with the former variance definition). At this point our aim is to show that Minimum Uncertainty Coherent States (MUCS) are states that minimize Heisenberg principle, i.e. $(\Delta q)^2(\Delta p)^2 = \hbar/4$. This can be done as follows: consider first two generic non-commmutating hermitian operators A, B

$$[\hat{A}, \hat{B}] = i\hat{G}$$

where G is another general operators. The fact that they are hermitian ensures that G is too, namely $G = -i[A, B] = i(BA - AB) = i(AB - BA)^\dagger = (-i[A, B])^\dagger = G^\dagger$. In this way, the Heisenberg principle claims

$$\Delta\hat{A}\Delta\hat{B} \geq |\langle G\rangle|^2/4 \tag{3.2.1.1}$$

Taking now into account non-hermitian operator defined as $\hat{A} + i\sigma\hat{B}$, where $\sigma = \frac{\langle\hat{G}\rangle}{2\Delta_B^2}$ (for simplicity we will denote $\Delta B := \Delta_B$), we are going to prove that the eigenvalues of this operator are characterized by minimum uncertainty, i.e. Eq.(3.2.1.1) is a strict equality:

$$(A + i\sigma B)|\psi\rangle = \lambda|\psi\rangle \quad \rightarrow \quad \Delta_A\Delta_B = \frac{\langle G\rangle}{2}$$

where ψ is some physical state of the system. This is immediately obtained noticing that the eigenvalue $\lambda = \langle A\rangle + i\sigma\langle B\rangle$. Therefore we can rewrite the eigenvalue equation as

$$(A - \langle A\rangle)|\psi\rangle = -i\sigma(B - \langle B\rangle)|\psi\rangle$$

and then if the term $(A - \langle A\rangle)$ acts on both side we find

$$(A - \langle A\rangle)^2|\psi\rangle = -i\sigma(A - \langle A\rangle)(B - \langle B\rangle)|\psi\rangle$$

with the product $(A - \langle A\rangle)$ that can be manipulated as

$$(A - \langle A\rangle) = [A - \langle A\rangle, B - \langle B\rangle] + (B - \langle B\rangle)(A - \langle A\rangle) = iG + (B - \langle B\rangle)(A - \langle A\rangle) \tag{3.2.1.2}$$

where we have used $[A - \langle A\rangle, B - \langle B\rangle] = [A, B] = iG$. Our eigenvalue equation thus became

$$(A - \langle A\rangle)^2|\psi\rangle = \sigma G|\psi\rangle + (i\sigma)^2(B - \langle B\rangle)^2|\psi\rangle,$$

and we just need to project $|\psi\rangle$ on the latter equation to determine the variance

$$\Delta_A^2 = \langle\psi|(A - \langle A\rangle)^2|\psi\rangle = -i\sigma\langle\psi|iG + (B - \langle B\rangle)(A - \langle A\rangle)|\psi\rangle = \sigma\langle\psi|G|\psi\rangle - \sigma^2\langle\psi|(B - \langle B\rangle)^2|\psi\rangle = \frac{\langle G\rangle^2}{\Delta_B^2}$$

from which the direct equality is now proven

$$\Delta_A^2\Delta_B^2 = \frac{\langle G\rangle^2}{4}.$$

3.2.2 Annihilation operator coherent states

Let us now resume the Hamiltonian of an harmonic oscillator,

$$H = \frac{p^2}{2m} + \omega^2\frac{m}{2}q^2$$

which we now know to be associated with the above mentioned *Schrödinger algebra* $\mathcal{A}_S$. The latter is said to be the Hamiltonian generating algebra for the HO in that it can be expressed as a quadratic function of the algebra generators q, and p. In this way, $\mathcal{A}_S$ is the Hamiltonian generating algebra for any one-dimensional potential system described by $H = p^2/2m + V(q)$ (where $V(q)$ as potential energy) or, more in general, for any system whose Hamiltonian is such that $H = F(q, p)$. In this sense it is appropriate introducing the annihilation operator as

$$a = \frac{mq\omega - ip}{\sqrt{2m\hbar\omega}} \tag{3.2.2.1}$$

since it allows us to rewrite

$$q = \sqrt{\frac{\hbar}{2m\omega}}(a^\dagger + a)$$
$$p = \sqrt{\frac{m\hbar\omega}{2}}(a^\dagger - a)$$

and the Hamiltonian as

$$H = \hbar\omega\left(n + \frac{1}{2}\right) \tag{3.2.2.2}$$

with the number operator $\hat{n} = a^\dagger a$ and where we used the commutation relation $[a, a^\dagger] = \mathbb{I}$. Equation (3.2.2.2) puts into evidence that the so called *Weyl-Heisenberg algebra*, generated by

$$\mathcal{A}_{WH} = \{\mathbb{I}, a^\dagger, a\}$$

is also an Hamiltonian generating algebra for the HO, in that H can be expressed in terms of quantities ($\mathbb{I}, a$, and $a^\dagger$) with well defined commutators

$$[a, n] = [a, a^\dagger]a = a, \quad [a^\dagger, n] = a^\dagger[a^\dagger, a] = -a^\dagger.$$

Observing these relations, one, in principle, can recognize that H can be written within a more general algebraic structure, namely the *Weyl algebra*. Indeed, this algebra will turn out to be a *dynamical algebra*, ie. if an algebra is such that some Hamiltonian can be written as a linear combination of its generator, then such an algebra is referred to as the dynamical algebra for the Hamiltonian under examination. However, entering in details of this is not our purpose, and we leave the complete discussion to [51].
Equation (3.2.2.2) also tells us that solving the eigenvalue problem for HO, adds up to diagonalizing the number operator n. This can be done by exploiting the commutation relations. In fact, denoting by $|s\rangle$ a generic (normalized) eigenstate of n ($n|s\rangle = s|s\rangle$), and by using commutator $[a, n] = a$ one has

$$n|s\rangle = (an - a)|s\rangle = as|s\rangle - a|s\rangle = (s - 1)a|s\rangle$$

showing that $a|s\rangle$ is an eigenstate of n with eigenvalue $s-1$. Using the communtator $[a^\dagger, n] = -a^\dagger$, one can repeat the same procedure obtaining

$$na^\dagger|s\rangle = (s + 1)a^\dagger|s\rangle$$

proving that $a^\dagger|s\rangle$ is an eigenstate of n with eigenvalue $s + 1$. Imposing the normalization condition $\langle s \pm 1|s \pm 1\rangle = 1$ yields to $a|s\rangle = \sqrt{s}|s1-\rangle$, and $a^\dagger|s\rangle = \sqrt{s+1}|s + 1\rangle$. The latter ones

can be recast as

$$a^m|s\rangle = \sqrt{s}a^{m-1}|s-1\rangle = \sqrt{\frac{s!}{(s-m)!}}|s-1\rangle$$
$$(a^\dagger)^m|s\rangle = \cdots = \sqrt{\frac{(s+m)!}{s!}}|s+1\rangle.$$

Therefore, we can now take expression (3.2.2.1), and have a look at the eigenstates of the annihilation operator [51]

$$a|\alpha\rangle = \alpha|\alpha\rangle,$$

expanding these states on the eigenfunctions basis to get

$$a|\alpha\rangle = a\sum_{n=0}^{\infty} f_n|n\rangle = \sum_{n=1}^{\infty}\sqrt{n}f_n|n-1\rangle = \sum_{n+1}^{\infty}\sqrt{n+1}f_n|n+1\rangle = \alpha|\alpha\rangle = \alpha\sum_{n=0}^{\infty} f_n|n\rangle$$

where the coefficients f_n of the series are related by the recursive relation $\sqrt{n}f_n = \alpha f_{n-1}$. In this way, we end up with

$$f_n = \frac{\alpha}{\sqrt{n}}f_{n-1} = \frac{\alpha^2}{\sqrt{n}\sqrt{n-1}}f_{n-2} = \cdots = \frac{\alpha^n}{\sqrt{n!}}f_0$$

that leads to

$$|\alpha\rangle = f_0\sum_{n=0}^{\infty}\frac{\alpha^n}{\sqrt{n!}}f_0$$

with f_0 determined due to the normalization condition

$$1 = \langle\alpha|\alpha\rangle = |f_0|^2\sum_n\frac{|\alpha|^2 n}{n!} = |f_0|^2 e^{|\alpha|^2}$$

from which

$$|\alpha\rangle = e^{-\frac{|\alpha|^2}{2}}\sum_{n=0}^{\infty}\frac{\alpha^n}{\sqrt{n!}}|n\rangle \tag{3.2.2.3}$$

The last step now consists in evaluating the uncertainty relation of q and p over the eigenstates (3.2.2.3):

$$\langle q\rangle = \frac{\hbar}{2m\omega}(\alpha+\alpha*)$$
$$\langle p\rangle = i\frac{\hbar m\omega}{2}(\alpha+\alpha^*)$$
$$\langle q^2\rangle = \frac{\hbar}{2m\omega}[(\alpha+\alpha^*)^2+1]$$
$$\langle p^2\rangle = \frac{\hbar}{2m\omega}[1-(\alpha-\alpha^*)^2]$$

from which finally

$$\begin{aligned} \Delta_q^2 &= \langle q^2\rangle - \langle q\rangle^2 = \frac{\hbar}{2m\omega} \\ \Delta_p^2 &= \langle p^2\rangle - \langle p\rangle^2 = \frac{\hbar\omega m}{2} \end{aligned} \quad \Rightarrow \quad \Delta_q^2\Delta_p^2 = \hbar/4 \tag{3.2.2.4}$$

Equation (3.2.2.4) exactly shows how the annihilation operator's eigenstates $|\alpha\rangle$ are minimum uncertainty states, namely they are annihilation operator coherent states (AOCS). This means that AOCS $\rightarrow$ MUCS.

3.2.3 Displacement operator coherent states

Finally, let's have a closer look at the definition of a coherent state as the result of the displacement operator on the vacuum state of the HO

$$|\alpha\rangle = D(\alpha)|0\rangle$$

with the already defined displacement operator $D(\alpha) = \exp(\alpha a^\dagger - \alpha^* a)$. Using the operator identity (Baker-Campbell-Hausdorff) [45]

$$e^{A+B} = e^A e^B e^{-[A,B]/2}$$

which only holds when

$$[A,[A,B]] = [B,[A,B]] = 0$$

we can write $D(\alpha)$ as

$$D(\alpha) = e^{-\frac{|\alpha|^2}{2}} e^{\alpha a^\dagger} e^{-\alpha^* a} \tag{3.2.3.1}$$

Now, since $a|0\rangle = 0$ implies that also $e^{\alpha^* a}|0\rangle = 0$ we can easily evaluate the action of the operator on the ground state

$$D(\alpha)|0\rangle = |\alpha\rangle = e^{-\frac{|\alpha|^2}{2}} e^{\alpha a^\dagger}|0\rangle = e^{-\frac{|\alpha|^2}{2}} \sum_{k=0}^{\infty} \frac{\alpha^k}{k!}\sqrt{k!}|k\rangle = e^{-\frac{|\alpha|^2}{2}} \sum_{k=0}^{\infty} \frac{\alpha^k}{\sqrt{k!}}|k\rangle$$

where we notice that the last expression is precisely the same as Eq.(3.2.2.3). We also would like to point out some important general properties of the displacement operator

$$\begin{aligned} &D^\dagger(\alpha) = D^{-1}(\alpha) = D(-\alpha) \\ &D^\dagger(\alpha)\; a\; D(\alpha) = a + \alpha \\ &D^\dagger(\alpha)\; a^\dagger\; D(\alpha) = a^\dagger + \alpha^* \\ &D(\alpha+\beta) = D(\alpha)D(\beta)e^{-i\mathrm{Im}\{\alpha\beta^*\}} \end{aligned} \tag{3.2.3.2}$$

Furthermore one could also evaluate the subsequent action of two displacement operators using this last property

$$D(\alpha_1)D(\alpha_2) = e^{\alpha_2 a^\dagger - \alpha_2 a} e^{\alpha_1 a^\dagger - \alpha_1 a} = D(\alpha_1+\alpha_2)e^{-i\mathrm{Im}\{\alpha_2\alpha_1^*\}}$$

where the latter result adds up to say that the application of a displacement operator on a coherent state results, up to a phase factor, into another coherent state:

$$D(\alpha_2)|\alpha_1\rangle = D(\alpha_2)D(\alpha_1)|0\rangle = e^{-i\mathrm{Im}\{\alpha_2\alpha_1^*\}}|\alpha_1+\alpha_2\rangle$$

This shows us how actually $D(\alpha)$ displaces the complex number which labels the coherent state. In this sense, the set of all the possible coherent states that come from the action of displacement operators on the ground state, is referred as

$$\{|\alpha\rangle = D(\alpha)|0\rangle, \quad \alpha \in \mathbf{C}\}$$

also called *coherent-state manifold*. This entail that, from the above definitions of the field coherent states, one sees that the displacement operator is a finite transformation operator in the complex α plane, that is, one to one correspondence between the coherent states $|\alpha\rangle$ and points in the complex α plane.

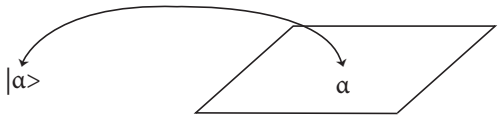

Figure 3: One to one correspondence between $|\alpha\rangle$ and points in the complex α plane.

3.3 Squeezed states

The uncertainty principle has posed a question to quantum physicists: is it possible to "beat" it? As far as we know this, for example, could be a limit in situations where we want to code and transmit information. However, if we think about it, the uncertainty principle is simply a statement about areas in phase space, and noise levels in different quadratures are statements about intersections of uncertainty ellipses with these axes. Any procedure that can deform, or squeeze, the uncertainty circle to an ellipse can in principle be used for noise reduction in one of the quadratures. Such squeezing does not violate the uncertainty principle; rather, it places the larger uncertainty in a quadrature not involved in the information transmission process. In this sense, a general class of minimum-uncertainty states is known as *squeezed states*. The procedure for squeezing the error ellipse that we will follow is given by Caves in 1981 [52], although he was not the first to give it, it is fair to mention the work of Yuen in 1976 [53] and Hollenhorst in 1979 [54] that introduced the term "squeezed states", and, of course, the pioneer worked in 1926 of Schrödinger [44], in connection with the classical states of the quantum harmonic oscillators.
We shall begin our discussion considering the properties of a single-mode field. We may write the annihilation operator a as a linear combination of two Hermitian operators

$$a = \sqrt{2}X_1 + i\sqrt{2}X_2 \tag{3.3.1}$$

obeying the following commutation relation

$$[X_1, X_2] = i.$$

The expectation values of X_1 and X_2 represent the real and imaginary parts of the complex amplitude, and they give dimensionless amplitudes for the two quadratures. Clearly it follows that the resulting uncertainty principle is $\Delta X_1 \Delta X_2 \geq 1/4$. The complex amplitude of a single mode is a constant of the motion, i.e. it is constant in the Heisenberg picture, thus, in Eq.(3.3.1), X_1, X_2 and a are Heisenberg-picture operators. There is a phase factor in the relation between the complex amplitude and the annihilation operator; this phase corresponds to the freedom to

make rotations in the complex-amplitude plane, since we can define them as

$$X_1(\theta) = \frac{1}{\sqrt{2}}\left(a^\dagger e^{i\theta} + a e^{-i\theta}\right)$$
$$X_2(\theta) = \frac{i}{\sqrt{2}}\left(a^\dagger e^{i\theta} - a e^{-i\theta}\right)$$

What we have previously seen is that the coherent state $|\alpha\rangle$, which has mean complex amplitude $\langle\alpha\rangle$, is conveniently represented by an "error circle" in a complex-amplitude plane whose axes are X_1, and X_2. On the other hand, the squeezed states have less noise in one quadrature than in the other. For this reason, they are represented by an ellipse on the quadrature planes, as shown in Fig.(2). Such states may be generated by using the unitary squeezing operator

$$S(\epsilon) = \exp[1/2\epsilon^* a^2 - 1/2\epsilon a^{\dagger 2}], \quad \epsilon = re^{i\theta} \tag{3.3.2}$$

where ϵ is an arbitrary complex number. Note the squeezing operator obeys the relations

$$S^\dagger(\epsilon) = S^{-1}(\epsilon) = S(-\epsilon)$$

and acts on the raising, lowering and quadrature operators as

$$S^\dagger(\epsilon) a S(\epsilon) = a\cosh r - a^\dagger e^{i\theta}\sinh r$$
$$S^\dagger(\epsilon) a^\dagger S(\epsilon) = a^\dagger\cosh r - a e^{-i\theta}\sinh r$$
$$S^\dagger(\epsilon)(Y_1 + iY_2)S(\epsilon) = Y_1 e^{-r} + iY_2 e^{r}$$

where

$$Y_1 + iY_2 = (X_1 + iX_2)e^{-i\theta/2}$$

is a rotated complex amplitude. The squeezing operator thus squeezes one component of the (rotated) complex amplitude, and it amplifies the other one. The degree of attenuation and amplification is determined by $r = |\epsilon|$, which will be called the *squeezing factor*. In this sense, the squeezed state $|\alpha, \epsilon\rangle$ is obtained by first squeezing the vacuum and then displacing it

$$|\alpha, \epsilon\rangle = D(\alpha)S(\epsilon)|0\rangle \tag{3.3.3}$$

To conclude, a squeezed state has the following expectation values and variances

$$\begin{aligned}
&\langle X_1 + iX_2\rangle = \langle Y_1 + iY_2\rangle e^{i\theta/2} = \alpha \\
&\Delta Y_1 = \frac{1}{2}e^{-r}, \quad \Delta Y_2 = \frac{1}{2}e^{r} \\
&\langle N\rangle = |\alpha|^2 + \sinh^2 r \\
&(\Delta N)^2 = |\alpha\cosh r + -\alpha^* e^{i\theta}\sinh r|^2
\end{aligned} \tag{3.3.4}$$

Note that the squeezed state $|\alpha, \epsilon\rangle$ has the same expected complex amplitude as the corresponding coherent state $|\alpha\rangle$, and it is a minimum uncertainty state for Y_1 and Y_2. The difference lies in its unequal uncertainties for Y_1, Y_2. In the complex plane, as already shown in Fig.(2), the coherent-state error circle has been squeezed into an error ellipse of the same area. Squeezed states are constantly used in quantum optics for various applications, and as we will see in Chapter 5 it is possible to obtain a reduction of quantum noise (output squeezing) by radiation pressure in optomechanical system [14].

3.3.1 Multimode squeezed states

Multimode squeezed states are important since many devices produce light which is correlated at the two frequencies ω_1 and ω_2. In this way, the squeezing exists not in the single modes but in the correlated state formed by the two modes. A two-mode squeezed state may be defined by [55, 56]

$$|\alpha_1, \alpha_2\rangle = D_1(\alpha_1)D_2(\alpha_2)S(\xi)|0\rangle \tag{3.3.1.1}$$

where the displacement operator is

$$D_j(\alpha) = \exp\left(\alpha a_j^\dagger - \alpha^* a_j\right), \quad j = 1, 2.$$

and the two-mode squeezing operator is

$$S(\xi) = \exp\left(\xi^* a_1 a_2 - \xi a_1^\dagger a_2^\dagger\right)$$

As a generalization of the previous section, it follows the squeezing operator transforms the annihilation operators as

$$S^\dagger(\xi)a_{1,2}S(\xi) = a_{1,2}\cosh r - a_{2,1}^\dagger e^{i\theta}\sinh r, \qquad \xi = re^{i\theta}$$

and gives the following expectation values

$$\begin{aligned}
&\langle a_{1,2}\rangle = \alpha_{1,2} \\
&\langle a_{1,2}a_{1,2}\rangle = \alpha_{1,2}^2 \\
&\langle a_1 a_2\rangle = \alpha_1\alpha_2 - e^{i\theta}\sinh r\cosh r \\
&\langle a_{1,2}^\dagger a_{1,2}\rangle = |a_{1,2}|^2 + \sinh^2 r.
\end{aligned} \tag{3.3.1.2}$$

Thanks to these, one can immediately compute the mean and variance of the quadrature operator $\hat{X}$ in a two-mode squeezed state

$$\langle\hat{X}\rangle = 2(\mathrm{Re}\,\{\alpha_1\} + \mathrm{Re}\,\{\alpha_2\}) \tag{3.3.1.3}$$

$$\mathrm{Var}(\hat{X}) = \left(e^{-2r}\cos^2\frac{\theta}{2} + e^{2r}\sin^2\frac{\theta}{2}\right) \tag{3.3.1.4}$$

where the quadrature is generalized in the two-mode case to

$$\hat{X} = \frac{1}{\sqrt{2}}\left(a_1 + a_1^\dagger + a_2 + a_2^\dagger\right).$$

Actually, this definition is a particular case of a more general one. It corresponds to the degenerate situation in which the frequencies of the two modes are set to be equal. These results for two-mode squeezed states will be used in the analyses of optomechanical systems given in Chapter 7. Furthermore, it is very interesting to see that squeezed states can have an immense range of situations where they are used. For example, it was shown in [57] that the vacuum quantum state in a black-hole space-time is given, for each mode, by a two-mode squeezed vacuum, showing us the close relationship between the theory of particle creation in external fields and the theory of quantum-mechanical squeezed states. In 1990 Grishchuk and Sidorov explained how primordial perturbations, created from zero-point quantum fluctuations in the course of

cosmological evolution, should be in squeezed states. Generally speaking, one can say that the variable gravitational field of the cosmological evolution is a "phase-sensitive amplifier which squeezed the vacuum". The important feature attributed to the phenomenon of squeezing, is that the variances in the amplitude distribution of gravitational waves are very large, while the variances in the phase distribution are practically equal to zero. It is known that to achieve squeezing, in the case of light generated under laboratory conditions, requires some experimental effort. In contrast with this, the squeezed gravitational waves are produced, are given for free and with a much greater amount of squeezing. Unfortunately, the electromagnetic waves cannot be squeezed in the course of cosmological expansion in a similar way, since they do not interact with the external gravitational field in the same manner as the gravitational waves do.
Grishchuk and Sidorov in 1990, and Kiefer in [58], also pointed out how Hawking's process of black-hole evaporation [59] is tightly linked with, again, two-mode squeezed states, turning out that these two areas of research are intimately related.

3.3.2 Einstein-Podolsky-Rosen paradox

To conclude this section, we would like to make a small introduction to what we will see in the next chapter, and also in Chapter 8, where we will work with squeezed states which will turn out to be entangled states. It is therefore necessary to mention the Einstein-Podolsky-Rosen paradox, which has been a fundamental work for studying entangled states, and in which they asked themselves: "Can Quantum-Mechanical Description of Physical reality be considered complete ?" [60]. In their article, the essential step was to introduce correlated pure states of two particles (or photons) of the form

$$|\Psi\rangle = \sum_n p_n |a_n\rangle_1 \otimes |b_n\rangle_2, \tag{3.3.2.1}$$

where p_n are numerical coefficients that sum up to 1, and $|a_n\rangle_1$, $|b_n\rangle_2$ are orthonormal eigenstates for some operators $\hat{A}_1$ and $\hat{B}_2$ of particles 1 and 2, respectively. Suppose now someone was measuring operator $\hat{A}_1$ on particle 1 long after the interaction between the particles has ended, and the two particles were space-like separated. If the result is some eigenvalue a_n, particle 1 must therefore be considered to be in the state $|a_n\rangle_1$, while particle 2 must be in the state $|b_n\rangle_2$, because of the collapse of the wave function. As the state of particle 2 is now an eigenstate of $\hat{B}_2$, we can predict with probability one that the physical quantity represented by $\hat{B}_2$ if measured, will give the result b_n. Thus we can predict the value of this physical quantity for particle 2 without in any way interacting with it.
Suppose, however, that instead of measuring $\hat{A}_1$ on particle 1 we measured some other observable, call it $\hat{C}_1$, with eigenstates $|c_n\rangle_1$, for which holds $[\hat{A}_1, \hat{C}_1] \neq 0$. We then have to rewrite the state in (3.3.2.1) as

$$|\Psi\rangle = \sum_n |c_n\rangle_1 \otimes |d_n\rangle_2 \tag{3.3.2.2}$$

where now $|d_n\rangle_2$ is an eigenstate of some other operator $\hat{D}_2$ for particle 2. If the result c_n is obtained from the measurement on particle 1, particle 2 must be in the state $|d_n\rangle_2$ for which a measurement of $\hat{D}_2$ must give exactly d_n as the result. Thus depending on what we choose to measure on particle 1 the state of particle 2 after the measurement, can be an eigenstate of two quite different operators. The EPR argument now raises one very important question. Is it possible that the two operators on particle 2, $\hat{B}_2$ and $\hat{D}_2$, do not commute? If this were the case the EPR argument establishes that, depending on what is measured on particle 1, we can predict with certainty the values of physical quantities, represented by non-commuting operators

without in any way interacting with this particle. By explicit construction Einstein, Podolsky and Rosen showed that this is indeed possible.
EPR claimed that "if without in any way disturbing a system, we can predict with certainty (i.e. with probability equal to unity), the value of a physical quantity, then there exists an element of physical reality corresponding to that quantity".
Assuming that the wave function does contain a complete description of the two-particle system it would seem that the argument of EPR establishes that it is possible to assign two different states ($|b_n\rangle_2$ and $|d_n\rangle_2$) to the same reality. Nevertheless, two physical quantities represented by operators which do not commute cannot have simultaneous reality. The EPR paradox concluded that the quantum mechanical description of physical reality given by the wave function is not complete.

3.4 Linear Detection of optical fields

To detect optical fields, the most common detection techniques are linear, i.e. they provide signals that are proportional to the intensity of the optical field. Such techniques can be understood through the example of direct detection of a bright field. The most common devices in practice involve a transition where a photon is absorbed. This has important consequences since this type of counter is insensitive to spontaneous emission. At this stage, we shall assume we have an ideal detector working on an absorption mechanism which is sensitive to the field $E^{(+)}(\mathbf{r},t)$ at the space-time point $(\mathbf{r},t)$. We will follow the treatment of Glauber [7] and the mathematical description given by [35].
The transition probability of the detector for absorbing a photon at position $\mathbf{r}$ and time t is proportional to

$$T_{if} = |\langle f|E^{(+)}(\mathbf{r},t)|i\rangle|^2 \tag{3.4.1}$$

where $|i\rangle$ and $|f\rangle$ are the initial and final states of the field. We do not measure the final state of the field but only the total counting rate. To obtain the latter we must sum over all states of the field which may be reached from the initial state by an absorption process. We can extend the sum over a complete set of final states since the states which cannot be reached (e.g., states $|f\rangle$ which differ from $|i\rangle$ by two or more photons) will not contribute to the result as they are orthogonal to $E^{(+)}(\mathbf{r},t)|i\rangle$. In this way, the total counting rate or average field intensity is

$$\begin{aligned} I(\mathbf{r},t) = \sum_f T_{fi} &= \sum_f \langle i|E^{(-)}(\mathbf{r},t)|f\rangle\langle f|E^{(+)}(\mathbf{r},t)|i\rangle \\ &= \langle i|E^{(-)}(\mathbf{r},t)E^{(+)}(\mathbf{r},t)|i\rangle, \end{aligned}$$

where we have used the e completeness relation relation $\sum_f |f\rangle\langle f| = 1$. The above result assumes that the field is in a pure state $|i\rangle$. As we know, the result may be generalized to a statistical mixture state by averaging over initial states with the probability p_i, i.e.

$$I(\mathbf{r},t) = \sum_i p_i \langle i|E^{(-)}(\mathbf{r},t)E^{(+)}(\mathbf{r},t)|i\rangle.$$

This can be recast as

$$I(\mathbf{r},t) = \mathrm{tr}\left\{\rho E^{(-)}(\mathbf{r},t)E^{(+)}(\mathbf{r},t)\right\}$$

with ρ density operator defined by

$$\rho = \sum_i p_i |i\rangle\langle i|.$$

If, for example, the field is initially in the vacuum state

$$\rho = |0\rangle\langle 0|,$$

then the intensity is

$$I(\mathbf{r}, t) = \langle 0|E^{(-)}(\mathbf{r}, t)E^{(+)}(\mathbf{r}, t)|0\rangle = 0.$$

The normal ordering of the operators (that is, all annihilation operators are to the right of all creation operators) yields zero intensity for the vacuum. This is a consequence of our choice of an absorption mechanism for the detector. Had we chosen a detector working on a stimulated emission principle, problems would arise with vacuum fluctuations. More generally the correlation between the field at the space-time point $\mathbf{x} = (\mathbf{r}, t)$ and the field at the space-time point $\mathbf{x}' = (\mathbf{r}', t')$ may be written as the correlation function

$$G^{(1)}(\mathbf{x}, \mathbf{x}') = \mathrm{tr}\left\{\rho E^{(-)}(\mathbf{x})E^{(+)}(\mathbf{x}')\right\},$$

where the first-order correlation function of the radiation field is sufficient to account for classical interference experiments, such as Young's interference experiment the shows how a definition of first-order optical coherence arises from considerations of the fringe visibility. Moreover, such a total rate is to be interpreted as a probability per unit time that one photon is recorded at $\mathbf{r}$ at time t and another at $\mathbf{r}'$ at time t'.

3.5 Phase-referenced tecniques: Homodyne and Heterodyne detection

Homodyne and Heterodyne are two phase-referenced detection techniques that find wide use in coherent communications, quantum optics, quantum optomechanics, and also microwave electronics. This techniques are well compared to direct detection in Fig.(4). As we can notice the

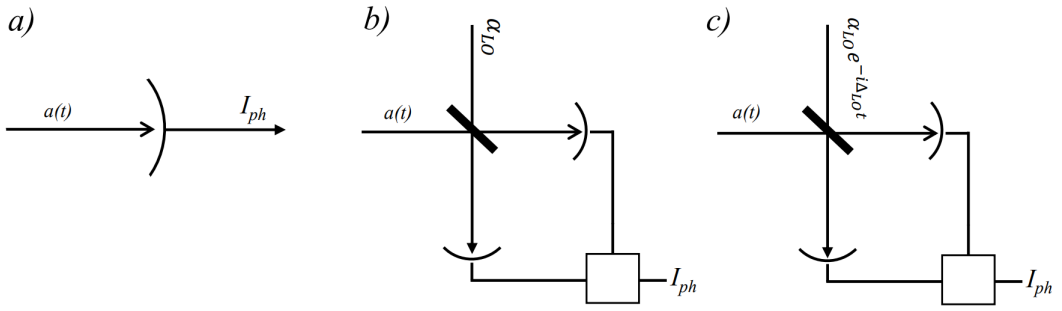

Figure 4: Sketch of direct (a), homodyne (b), and heterodyne (c) detection of an optical field, where $a(t)$ is the input field to be measured and I_{ph} the resulting photo-electron current. In homodyne detection the input field is interfered on a 50/50 beam splitter with a bright local oscillator that has the same optical carrier frequency. The phase of the local oscillator α_{LO} determines the measured optical quadrature. In heterodyne detection an offset local oscillator carrier frequency is used, resulting in a temporally oscillating phase relative to the input field. The measured optical quadrature therefore also oscillates with time.

main difference between direct and phase-referenced detection, is that in the second one the detected field is interfering with a bright local oscillator field. Specifically, in homodyne detection,

the local oscillator field (LO) has the same carrier frequency, while in heterodyne detection is used a carrier frequency that is offset from the detected field frequency by Δ_{LO}.
Starting with homodyne detection, consider two fields $E_1(\mathbf{r},t)$ and $E_2(\mathbf{r},t)$ of the same frequency, combined on a beam splitter with transmittivity η. We can expand the two incident fields into their positive and negative frequency components

$$E_1(\mathbf{r},t) = i\sqrt{\frac{\hbar\omega}{2V\varepsilon_0}}(a_1 e^{i(\mathbf{k}\cdot\mathbf{r}-\omega t)} - a_1^\dagger e^{-i(\mathbf{k}\cdot\mathbf{r}-\omega t)})$$
$$E_2(\mathbf{r},t) = i\sqrt{\frac{\hbar\omega}{2V\varepsilon_0}}(a_2 e^{i(\mathbf{k}\cdot\mathbf{r}-\omega t)} - a_2^\dagger e^{-i(\mathbf{k}\cdot\mathbf{r}-\omega t)})$$

where a_1, a_2 are boson operators which characterise E_1 and E_2, respectively. Both fields are taken to have the same sense of polarization. The total field after combination is given by

$$E_T = i\sqrt{\frac{\hbar\omega}{2V\varepsilon_0}}(ce^{i(\mathbf{k}\cdot\mathbf{r}-\omega t)} - c^\dagger e^{-i(\mathbf{k}\cdot\mathbf{r}-\omega t)})$$

where

$$c = \sqrt{\eta}a_1 + \sqrt{1-\eta}a_2$$

The photon detector, of course, responds to the moments of $c^\dagger c$, and we thus define the number operator $\hat{N} = \langle c^\dagger c\rangle$. In this sense, the mean photo-electron current in the detector is proportional to $\langle c^\dagger c\rangle$ which is given by

$$I_{\text{ph}} \propto \langle c^\dagger c\rangle = \eta\langle a_1^\dagger a_1\rangle + (1-\eta)\langle a_2^\dagger a_2\rangle + \eta(1-\eta)(\langle a_1^\dagger a_2\rangle + \langle a_1 a_2^\dagger\rangle). \tag{3.5.1}$$

Let us take the field E_2 to be the local oscillator and assume it to be in a coherent state of large amplitude $\beta \in \mathbb{R}$. Then we may neglect the first term in (3.5.1) and write I_{ph} in the form

$$I_{\text{ph}} \propto \langle c^\dagger c\rangle \approx (1-\eta)|\beta|^2 + \eta(1-\eta)\sqrt{2}\beta\langle\hat{X}(\theta)\rangle$$

with the quadrature operator

$$\hat{X}(\theta) \equiv \frac{1}{\sqrt{2}}(a_1 e^{-i\theta} + a_1^\dagger e^{i\theta}) \tag{3.5.2}$$

and θ is the phase of β. This is an important result, as it shows us that the mean photo-current in the detector is proportional to the mean quadrature phase amplitude of the signal field defined with respect to the local oscillator phase. If we also change $\theta \to \theta + \pi/2$ we can determine the mean amplitude of the two canonically conjugate quadrature phase operators (namely $\hat{X}$ and $\hat{P}$). We now shall make a consideration of the fluctuations in the photo-current. For a local oscillator in a coherent state the variance of $c^\dagger c$ is

$$\text{Var}(\hat{N}) = (1-\eta)^2|\beta|^4 + 2\eta^2(1-\eta)^2|\beta|^2\text{Var}(\hat{X}_\theta). \tag{3.5.3}$$

The first term here represents reflected local oscillator intensity fluctuations. If this term is subtracted out, the photo-current fluctuations are determined by the variances in $\hat{X}_\theta$, i.e. the measured quadrature-phase operator. To subtract out the contribution of the reflected local oscillator field balanced homodyne detection may be used. In this scheme, the output from both ports of the beam splitter is directed to a photodetector, and the resulting currents are combined with appropriate phase shifts before subsequent analysis. Balanced homodyne detection

realizes direct measurement of the signal field quadrature-phase operators [61]. Alternatively, the contribution from the local oscillator intensity fluctuations may be reduced by making the transmissivity $\eta \approx 1$, in which case the dominant contribution to $\mathrm{Var}(\hat{N})$ comes from the second term in (3.5.3).
Heterodyne detection is essentially equivalent to the homodyne case, except that the frequency of the local oscillator field is offset from the frequency of the field to be detected by $\Delta_{LO} = \omega_{LO} - \omega_L$ (ω_L is the detected field frequency). Analogously, one could show that

$$I_{\mathrm{ph}}^{\mathrm{het}} \propto \langle \hat{X}(\theta - \Delta_{LO} t) \rangle \tag{3.5.4}$$

meaning that the output signal of the probed field by heterodyne detection, oscillates in time at a frequency given by the detuning of the local oscillator.

4 Entanglement measures

When two quantum systems come to interact, some quantum correlation is established between the two of them. This correlation persists even when the interaction is switched off and the two systems are spatially separated. If we measure a local observable on the first system, its state collapses in an eigenstate of that observable. In the ideal case of no environmental decoherence, the state of the second system is instantly modified. The question then arises about what is the mechanism responsible for this action at a distance. In this sense, quantum entanglement refers to correlations between the results of measurements made on subsystems of a system that cannot be explained in terms of classical statistical correlations. For example, one may argue that this system contains quantum correlations if the observables, associated with the different subsystems, are correlated and their correlations cannot be reproduced with purely classical means. This implies that some form of inseparability or non-factorizability is necessary to properly take into account those correlations, as in the case of a pure quantum state, where the entanglement is defined as the impossibility of factorization of that state. Nevertheless, in the real world, we usually meet physical systems which interact with the environment getting then entangled with it. This process, changing the state of our system from pure to mixed one, decreases the internal entanglement of the system sometimes even destroying it completely. Thus one usually faces the following process

$$|\Psi\rangle\langle\Psi| \longrightarrow \rho_{AB} \tag{4.1}$$

However it has been shown [62, 63] that there are cases when the system in a mixed state ρ_{AB} still possesses entanglement, and the density matrices of those systems are called inseparable. Mathematically, ρ_{AB}, defined on the Hilbert space $\mathcal{H} = \mathcal{H}_{\mathcal{A}} \otimes \mathcal{H}_{\mathcal{B}}$, is called inseparable (separable) if it cannot (can) be represented as a convex combination of product states [64, 65]

$$\rho_{AB} = \sum_{i=1}^{N} p_i \rho_A^i \otimes \rho_B^i, \tag{4.2}$$

where ρ_A^i and ρ_B^i are subsystems' states and of course $\sum_{i=1}^{N} p_i = 1$.
The simplest example [66] of such a state is the Bell state with the two $\frac{1}{2}$ - spin particles labeled by A and B

$$\Psi = \frac{1}{\sqrt{2}} = (|\uparrow\rangle_A|\downarrow\rangle_B - |\downarrow\rangle_A|\uparrow\rangle_B), \tag{4.3}$$

or any state which can be obtained from the above one by means of product unitary transformation. The properties of the states of this kind are responsible for profoundly non-classical phenomena like quantum cryptography via Bell inequalities [67, 68], which will be discussed later on in Chapter 9.
Let us now take into account the paradigmatic situation of two observers Alice and Bob being in two distant laboratories. There is a source of pairs of particles between two laboratories which sends one member of any pair to each of them. Alice and Bob are allowed to perform any quantum operations on particles in their laboratories and communicate with each other via some classical channel (e.g. by telephone). Usually, they are also allowed to discard some particles. We shall refer to all those operations as to $LQCC$ ones (Local Quantum Operations and Classical Communication). Since Alice and Bob can only interact classically, then some operations are certainly unavailable for them. For example, if they share a pair of particles that are non-entangled, it is impossible to entangle those particles with each other. Now the basic task is to find the best

Alice and Bob can do under the above restrictions to reverse somehow the process (4.1). This leads to the so-called idea of distillation of noisy entanglement via local quantum operations and classical communication [69, 66]. We now rapidly describe some of the entanglement measures introduced by [70, 65], but from Sec. 4.1 we will focus particularly on one specific obtained result in the context of separability criteria, namely the Peres–Horodecki condition [71, 72], qualifying and quantifying entanglement in Gaussian states for continuous-variable systems.
In this way, referring to the paradigmatic situation of two distant laboratories, to quantify the entanglement of any quantum state ρ_{AB}, there arise natural postulates which must be satisfied by any measure of entanglement E:

- $E(\rho_{AB}) \geq 0$ and $E(\rho_{AB}) = 0$ if ρ_{AB} is separable,
- $E(\rho_{AB})$ is invariant under the product unitary operations $U_A \otimes U_B$,
- $E(\rho_{AB})$ cannot be increased by any $LQCC$ operation.

It is now well understood that entanglement in a pure bipartite quantum state $|\Psi\rangle$ is equivalent to the degree of mixedness of each subsystem. Accordingly, it can be properly quantified by the entropy of entanglement $E_V(|\Psi\rangle)$, defined as the von Neumann entropy of the reduced density matrices. We first introduce the latter as a measure of the degree of information contained in a quantum (Gaussian) state, which corresponds to the amount of knowledge that we possess *a priori* on predicting the outcome of any state's measure. Therefore, the von Neumann entropy of a quantum state ρ_{AB} is defined as

$$S(\rho_{AB}) = -\mathrm{tr}\rho_{AB} \log \rho_{AB}$$

In this way, the entropy of entanglement reads [3]

$$E_V(\Psi\rangle) = S(\rho_A^i)S(\rho_B^i) = -\sum_{k=1}^{d} \lambda_k^2 \log \lambda_k^2 \tag{4.4}$$

where $\rho_B^i = \mathrm{tr}_A \left\{ |\Psi_{AB}^i\rangle\langle\psi_{AB}^i| \right\}$ and viceversa for ρ_A^i. As already mentioned, it can be shown [73] that $E_V(|\Psi\rangle)$ cannot increase under $LQCC$ performed on the state $|\Psi\rangle$. Moreover, the entropy of entanglement is by definition invariant under local unitary operations

$$E_V((\hat{U}_1 \otimes \hat{U}_2)|\Psi\rangle) = E_V(|\Psi\rangle).$$

On the other hand, if we deal with a mixed quantum state the difficulty lies in the fact that the decomposition of equation (4.2) is not unique: apart from pure states, there exist infinitely many decompositions of a generic ρ_{AB}, meaning that the mixed state can be prepared in infinitely many different ways. This has important consequences on the determination of mixed-state entanglement.

4.1 Mathematical description of continuous-variable systems and Gaussian States

Before analyzing the Peres–Horodecki criteria, we prefer to introduce a mathematical description of Gaussian states for continuous-variable (CV) systems. To this end, we will rely on what has been discussed in [74].
A continuous-variable (CV) system of N canonical bosonic modes is described by a Hilbert

[3] Notice that the purity of a state ρ is given by $\mathrm{tr}(\rho^2) = \sum_k \lambda_k^2$, with λ_k eigenvalues.

space $\mathcal{H} = \bigotimes_{k=1}^{N} \mathcal{H}_k$ resulting from the tensor product structure of infinite-dimensional Fock spaces $\mathcal{H}_k$'s, each of them associated with a single mode. For instance, one can think of the non-interacting quantized electromagnetic field, whose Hamiltonian describes a system of an arbitrary number N of harmonic oscillators of different frequencies ω_k. We have already seen the expressions of the quadrature phase operators (position and momentum) for each mode, but now we want to collect them together in the vector

$$\hat{R} = (\hat{q}_1, \hat{p}_1, \ldots, \hat{q}_N, \hat{p}_N)^T,$$

which enables us to write in compact form the bosonic commutation relations between the quadrature phase operators,

$$[\hat{R}_k, \hat{R}_j] = i\Omega_{k,j}$$

where Ω is the symplectic form

$$\Omega = \bigoplus_{k=1}^{N} \omega, \quad \omega = \begin{pmatrix} 0 & 1 \\ -1 & 0 \end{pmatrix}$$

In this way, the space $\mathcal{H}_k$ is spanned by the Fock basis $\{|n\rangle_k\}$ of eigenstates of the number operator $\hat{n}_k = \hat{a}_k^\dagger \hat{a}_k$.
States with central importance in quantum optics and quantum information are the Gaussian states. The set of Gaussian states is, by definition, the set of states with Gaussian characteristic functions and quasi-probability distributions on the quantum phase space. Gaussian states include coherent, squeezed, and thermal states, and the most general Gaussian state is precisely a thermal squeezed displaced state. Their entanglement properties will thus be the main subjects of these sections. From the definition, it follows that a Gaussian state ρ is completely characterized by the first and second statistical moments of the quadrature field operators, which will be denoted, respectively, by the vector of first moments $\mathbf{R} = (\langle \hat{R}_1 \rangle, \ldots, \langle \hat{R}_N \rangle)$ and by the covariance matrix (CM) $\boldsymbol{\sigma}$ of elements

$$\boldsymbol{\sigma}_{i,j} = \frac{1}{2}\langle \hat{R}_i \hat{R}_j + \hat{R}_j \hat{R}_i \rangle - \langle \hat{R}_i \rangle \langle \hat{R}_j \rangle.$$

Furthermore, the Wigner function of a Gaussian state can be written as follows in terms of phase-space quadrature variables

$$W(R) = \frac{e^{-\frac{1}{2} R \boldsymbol{\sigma}^{-1} R^T}}{\pi \sqrt{\mathrm{Det}\boldsymbol{\sigma}}},$$

where R stands for the real phase-space vector $(q_1, p_1, \ldots, q_N, p_N)$ belongs to the phase space Γ. Therefore, despite the infinite dimension of the associated Hilbert space, the complete description of an arbitrary Gaussian state is given by the $2N \times 2N$ covariance matrix. In the following, $\boldsymbol{\sigma}$ will be assumed indifferently to denote the matrix of second moments of a Gaussian state or the Gaussian state itself. In the language of statistical mechanics, the elements of the CM are the two-point correlation functions between the $2N$ canonical continuous variables.
We also notice that the entries of the CM can be expressed as energies by multiplying them by the level spacing $\hbar\omega_k$, where ω_k is the frequency of each mode. In this way, $\mathrm{tr}\boldsymbol{\sigma}$ is related to the mean energy of the state. Since $\boldsymbol{\sigma}$ contains the complete locally invariant information on a Gaussian state, we can expect some constraints existing to be obeyed by any CM, reflecting,

in particular, the requirements of positive semidefiniteness of the associated density matrix ρ. Indeed, such condition together with the canonical commutation relations implies

$$\boldsymbol{\sigma} + i\Omega \geq 0. \tag{4.1.1}$$

Eq.(4.1.1) is the necessary and sufficient condition the matrix $\boldsymbol{\sigma}$ has to fulfil to be a CM corresponding to a physical Gaussian state. We note that such a constraint implies $\boldsymbol{\sigma} \geq 0$. For future convenience, let us define the CM $\boldsymbol{\sigma}_{1\ldots N}$ of N-mode Gaussian state in terms of two-by-two submatrices as

$$\boldsymbol{\sigma}_{1\ldots N} = \begin{pmatrix} \boldsymbol{\sigma}_1 & \varepsilon_{1,2} & \cdots & \varepsilon_{1,N} \\ \varepsilon_{1,2}^T & \ddots & \ddots & \vdots \\ \vdots & \ddots & \ddots & \varepsilon_{N-1,N} \\ \varepsilon_{1,N}^T & \cdots & \varepsilon_{N-1,N}^T & \boldsymbol{\sigma}_N \end{pmatrix}. \tag{4.1.2}$$

Each diagonal block $\boldsymbol{\sigma}_k$ is respectively the local CM corresponding to the reduced state of mode k, for all $k = 1, \ldots, N$. On the other hand, the off-diagonal matrices $\varepsilon_{i,j}$ encode the correlations between subsystems i and j. We shall mention the explicit form of the CM for a two-mode squeezed state (with squeezing factor r), since, as we will see in Chapter 8, two-mode squeezed states are of key importance as entangled resources for practical implementations of CV quantum information protocols. The CM thus will be

$$\boldsymbol{\sigma}_{i,j}(r) = \begin{pmatrix} \cosh 2r & 0 & \sinh 2r & 0 \\ 0 & \cosh 2r & 0 & -\sinh 2r \\ \sinh 2r & 0 & \cosh 2r & 0 \\ 0 & -\sinh 2r & 0 & \cosh 2r \end{pmatrix}. \tag{4.1.3}$$

In the limit of infinite squeezing ($r \to \infty$), the state approaches the ideal EPR state [60], a simultaneous eigenstate of total momentum and relative position of the two subsystems, which thus share infinite entanglement. The EPR state is not normalizable and unphysical. However, in principle, an EPR state can be approximated with an arbitrarily high degree of accuracy by two-mode squeezed states with sufficiently large squeezing.

4.2 Separability Criterion for density matrices

The Peres–Horodecki criterion (PH) [71, 64] is based on the operation of partial transposition of the density matrix of a bipartite system, obtained by performing transposition with respect to the degrees of freedom of one subsystem only. PH criterion states that if a state ρ is separable then its partial transpose ρ^{T_1} (with respect, e.g., to subsystem S_1) is a valid density matrix, in particular positive semidefinite, $\rho^{T_1} \geq 0$. Obviously, the same holds for ρ^{T_2}. Positivity of the partial transpose (PPT) is therefore a necessary condition for separability. Note that the converse (i.e. $\rho_1^T \geq 0 \to \rho$ separable) is in general false, but it has been proven true for low dimensional systems, e.g. bipartite systems with Hilbert state space of dimensionality 2×2. The PPT criterion has been generalized to continuous-variable systems by Simon [75], who showed how, in infinite-dimensional Hilbert spaces, the PPT criterion is necessary and sufficient for the separability of all N-mode Gaussian states. Under partial transposition, the CM $\boldsymbol{\sigma}_{A|B}$, where subsystem S_A groups N_A modes, and subsystem S_B is formed by N_B modes, is transformed into a new matrix

$$\tilde{\boldsymbol{\sigma}}_{A|B} \equiv \boldsymbol{\theta}_{A|B} \boldsymbol{\sigma}_{A|B} \boldsymbol{\theta}_{A|B},$$

with

$$\boldsymbol{\theta}_{A|B} = \mathrm{diag}\left\{\underbrace{1,-1,1,-1,\ldots,1,-1}_{2N_A},\underbrace{1,1,1,1,\ldots,1,1}_{2N_B}\right\}.$$

Referring to the notation of equation (4.1.2), the partially transposed matrix $\tilde{\boldsymbol{\sigma}}_{A|B}$ differs from $\boldsymbol{\sigma}_{A|B}$ by a sign flip in the determinants of the internal correlation matrices, $\mathrm{Det}\varepsilon_{ij}$, with modes $i \in S_A$ and modes $j \in S_B$. In this way, the PPT criterion yields that a Gaussian state $\boldsymbol{\sigma}_{A|B}$ (with $N_A = 1$ and N_B arbitrary) is separable if and only if the partially transposed $\tilde{\boldsymbol{\sigma}}_{A|B}$ satisfies the uncertainty principle equation

$$\tilde{\boldsymbol{\sigma}}_{A|B} + i\Omega \geq 0. \tag{4.2.1}$$

This property in turn reflects the positivity of the partially transposed density matrix ρ^{T_A} associated with the state ρ. We have therefore demonstrated the existence of 'bisymmetric' (N_A+N_B)-mode Gaussian states for which PPT is equivalent to separability.

4.2.1 Negativity and inseparable mixed states

An important class of entanglement measures is defined by the negativities [76], which quantify the violation of the PPT criterion for separability, i.e. how much the partial transposition of ρ fails to be positive. The negativity $\mathcal{N}(\rho)$ [77, 78] is defined as

$$\mathcal{N}(\rho) = \frac{||\rho^{T_i}||_1 - 1}{2}, \tag{4.2.1.1}$$

where

$$||\hat{\mathcal{O}}||_1 = \mathrm{tr}\sqrt{\hat{\mathcal{O}}^\dagger\hat{\mathcal{O}}}$$

is the trace norm of the operator $\hat{\mathcal{O}}$. The negativity has the advantage of being a computable measure of entanglement, being

$$\mathcal{N}(\rho) = \max\left\{0, -\sum_k \lambda_k^-\right\}, \tag{4.2.1.2}$$

where $\left\{\lambda_k^-\right\}$ are the negative eigenvalues of the partial transpose. The negativity can be defined for CV systems as well [78], even though a related measure is more often used, the logarithmic negativity $E_{\mathcal{N}}(\rho)$

$$E_{\mathcal{N}}(\rho) = \log||\rho^{T_i}|| = \log[1 + 2\mathcal{N}(\rho)]. \tag{4.2.1.3}$$

The logarithmic negativity is an additive quantity and consists of an upper bound for the distillable entanglement. Both the negativity and the logarithmic negativity fail to be continuous in trace norm on infinite-dimensional Hilbert spaces; however, this problem can be circumvented by restricting to physical states of finite mean energy [79]. The great advantage of the negativities is that they are easily computable for general Gaussian states; they provide a proper quantification of entanglement, directly quantifying the degree of violation of the necessary and sufficient PH criterion for separability.
We conclude this section discussing the characterization of the prototypical entangled states of

CV systems, i.e. the two-mode Gaussian states. For these states, let us recall the expression of their CM in a general way as (e.g, see 4.1.3)

$$\boldsymbol{\sigma} = \begin{pmatrix} \boldsymbol{\alpha} & \boldsymbol{\gamma} \\ \boldsymbol{\gamma}^T & \boldsymbol{\beta} \end{pmatrix} = \begin{pmatrix} a & 0 & c_+ & 0 \\ 0 & a & 0 & c_- \\ c_+ & 0 & b & 0 \\ 0 & c_- & 0 & b \end{pmatrix}. \tag{4.2.1.4}$$

For two-mode states, the uncertainty principle in Equation (4.1.1) can be recast as a constraint on $\mathrm{Det}\boldsymbol{\sigma}$ and $\Delta(\boldsymbol{\sigma}) = \mathrm{Det}\boldsymbol{\alpha} + \mathrm{Det}\boldsymbol{\beta} + 2\mathrm{Det}\boldsymbol{\gamma}$ [80],

$$\Delta(\boldsymbol{\sigma}) \leq 1 + \mathrm{Det}\boldsymbol{\sigma}. \tag{4.2.1.5}$$

The eigenvalues of a two-mode Gaussian state will be denoted as ν_- and ν_+, where $\nu_- \leq \nu_+$, and they will be obtained by the following

$$2\nu_\mp^2 = \Delta(\boldsymbol{\sigma}) \mp \sqrt{\Delta(\boldsymbol{\sigma})^2 - 4\mathrm{Det}\boldsymbol{\sigma}}.$$

In this way, the PPT condition for separability, equation (4.2.1), has a very simple form for two-mode Gaussian states. In these terms, partial transposition corresponds to flipping the sign of $\mathrm{Det}\boldsymbol{\gamma}$, i.e.

$$\boldsymbol{\sigma} = \begin{pmatrix} \boldsymbol{\alpha} & \boldsymbol{\gamma} \\ \boldsymbol{\gamma}^T & \boldsymbol{\beta} \end{pmatrix} \xrightarrow{\rho \to \rho^{\mathrm{T}_i}} \tilde{\boldsymbol{\sigma}} = \begin{pmatrix} \boldsymbol{\alpha} & \tilde{\boldsymbol{\gamma}} \\ \tilde{\boldsymbol{\gamma}}^T & \boldsymbol{\beta} \end{pmatrix},$$

with $\mathrm{Det}\boldsymbol{\gamma} = -\mathrm{Det}\tilde{\boldsymbol{\sigma}}$. Accordingly, $\Delta(\boldsymbol{\sigma})$ is mapped into $\Delta(\tilde{\boldsymbol{\sigma}}) = \mathrm{Det}\boldsymbol{\alpha} + \mathrm{Det}\boldsymbol{\beta} - 2\mathrm{Det}\boldsymbol{\gamma}$, and the eigenvalues will be given by

$$2\tilde{\nu}_\mp^2 = \Delta(\tilde{\boldsymbol{\sigma}}) \mp \sqrt{\Delta(\tilde{\boldsymbol{\sigma}})^2 - 4\mathrm{Det}\boldsymbol{\sigma}}.$$

In this sense, the state $\boldsymbol{\sigma}$ is separable if and only if $\tilde{\nu}_- \geq 1$. Therefore, the logarithmic negativity equation reads

$$E_{\mathcal{N}} = \max\left\{0, -\log\tilde{\nu}_-\right\}, \tag{4.2.1.6}$$

as for the biggest eigenvalue of the partial transpose one has $\tilde{\nu}_+ > 1$ for all two-mode Gaussian states. Note that from previous equations the following necessary condition for two-mode entanglement follows

$$\boldsymbol{\sigma} \text{ entangled } \implies \mathrm{Det}\boldsymbol{\gamma} < 0.$$

4.3 Inseparability Criterion for CV Systems: Duan bound violation

The last criterion we want to analyze is directly linked to the inseparability of a CV system, and it will be the one utilized in all the calculations of Chapter 8. The Duan bound violation [81] is an inseparability criterion based on the total variance of a pair of Einstein-Podolsky-Rosen type operators, for continuous variable systems, providing a sufficient condition for entanglement of any bipartite state. Furthermore, for all Gaussian states, this criterion turns out to be a necessary and sufficient condition for inseparability.
As we have already seen, a quantum state ρ of two modes 1 and 2 is separable if, and only if, it can be expressed in the following form

$$\rho = \sum_i p_i \rho_1^i \otimes \rho_2^i,$$

where where we assume ρ_1^i and ρ_2^i to be normalized states of the modes 1 and 2, respectively, and $p_i \geq 0$ to satisfy $\sum_i p_i = 1$. In this sense, a maximally entangled continuous-variable state can be expressed as a co-eigenstate of a pair of EPR type operators, such as $\hat{x}_1 + \hat{x}_2$ and $\hat{p}_1 + \hat{p}_2$. Of course, the maximally entangled continuous-variable states are not physical, but for the physically entangled continuous-variable states, the two-mode squeezed states, the total variance of these two operators will rapidly tend to zero by increasing the degree of squeezing. We consider the following type of EPR-like operators:

$$\begin{aligned} \hat{u} &= |a|\hat{x}_1 + \frac{1}{a}\hat{x}_2 \\ \hat{v} &= |a|\hat{p}_1 - \frac{1}{a}\hat{p}_2 \end{aligned} \tag{4.3.1}$$

with the assumption that a is an arbitrary (nonzero) real number. In this way, we can state the following sufficient criterion for inseparability [81]:

- For any inseparable quantum state ρ, the total variance of a pair of EPR-like operators defined by Eqs. (4.3.1) with the commutators $[\hat{x}_j, \hat{p}_{j'}] = i\delta_{jj'}$ satisfies the inequality

$$\langle(\Delta\hat{u})^2\rangle_\rho + \langle(\Delta\hat{v})^2\rangle_\rho < a^2 + \frac{1}{a^2} \tag{4.3.2}$$

  with the variances $\langle(\Delta\hat{u})^2\rangle := \langle\hat{u}^2\rangle - \langle\hat{u}^2\rangle$ and $\langle(\Delta\hat{v})^2\rangle := \langle\hat{v}^2\rangle - \langle\hat{v}^2\rangle$. We leave the proof of latter result in the Appendix A.

A natural question could be how strong is this bound. Is it strong enough to ensure that, if inequality in the form of Eq.(4.3.2) is satisfied, the state necessarily becomes inseparable? It is very difficult to consider this problem for arbitrary continuous variable states. However, in experiments and protocols for quantum communication [82, 83, 84], continuous variable entanglement is generated by two-mode squeezing or by beam splitters, and all of these processes lead to Gaussian states. So, we will limit ourselves to consider Gaussian states only, which are of great practical importance. Regarding this, we find out that the inequality 4.3.2 indeed gives a necessary and sufficient inseparability criterion for all of the Gaussian states.
Regarding our work, in Chapter 8 we will exploit these criteria for studying optomechanical entanglement, focusing particularly on two-mode systems [85, 86, 87], for which it was first demonstrated for a superconductive microwave optomechanical system in 2013 by Palomaki, Teufel *et al* [24], and for massive mechanical oscillators in 2018 by Massel, Ockeloen-Korppi *et al* [88].

4.4 Bell Inequalities and non-locality: the Alain Aspect Experiment

In Quantum Physics, non-locality refers to the phenomenon by which the statistical measurement of a multi-partite quantum system does not admit an interpretation in terms of a local realistic theory. Quantum nonlocality has been experimentally verified under different physical assumptions [89, 90, 91, 92]. Any physical theory that aims at superseding or replacing quantum theory should account for such experiments and therefore cannot fulfill local realism; quantum nonlocality is a property of the universe that is independent of our description of nature.
Already the early days of quantum mechanics were characterized by debates over the applicability of established classical concepts to the new formulation of mechanics. The issues became quite distinct in the protracted exchange between A. Einstein and N. Bohr, culminating with the EPR-paper [60] and Bohr's response in 1935 [93].
Thereafter the matter rested until 1964 when J.S. Bell [67] opened up the possibility of directly

testing the consequences of the EPR premises. In the following, we will discuss the analysis of Bell in the context of correlated photon states, as treated in [35].
As we have seen in the EPR argument, it would seem necessary to search for a more complete physical theory than quantum mechanics. To obtain such a theory, quantum mechanics should be supplemented by additional, perhaps inaccessible, variables. Bell's argument consists of considering a system in which correlated photon polarization states are produced, as shown in Fig.(5). The two photons are emitted in opposite directions (by conservation of momentum)

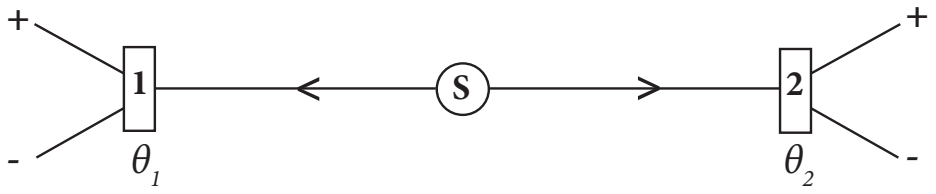

Figure 5: Sketch of the experiment of Aspect et al. [89] to test the Bell's inequality. S is a source of two polarised photons. 1 and 2 label polarisation analysers, with orthogonal output channels labelled + and −. The polarisation analysers are set at angles θ_1, θ_2.

with correlated polarisation states. Each photon passes through separate polarisation analyzers, emerging in either the horizontal (+) channel, or the vertical channel (−) of each analyzer. Initially let us assume that the horizontal polarisation is chosen to be orthogonal to the plane of the experiment. Let $a_\pm(b\pm)$ be the annihilation operator for the horizontally (+) or vertically (−) polarised mode for the field travelling to analyser 1 or analyser 2. The state of the two photons may be written as Bell's state

$$|\Psi\rangle = \frac{1}{\sqrt{2}} = (a_+^\dagger b_+^\dagger + a_-^\dagger b_-^\dagger)|0\rangle,$$

with $|0\rangle$ as vacuum state.
Using the notation $|n_1, n_2, n_3, n_4\rangle$ to denote n_1 photons in mode a_+, n_2 photons in mode a_-, n_3 photons in mode b_+ and n_4 photons in mode b_-, the state may be rewritten as

$$\Psi\rangle = \frac{1}{\sqrt{2}}(|1,0,1,0\rangle + |0,1,0,1\rangle).$$

If the photon in analyser 1 is detected in the (+) channel, the state of the photon directed towards 2 must be polarised in the horizontal direction. This correlation is thus precisely of the kind required for the EPR experiment. Of course, we are free to measure the polarisation in any direction simply rotating the analysers through the angles θ_1 and θ_2 for detector 1 and 2, respectively. The detected modes in this case are orthogonal transformations of the modes $a_\pm$ and $b_\pm$;

$$\begin{aligned} c_+ &= a_+ \cos\theta_1 + a_- \sin\theta_1 \\ c_- &= -a_+ \sin\theta_1 + a_- \cos\theta_1 \\ d_+ &= b_+ \cos\theta_2 + b_- \sin\theta_2 \\ d_- &= -b_+ \sin\theta_2 + b_- \cos\theta_2 \end{aligned} \tag{4.4.1}$$

In this way, the detectors placed after the polarisers measure the intensities $\langle I_1^\pm\rangle$ and $\langle I_2^\pm\rangle$, while the correlators measure $\langle I_1^+ I_2^+\rangle$, and so on. Indeed, for the two-photon state $\langle I_i^\pm\rangle = P_i^\pm$ is the

probability for one count in the + or − channel of detector i (obviously these moments depend on θ_1 and θ_2).
At this point, what Bell does is to suppose that in a complete theory these functions also depend on a variable λ which remains hidden from direct determination. This variable is distributed according to some density $\rho(\lambda)$. In general, we may write

$$\langle I_1^{\pm} I_2^{\pm} \rangle = \int \rho(\lambda) I_1^{\pm}(\theta_1, \theta_2, \lambda) I_2^{\pm}(\theta_1, \theta_2, \lambda) d\lambda$$

where I_1^+ denotes the expected intensity at detector 1 given a value for λ, i.e.

$$I_1^+(\theta_1, \theta_2, \lambda) = \int I_1^+ \rho(I_1^+ | (\theta_1, \theta_2, \lambda)) dI_1^+.$$

It is reasonable to assume that for a given value of λ the results at 1 cannot depend on the angle θ_2 chosen at 2, (and conversely). This is the "locality assumption", and can be written as

$$\begin{aligned} I_1^+(\theta_1, \theta_2, \lambda) &= I_1^+(\theta_1, \lambda) \\ I_2^+(\theta_1, \theta_2, \lambda) &= I_2^+(\theta_2, \lambda). \end{aligned}$$

Considering now the correlation functions

$$E(\theta_1, \theta_2) = \frac{\langle (I_1^+ - I_1^-)(I_2^+ - I_2^-) \rangle}{\langle (I_1^+ + I_1^-)(I_2^+ + I_2^-) \rangle}, \tag{4.4.2}$$

and assuming a local hidden variable theory we may write

$$E(\theta_1, \theta_2) = N^{-1} \int f(\lambda) S_1(\lambda, \theta_1) S_2(\lambda, \theta_2) d\lambda,$$

where

$$\begin{aligned} S_1(\lambda, \theta_1) &= \frac{I_1^+(\lambda, \theta_1) - I_1^-(\lambda, \theta_1)}{I_1(\lambda)} \\ S2(\lambda, \theta_2) &= \frac{I_2^+(\lambda, \theta_2) - I_2^-(\lambda, \theta_2)}{I_2(\lambda)} \\ f(\lambda) &= \rho(\lambda) I_1(\lambda) I_2(\lambda) \\ I_j(\lambda) &= I_j^+(\lambda, \theta_j) + I_j^-(\lambda, \theta_j) \qquad j = 1, 2. \end{aligned}$$

The latter equations correspond to the intensity of light measured at 1 or 2 when the polarisers are removed. The normalisation N is

$$N = \int f(\lambda) d\lambda.$$

The functions $|S_1(\lambda, \theta_1)|$ and $|S_2(\lambda, \theta_2)|$ are bounded by

$$\begin{aligned} |S_1(\lambda, \theta_1)| &\leq 1 \\ |S_2(\lambda, \theta_2)| &\leq 1. \end{aligned} \tag{4.4.3}$$

To obtain a statistical quantity we need to consider how $E(\theta_1, \theta_2)$ changes as the orientation of the polarisers are changed. With this in mind, consider $E(\theta_1, \theta_2) - E(\theta_1, \theta_2')$. This quantity can

be expressed as

$$E(\theta_1,\theta_2) - E(\theta_1,\theta_2') = N^{-1}\int d\lambda f(\lambda) S_1(\lambda,\theta_1) S_2(\lambda,\theta_2)[1 \pm S_1(\lambda,\theta_1') S_2(\lambda,\theta_2')]$$
$$- N^{-1}\int d\lambda f(\lambda) S_1(\lambda,\theta_1) S_2(\lambda,\theta_2')[1 \pm S_1(\lambda,\theta_1') S_2(\lambda,\theta_2)].$$

Then using (4.4.3)

$$|E(\theta_1,\theta_2) - E(\theta_1,\theta_2')| \leq N^{-1}\int d\lambda f(\lambda)[1 \pm S_1(\lambda,\theta_1') S_2(\lambda,\theta_2')]$$
$$+ N^{-1}\int d\lambda f(\lambda)[1 \pm S_1(\lambda,\theta_1') S_2(\lambda,\theta_2)]$$
$$= 2 \pm [E(\theta_1',\theta_2') + E(\theta_1',\theta_2)].$$

Finally, we obtain the Bell inequality

$$|B| \leq 2 \tag{4.4.4}$$

with

$$|B| = E(\theta_1,\theta_2) - E(\theta_1,\theta_2') + E(\theta_1',\theta_2') + E(\theta_1',\theta_2).$$

This particular Bell inequality is known as the Clauser–Horne–Shimony–Holt (CHSH) inequality. It is worthy to mention that there are states of the field which violate the inequality (4.4.4). However,if state of the field can be represented by a positive, normalisable Glauber–Sudarshan P-representation, no violation of this inequality is possible. For simplicity, we leave the demon-

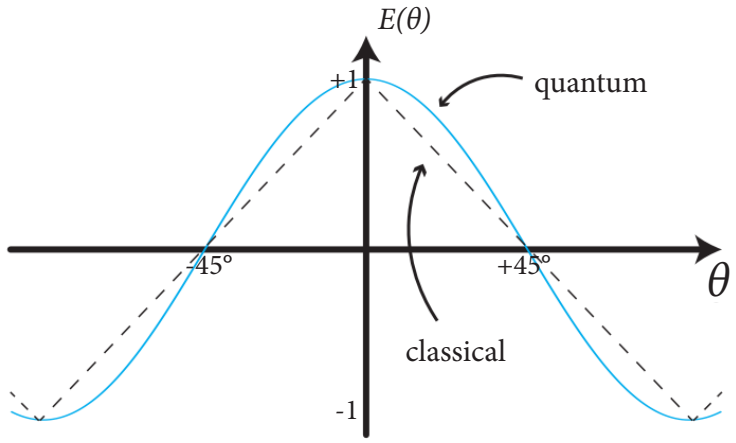

Figure 6: Comparison of the correlation of polarisations as a function of the relative angle of the polarisation analysers. Quantum mechanical prediction against classical one. For ideal polarisers the curves would reach the values ±1.

stration of this to [35]. The correlation function $E(\theta_1,\theta_2)$ may be evaluated directly for the Bell's state using Eq.(4.4.1). One finds,

$$E(\theta_1,\theta_2) = \cos 2\psi$$

where

$$\psi \equiv \theta_1 - \theta_2.$$

In this sense, if we choose

$$\psi = \theta_2 - \theta_1 = \theta_1' - \theta_2 = \theta_1' - \theta_2' = \frac{1}{3}(\theta_1 - \theta_2'),$$

we end with

$$B = 3\cos 2\psi - \cos 6\psi.$$

When $\psi = 22.5^\circ$, $B = 2\sqrt{2}$ showing showing a clear violation of the Bell inequality $|B| \leq 2$. This violation has convincingly been demonstrated in the experiment of Aspect [68]. In this experiment the polarisation analysers were essentially beam splittters with polarisation-dependent transmittivity. Ideally, one would like to have the transmittivity (T^+) for the modes a_+ and b_+ equal to one, and the reflectivity (R^-) for the modes a_- and b_- also equal to one. However, in the experiment the measured values were $T_1^+ = R_1^- = 0.950$, $T_1^- = R_1^+ = 0.007$ and $T_2^+ = T_2^- = 0.930$, $T_2^- = R_2^+ = 0.007$. The observed value was 2.697 ± 0.015, in quite good agreement with quantum theory and a clear violation of the Bell inequality. The above Fig.(6) shows a plot of the theoretical and experimental results as a function of ψ.

5 Optomechanical Systems

In optomechanical systems, an electromagnetic field is used for the measurement and control of one or more mechanical resonators. This field is usually confined within a cavity, providing resonant enhancement of the field strength and sensitivity to mechanical displacements. The coupling with the mechanical oscillator can be done in different ways, such as through the effects of radiation pressure, optical gradient forces, the Doppler effect, or photothermal forces.
Radiation pressure is a scattering force that arises due to the reflection of light, owing to the momentum associated with it. Optical gradient forces (also known as dipole forces) arise from the spatial variation of optical intensity. The Doppler effect is typically very weak [94], requiring a mirror with a strong dependence of reflectivity on wavelength [95]. Further, photothermal effects, arising from temperature gradients induced by the uneven absorption of light, are inherently dissipative [96]. In the following we shall focus on radiation pressure, following also the mathematical treatment in [42, 97, 25, 37, 11].
We shall begin by deriving the full interaction Hamiltonian for dispersive optomechanics within an optical cavity, and we then examine the dynamics of dispersive optomechanics. We then derive the linearised optomechanical Hamiltonian and finally introduce quantum optomechanical parameters.

5.1 Basic radiation pressure interaction

Radiation pressure was first demonstrated experimentally over one hundred years ago [3, 2]. The static effect of radiation pressure on an optomechanical cavity is bistability [98]. The dynamic effect of radiation pressure, associated with a finite cavity lifetime, is a frequency shift and modified damping of the mechanical resonator [99, 100, 16].
At its most basic level, the radiation pressure interaction between light and matter involves an exchange of momentum between light and a mechanical degree of freedom. Before examining this interaction in detail, it is worthwhile to consider the basic example of a single photon reflecting from the mirrored surface of a mechanical harmonic oscillator. The impact of the photon on the oscillator will cause a momentum kick which will start oscillating. From a quantum perspective, the regime in which the maximum displacement of the oscillator is larger than its zero-point motion $x_{zp} = (\hbar/2m\omega_m)^{1/2}$ is clearly interesting. Since the momentum of a photon with wavelength λ is $\hbar/\lambda$, in the simple case where the photon reflects from the mechanical oscillator, it imparts a $2\hbar/\lambda$ momentum kick to the oscillator. After a quarter period this momentum kick results in a displacement of $\Delta q = 2\hbar/\lambda m\omega_m = 8\pi x_{zp}^2/\lambda$. Therefore, we arrive immediately at the condition

$$\frac{x_{zp}}{\lambda} > \frac{1}{8\pi}$$

for the recoil to exceed the oscillator zero-point motion. Notice that the latter equation is only intended to give a rough indication of a regime where quantum mechanics plays a role in the interaction between a field and a mechanical oscillator. A more rigorous treatment would include additional constraints, and it should be recognized that, for a high-quality mechanical oscillator, measurements should be made over many cycles of the oscillator rather than just one.

5.2 Quantisation

We have introduced the idea that quantum mechanics can play a significant role in the interaction between light and a macroscopic material object. Usually, we treat the mechanical displacement in terms of a simple scalar displacement field $u(\mathbf{x}, t)$, where $\mathbf{x}$ labels a point in the space. Typically

the interaction is elastic and the displacement field obeys a linear wave equation. In that case, we expand the scalar field in terms of harmonic modes

$$u(\mathbf{x},t) = \sum_k \alpha_k(t)\phi_k(\mathbf{x}) + \alpha_k^*(t)\phi_k(\mathbf{x})$$

where $\phi_k(\mathbf{x})$ are a suitable set of spatial mode functions. The amplitudes $\alpha_k(t)$ obey equations of motion equivalent to those of independent harmonic oscillators

$$\dot{\alpha}_k(t) = -i\omega_k\alpha_k(t).$$

In passing to the quantum description, we simply replace each of these harmonic oscillators with a quantum harmonic oscillator using

$$\alpha_k(t) \to \hat{a}_k(t)$$
$$\alpha_k^*(t) \to \hat{a}_k^\dagger(t)$$

with canonical commutation relations $[\hat{a}_k(t), \hat{a}_k'^\dagger(t)] = \delta_{k,k'}$. In most cases, we can restrict the discussion to the response of a single mode a_0 with frequency ω_0. As usual, we may introduce canonical position and momentum operators for this mode by

$$\hat{q} = \sqrt{\frac{\hbar}{2m_0\omega_0}}(a_0 + a_0^\dagger)$$
$$\hat{p} = -i\sqrt{\frac{\hbar m_0\omega_0}{2}}(a_0 - a_0^\dagger)$$

where m_0 is the effective mass of this particular harmonic mode.

5.3 Dispersive optomechanics (Fabry–Pérot cavity)

In dispersive optomechanics, the position of the mechanical oscillator is parametrically coupled to the resonance frequency of an optical cavity or microwave resonator. Radiation pressure imparted by the optical or microwave field allows the motion of the oscillator to be controlled, while the field leaving the cavity or resonator carries information about the resonance frequency and therefore the mechanical position. The interaction Hamiltonian describing the parametric interaction between the mechanical oscillator and the field can be easily established by considering the change in optical cavity[4] resonance frequency of a Fabry–Pérot cavity induced by a change in mechanical position.

In this way, let us consider a Fabry–Pérot cavity of bare length L with one end mirror forming part of a mechanical oscillator, as shown in Fig.(7). The motion of the mechanical oscillator shifts the length of the cavity with $L(q) = L - q$, where q is the displacement of the mechanical oscillator away from its equilibrium position and the minus sign is arbitrary, defining only the positive direction of mechanical motion. In a Fabry–Pérot cavity of length $L(q)$, the longitudinal optical modes have wavelengths

$$\lambda_j = \frac{2(L-q)}{j},$$

[4]Note that in this chapter we will discuss the physics of cavity optomechanical systems concerning optical cavities. However, it should be kept in mind that the physics is equally applicable to microwave resonators.

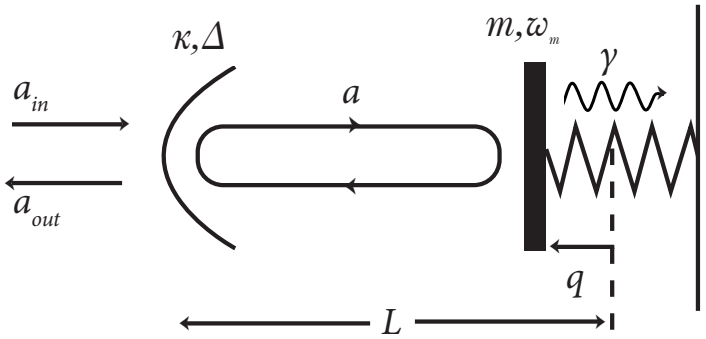

Figure 7: Representation of a canonical cavity optomechanical system. κ and L, are the cavity decay rate and bare length, respectively; while m, ω_m, and γ are respectively the effective mass, resonance frequency, and damping rate of the mechanical oscillator. a and $\hat{q}$ are the annihilation operator for the cavity field and the position operator for the mechanical oscillator, respectively; and a_{in} and a_{out} are the annihilation operators for the incident and output fields.

where j is the mode number. The mode frequencies are therefore

$$\omega_{c,j}(q) = \frac{2\pi c}{\lambda_j} = \frac{\pi c j}{L - q} \approx \omega_{c,j}(1 + \frac{q}{L})$$

where the approximation is valid as long as $q \ll L$, which is appropriate for the vast majority of cavity optomechanical systems, c is the speed of light, and $\omega_{c,j} \equiv \omega_{c,j}(0)$ is the bare optical resonance frequency of the cavity, with the subscript c used to label the cavity's resonance frequency. We see that the motion of the mechanical oscillator acts to linearly shift the optical resonance frequency. The frequency shift per meter is quantified by the optomechanical coupling strength G

$$\begin{aligned} G &\equiv \frac{\delta\omega_c(q)}{\delta q} \\ &= \frac{\omega_c}{L} \quad \text{(Fabry-Pérot cavity)} \end{aligned} \tag{5.3.1}$$

where we have omitted the mode number subscript j.
We can now proceed to the description of the interaction between the cavity field and the mechanical element. The energy of the light in a particular cavity mode is given by the energy per quantum, $\hbar\omega_c$, times the number, $\hat{n}(t)$, of photons in the cavity

$$H_c = \hbar\omega_c(q)\hat{n}$$

where we have explicitly included the dependence of the cavity frequency on the displacement of the mechanical oscillator. In the absence of the radiation pressure interaction, the energy of the mechanical oscillator is

$$H_m = \frac{p^2}{2m} + \frac{m\omega_m^2}{2}q^2,$$

where ω_m denotes the resonance frequency of the mechanical oscillator, and p and m are its momentum and mass, respectively. The total classical Hamiltonian is $H = H_c + H_m$.

The quantum description of the system is then given by replacing the classical variables with the corresponding operators $q \to \hat{q}$, $p \to \hat{p}$, $n \to a^\dagger a$ which satisfy the canonical commutation relations. The quantum optomechanical Hamiltonian is then

$$\hat{H} = \frac{\hat{p}^2}{2m} + \frac{m\omega_m^2}{2}\hat{q}^2 + \hbar\omega_c(\hat{q})a^\dagger a. \tag{5.3.2}$$

Introducing the raising and lowering operators for the mechanical excitations as $b^\dagger$ and b, which also satisfy the Boson commutation relation, enables us to write

$$\begin{aligned}\hat{H} &= \hbar(\omega_c + G\hat{q})a^\dagger a + \hbar\omega_m b^\dagger b \\ &= \hbar\omega_c a^\dagger a + \hbar\omega_m b^\dagger b + \hbar g_0 a^\dagger a(b^\dagger + b),\end{aligned} \tag{5.3.3}$$

where to arrive at Eq.(5.3.3) we have used the definition $\hat{q} = x_{zp}(b^\dagger + b)$, and we have defined the vacuum optomechanical coupling rate

$$g_0 \equiv G x_{zp}$$

which has units of $[s^{-1}]$. The single-photon optomechanical coupling rate, g_0, is one of the central parameters in the field of quantum optomechanics. It can be interpreted as the optical frequency shift induced by a mechanical displacement equal to the mechanical zero-point motion. Conversely, the radiation pressure from a single photon within the cavity acts to displace the mechanical oscillator. The ratio g_0/ω_m quantifies this displacement in units of the mechanical zero-point motion. Throughout the entire work we will use the annihilation operators a and b, respectively, for the cavity field and mechanical oscillator, and position and momentum operators $\hat{p}$ and $\hat{q}$ for the mechanical oscillator.
In the majority of cavity optomechanics experiments, since the optical cavity (or microwave resonator) resonance frequency ω_c is much larger than all other system rates, a situation commonly encountered is where the cavity is strongly driven to some large coherent amplitude $\alpha \equiv \langle a \rangle$.
For now, suppose that the cavity is driven at a frequency ω_p, detuned from the cavity resonance frequency. It is convenient to move into a rotating frame at the incident ω_p, and thereby remove the fast oscillations of the optical field. In this way, we can transform the terms in Eq.(5.3.3), with the result

$$\hat{H} = -\hbar\Delta a^\dagger a + \hbar\omega_m b^\dagger b + \hbar g_0 a^\dagger a(b^\dagger + b), \tag{5.3.4}$$

where here a is now in the rotating frame, and we have defined the detuning Δ between the optical cavity and the incident pump frequency as

$$\Delta \equiv \omega_p - \omega_c.$$

We shall keep in mind this form of the optomechanical Hamiltonian, as it will be at the center of our calculations in further sections.

5.4 Linearisation of optomechanical Hamiltonian

Let us make a small step back from Eq.(5.3.4), and take again the general optomechanical Hamiltonian

$$\hat{H} = \hbar\omega_c a^\dagger a + \hbar\omega_m b^\dagger b + \hbar g_0 a^\dagger a(b^\dagger + b).$$

Starting from here, we can write down the QLEs for the cavity and the mechanical mode,

$$\dot{a}(t) = -i\omega_c a - ig_0 a(b^\dagger + b) - \frac{\kappa}{2}a + \sqrt{\kappa}a_{\text{in}} \tag{5.4.1}$$

$$\dot{b}(t) = -i\omega_m b - \frac{\gamma}{2}b + \sqrt{\gamma}b_{\text{in}} - ig_0 a^\dagger a \tag{5.4.2}$$

where we have taken κ as external dissipation for our cavity, γ as dissipative constant of the mechanical resonator, and for simplicity of calculus we set $\hbar = 1$.
We can now expand, up to the first order, the cavity and the mechanical modes

$$a(t) = \alpha_0(t) + \delta a$$
$$b(t) = \beta_0(t) + \delta b.$$

This leads us to write down our equation (for the moment) up to zero order:

$$\dot{\alpha}_0(t) = -i\omega_c\alpha_0(t) - ig_0\alpha_0(t)(\beta_0^* + \beta_0) - \frac{\kappa}{2}\alpha_0(t) + \sqrt{\kappa}a_{\text{in}}$$
$$\dot{\beta}_0(t) = -i\omega_m\beta_0(t) - \frac{\gamma}{2}\beta_0(t) - ig_0|\alpha_0(t)|^2 + \sqrt{\gamma}b_{\text{in}}.$$

Furthermore, to manipulate the equation of motion for α_0, we can switch to an interaction picture that rotates with ω_p, meaning that $\alpha_0(t) = \alpha_{I,0}e^{-i\omega_p t}$. For simplicity, we just drop out the I-index. In this way, we obtain

$$\dot{\alpha}_0(t) + i(\omega_c - \omega_p)\alpha_0(t) = -ig_0\alpha_0(t)(\beta_0^* + \beta_0) - \frac{\kappa}{2}\alpha_0(t) + \sqrt{\kappa}a_{\text{in}}$$
$$\dot{\beta}_0(t) = -i\omega_m\beta_0(t) - \frac{\gamma}{2}\beta_0(t) - ig_0|\alpha_0(t)|^2 + \sqrt{\gamma}b_{\text{in}}$$

by calling $\Delta := \omega_p - \omega_c$, the latter can be recast as

$$\dot{\alpha}_0(t) - i\Delta\alpha_0(t) + ig_0\alpha_0(t)(\beta_0^* + \beta_0) + \frac{\kappa}{2}\alpha_0(t) = \sqrt{\kappa}a_{\text{in}}$$
$$\dot{\beta}_0(t) = -i\omega_m\beta_0(t) - \frac{\gamma}{2}\beta_0(t) - ig_0|\alpha_0(t)|^2 + \sqrt{\gamma}b_{in}.$$

At this point, we can impose stationary conditions $\dot{\alpha}_0(t) = 0$, $\dot{\beta}_0(t) = 0$, to find out

$$\alpha_0 = \frac{\sqrt{\kappa}}{-i\Delta + ig_0(\beta_0^* + \beta_0) + \frac{\kappa}{2}}a_{\text{in}} \tag{5.4.3}$$

$$\beta_0 = \frac{\sqrt{\gamma}}{i\omega_m + \frac{\gamma}{2}\beta_0 + ig_0|\alpha_0|^2}b_{\text{in}} \tag{5.4.4}$$

Now, we plug them into the previous ones and rewrite them up to the first order including also the deviations, keeping in mind $\dot{\alpha}_0(t) = 0, \dot{\beta}_0 = 0$. We end up with

$$\delta\dot{a}(t) = -i\omega_c\delta a - \frac{\kappa}{2}\delta a - ig_0\alpha_0(t)(\delta b^* + \delta b) - ig_0\delta a(\beta_0^* + \beta_0) + \sqrt{\kappa_e}\delta a_{in,e} + \sqrt{\kappa}\delta a_{\text{in}} \tag{5.4.5}$$

$$\delta\dot{b}(t) = -i\omega_m\delta b - \frac{\gamma}{2}\delta b - ig_0\left[\alpha_0(t)\delta a^* + \alpha_0^*(t)\delta a\right] + \sqrt{\gamma}\delta b_{\text{in}}. \tag{5.4.6}$$

We are left with some choices to make to extrapolate some physics out of our last equations. First of all, we can consider two types of reference systems, respectively for the cavity and the

mechanical resonator. We thus choose a frame that oscillates at ω_c for the optical cavity, while another one that oscillates at ω_m for the mechanical resonator. In this sense, we named:

$$\delta a \longrightarrow a$$
$$\delta b \longrightarrow b,$$

and our equations become:

$$\dot{a}(t) = -i\omega_c a - \frac{\kappa}{2}a + \sqrt{\kappa}a_{\text{in}} - ig_0\alpha_0 e^{-i\omega_p t}(b^\dagger + b) \tag{5.4.7}$$

$$\dot{b}(t) = -i\omega_m b - \frac{\gamma}{2}b + \sqrt{\gamma}b_{\text{in}} - ig_0[\alpha_0 a^\dagger + \alpha_0^* a]. \tag{5.4.8}$$

Let us first focus on the frame that rotates with ω_c for the optical cavity. In this picture, we will have $a = a_I e^{-i\omega_c t}$, where the index stems from the interaction frame. From now on, we will drop it. Our (5.4.7) will thus be

$$\dot{a}(t) = -\frac{\kappa}{2}a + \sqrt{\kappa}a_{\text{in}} - ig_0\alpha_0 e^{i(\omega_c-\omega_p)t}(b^\dagger + b),$$

and using $\Delta = \omega_p - \omega_c$, $b = b_I e^{-i\omega_m t}$ we obtain

$$\dot{a}(t) = -\frac{\kappa}{2}a + \sqrt{\kappa}a_{\text{in}} - ig_0\alpha_0 e^{-i\Delta t}(b^\dagger e^{i\omega_m t} + be^{-i\omega_m t}). \tag{5.4.9}$$

We can notice that in our expression we have terms like

$$b^\dagger e^{-it(\Delta-\omega_m)}$$
$$be^{-it(\Delta+\omega_m)},$$

which when $\Delta \simeq \omega_m$ (i.e.$\omega_p \simeq \omega_c+\omega_m$) allow us to cancel out the term $be^{-it(\Delta+\omega_m)}$ by Rotating Wave Approximation. On the other hand, when $\Delta \simeq -\omega_m$ (i.e. $\omega_p \simeq \omega_c - \omega_m$) we can get rid of the term $b^\dagger e^{-it(\Delta-\omega_m)}$, always by RWA.
The same procedure can be applied to the mechanical mode, focusing on the frame that rotates with ω_m. In this case, we find out

$$\dot{b}(t) = -\frac{\gamma}{2}b + \sqrt{\gamma}b_{\text{in}} - ig_0\left[\alpha_0 a^\dagger e^{-it(\Delta-\omega_m)} + \alpha_0^* a e^{it(\Delta+\omega_m)}\right]. \tag{5.4.10}$$

Analogously, we can distinguish the two cases depending on Δ:

- when $\Delta \simeq \omega_m$ the term $\alpha_0^* a e^{it(\Delta+\omega_m)}$ will be the one suppressed by RWA;

- when $\Delta \simeq -\omega_m$ the term $\alpha_0 a^\dagger e^{-it(\Delta-\omega_m)}$ will be the one suppressed by RWA.

At this point, we can collect our equations depending on the choice of Δ. When $\Delta \simeq \omega_m$ our equations motion will be of the form of

$$\dot{a}(t) = -\frac{\kappa}{2}a + \sqrt{\kappa}a_{\text{in}} - ig_0\alpha_0 b^\dagger \tag{5.4.11}$$

$$\dot{b}(t) = -\frac{\gamma}{2}b + \sqrt{\gamma}b_{\text{in}} - ig_0\alpha_0 a^\dagger, \tag{5.4.12}$$

and when $\Delta \simeq -\omega_m$

$$\dot{a}(t) = -\frac{\kappa}{2}a + \sqrt{\kappa}a_{\text{in}} - ig_0\alpha_0 b \tag{5.4.13}$$

$$\dot{b}(t) = -\frac{\gamma}{2}b + \sqrt{\gamma}b_{\text{in}} - ig_0\alpha_0^* a. \tag{5.4.14}$$

We have now obtained two sets of linearized equations of motion, depending on the detuning parameter Δ. The particular choice of Δ, as we can see, can give rise to two very distinct cases of fundamental importance in the study of optomechanical systems. Indeed, Eqs.(5.4.11) and (5.4.12) are referred as the blue detuning case. They could be thought as generated by $\mathcal{H}_{\mathcal{B}} = \hbar g(a^\dagger b^\dagger + ab)$, also called down-conversion Hamiltonian, with the linearised optomechanical coupling rate $g = -g_0\alpha_0$ measuring the strength of the coupling in this regime. On the other hand, Eqs.(5.4.13) and (5.4.14) are known as the the red detuning case, where the generating Hamiltonian is of the kind $\mathcal{H}_{\mathcal{R}} = \hbar g(a^\dagger b + ab^\dagger)$, also called beam splitter Hamiltonian.
In this way, we can rewrite our full linearized Hamiltonian as:

$$\hat{H} = -\hbar\Delta a^\dagger a + \hbar\omega_m b^\dagger b + \hbar g(a + a^\dagger)(b + b^\dagger). \tag{5.4.15}$$

Hamiltonian (5.4.15) will be the starting point in Chapter 7, in particular, using RWA, we will solve the equations of motion in the two cases. To do it, we will work into the Fourier space, and we will thus see the consequences of doing blue/red detuning to our optomechanical system.

5.5 Consequences of the Optomechanical Interaction

As an introduction for further sections, it is now convenient to introduce useful regimes in which we work with our optomechanical parameters. These regimes, called resolved sideband, large cooperativity, and strong coupling regime, can be summarised as follows:

- Resolved sideband regime when $\omega_m \gg \kappa$;
- Large cooperativity regime when the cooperativity $C = \frac{4g^2}{\gamma\kappa} \gg 1$;
- Strong coupling regime when $g \gg \gamma, \kappa$.

The first two are the most used to implement RWA to cool down the mechanical motion, down to its ground state, while the last one is the source of normal mode splitting. Both phenomena will be exhaustively treated in Sec. 6.1.1-6.1.2.

5.5.1 Standard Quantum Limit

To better understand these latter regimes, is worthwhile to explore which are the basic consequences of the optomechanical interaction. To do this, we follow what has been done by Bowen & Milburn [42].
Our aim is to describe the linearised interaction between light and a mechanical oscillator in a cavity optomechanical system, and quantify how the optical output field can be used to monitor the quantum state of the mechanics. Our purpose is to show that continuous measurement results in a quantum back-action that heats the mechanical oscillator and introduces a standard quantum limit on the accuracy of the measurement itself. Before introducing the effects of quantum measurement on the dynamics of the optomechanical systems, it is illustrative to consider

the simple example of quantum measurement of the position of a free mass.
Specifically, we wish to determine the position of the mass after some time τ by performing two sequential position measurements and we are interested in the effect of measurement back-action on the precision [101, 102, 103, 104]. This is a scenario [105, 106, 107] that is relevant, for example, in interferometric gravitational wave observatories that seek to observe ripples in space-time via the length changes that they induce in an interferometer. If the initial measurement localizes the position of the mass with a standard deviation $\sigma[\hat{q}(0)]$, the Heisenberg uncertainty principle tells us that the measurement must also introduce quantum back-action on the momentum of the oscillator, increasing its uncertainty to at least

$$\sigma[\hat{p}(0)] = \frac{\hbar}{2\sigma[\hat{q}(0)]}.$$

The mass will then freely evolve until the second measurement is performed at time τ. This evolution is, of course, governed by the free-particle Hamiltonian

$$\hat{H} = \frac{\hat{p}^2}{2m},$$

which yields the evolution

$$\hat{q}(\tau) = \hat{q}(0) + \frac{\tau}{m}\hat{p}(0).$$

In this way, the uncertainty in the measurement outcome is then entirely specified

$$\begin{aligned}\sigma^2[\hat{q}(\tau)] &= \sigma^2[\hat{q}(0) + \frac{\tau}{m}\hat{p}(0)] \\ &= \sigma^2[\hat{q}(0)] + \left(\frac{\tau}{m}\right)^2 \sigma^2[\hat{p}(0)] \\ &= \sigma^2[\hat{q}(0)] + \left(\frac{\hbar\tau}{2m}\right)^2 \frac{1}{\sigma^2[\hat{q}(0)]}.\end{aligned}$$

Here, by simply taking the sum of the uncertainty contributions from the position and momentum, we are assuming that the position and momentum of the mass are not correlated after the first measurement [5]. Indeed, no such correlations can exist if the mass is in a minimum uncertainty state, as described by $\sigma[\hat{p}(0)] = \frac{\hbar}{2\sigma[\hat{q}(0)]}$. The regime in which this assumption breaks down is interesting and can allow improved measurement precision. Since the last equation contains terms that scale both as $\sigma^2[\hat{q}(0)]$ and as $\sigma^{-2}[\hat{q}(0)]$, it is clear that an optimal measurement is the one that maximizes the accuracy of the measurement. It is straightforward to show that this optimum is

$$\sigma_{\mathrm{sql}}[\hat{q}(0)] = \sqrt{\frac{\hbar\tau}{2m}},$$

which leads us to a standard quantum limit for position measurement of a free mass

$$\sigma_{\mathrm{sql}}[\hat{q}(\tau)] = \sqrt{\frac{\hbar\tau}{m}}.$$

We see therefore that the presence of quantum measurement back-action provides a fundamental limit to the precision of position measurements. To make an example, since gravitational waves cause an oscillation in the relative length of the two arms of an interferometer, a differential position measurement is most sensitive to them if the first measurement is made when one arm of the interferometer is fully extended and the second is made when it is fully contracted.

[5] Specifically, $\langle\hat{q}(0)\hat{p}(0) + \hat{p}(0)\hat{q}(0)\rangle - 2\langle\hat{p}(0)\rangle\langle\hat{q}(0)\rangle = 0$.

5.5.2 Radiation pressure shot noise

We can now consider the effect of fluctuations in radiation pressure due to optical shot noise on the dynamics of a mechanical oscillator. This radiation pressure shot noise is the unavoidable quantum back-action on the oscillator. In general, shot noise is a type of noise which can be modeled by a Poisson process distribution. In optics, shot noise describes the fluctuations of the number of photons detected due to their occurrence independent of each other. This is therefore a consequence of discretization of the energy in the electromagnetic field in terms of photons. As we have seen in Chapter 3, in the case of photon detection, the relevant process is the random conversion of photons into photo-electrons, where only for squeezed state the number of photons measured, per unit time, can have fluctuations smaller than the square root of the expected number of photons counted in that period of time. Of course there are other mechanisms of noise in optical signals which often dwarf the contribution of shot noise. When these are absent, however, optical detection is said to be "photon noise limited" as only the shot noise (also known as "quantum noise") remains. In this case, the fluctuations in a photo-current scale as the square-root of the average intensity:

$$(\Delta I_{\rm ph})^2 := \langle (I_{\rm ph} - \langle I_{\rm ph}\rangle)^2\rangle \propto I_{\rm ph}.$$

In optical homodyne detection, the shot noise in the photodetector can be attributed to either the zero point fluctuations of the quantised electromagnetic field, or to the discrete nature of the photon absorption process [108]. However, shot noise itself is not a distinctive feature of quantised field and can also be explained through semiclassical theory. Shot noise also sets a lower bound on the noise introduced by quantum amplifiers which preserve the phase of an optical signal.
Throughout our discussion, we consider only the linearized dynamics of the optomechanical system (as discussed in Section 5.4). We therefore take the Markovian limit where the bath has no memory, for both the optical field and the mechanical oscillator, and make the Rotating Wave Approximation on the optical field, taking the cavity resonance frequency to be much higher than any other rates in the problem. In this regime, linearised equations of motion for the mechanical oscillator and optical field can be derived from the Hamiltonian of Eq.(5.4.15), using the Quantum Langevin Equations. The resulting equations of motion are

$$\begin{aligned}
\dot{\hat{X}} &= -\frac{\kappa}{2}\hat{X} + \sqrt{\kappa}\hat{X}_{\rm in} \\
\dot{\hat{Y}} &= -\frac{\kappa}{2}\hat{Y} + \sqrt{\kappa}Y_{\rm in} + -2g\hat{Q} \\
\dot{\hat{Q}} &= \omega_m \hat{P} \\
\dot{\hat{P}} &= -\omega_m \hat{Q} + \gamma\hat{P} + \sqrt{2}\gamma\hat{P}_{\rm in} - 2g\hat{X},
\end{aligned}$$

where we have taken the case of on-resonance optical driving ($\Delta = 0$) for simplicity, and we remind that throughout this work $\hat{X}$ and $\hat{Y}$ refer to the optical amplitude and phase quadratures, $\hat{Q}$ and $\hat{P}$ refer to the dimensionless mechanical position and mechanical momentum, κ and γ are optical and mechanical decay rates and g is the optomechanical coupling rate. On the other hand, the non-zero detuning case, as we will see in the next chapter, is also very interesting and allows for cooling and entanglement. Because we have chosen to drive the optical cavity on resonance ($\Delta = 0$), the quantum stochastic equations describing the optical amplitude and phase quadratures are independent. This is not the case for the mechanical oscillator, where the last two equations are easily combined into a single second-order differential equation

$$\ddot{\hat{Q}} + \gamma\dot{\hat{Q}} + \omega_m^2\hat{Q} = \sqrt{2\gamma}\omega_m\hat{P}_{\rm in} - 2g\omega_m\hat{X}.$$

This linear system of equations can then be solved directly in the frequency domain. Taking the Fourier transform, we obtain the steady-state solutions

$$\hat{X}(\omega) = \frac{\sqrt{\kappa}\hat{X}_{\text{in}}}{\kappa/2 - i\omega} \tag{5.5.1}$$

$$\hat{Y}(\omega) = \frac{\sqrt{\kappa}\hat{Y}_{\text{in}} - 2g\hat{Q}}{\kappa/2 - i\omega} \tag{5.5.2}$$

$$\hat{Q}(\omega) = \chi(\omega)\left(\sqrt{2\gamma}\hat{P}_{\text{in}} - 2g\hat{X}\right) \tag{5.5.3}$$

where we have defined the mechanical susceptibility as $\chi(\omega) \equiv \omega_m/(\omega_m^2 - \omega^2 - i\omega\gamma)$. Substituting Eq.(5.5.1) for the optical amplitude quadrature into Eq.(5.5.3), we arrive at the expression for the mechanical position

$$\hat{Q}(\omega) = \sqrt{2\gamma}\chi(\omega)\left(\hat{P}_{\text{in}} - \sqrt{2C_{\text{eff}}}\hat{X}_{\text{in}}\right),$$

where we have introduced the *effective optomechanical cooperativity*

$$C_{\text{eff}}(\omega) \equiv \frac{C}{(1 - 2i\omega/\kappa)^2}$$

with C being the *optomechanical cooperativity*

$$C \equiv \frac{4g^2}{\kappa\gamma}.$$

As we have just seen, the radiation pressure interaction perturbs the motion of a mechanical oscillator, introducing noise. This noise can be understood to be a direct consequence of the Heisenberg uncertainty principle between position and momentum. The interaction encodes position information on the optical field, leading to an increase in noise on the mechanical momentum.
Furthermore, we notice that, through radiation pressure, the optical shot noise contributes a heating term to the mechanical oscillator dynamics, with magnitude dependent on the effective optomechanical cooperativity. We see that this heating is attenuated at frequencies above the cavity linewidth ($\omega > \kappa$) since the incident optical fluctuations at these frequencies are off-resonance and therefore partially screened by the cavity. Particularly in the resolved sideband regime where $\omega_m \gg \kappa$ this attenuation has the effect of reducing the optomechanical interaction strength. Radiation pressure effects are widely seen in experiments with cold atomic gases. For instance, the radiation pressure back-action heating was first observed only in 2008 [109], in that case using a collective mechanical mode of a cloud of 9,000 ultracold atoms. In 2013 radiation pressure shot noise was observed for the first time for a mechanical resonance of a macroscopic mechanical oscillator using a 7 ng silicon nitride membrane [110].

6 Interaction phenomena between light and mechanics: cooling and amplification

In the previous chapter, we examined the linearised radiation pressure interaction between the optical field and mechanical oscillator in a cavity optomechanical system in the case that the optical cavity is coherently driven on resonance ($\Delta = 0$). In this chapter, we introduce radiation pressure coherent coupling between light and a mechanical oscillator, that occurs when an optical detuning is introduced. We discuss effects such as resolved sideband cooling, normal mode splitting, amplification, optomechanical entanglement between a cavity and mechanical oscillator, and also mechanical squeezing that arise from this coherent interaction.
We have previously seen how on-resonance ($\Delta = 0$) optical probing of mechanical motion showed that radiation pressure shot noise heats the mechanical oscillator. This back-action heating is a consequence of the fact that information about the mechanical motion is imprinted on the phase of the optical field, and is necessary to ensure that the Heisenberg uncertainty principle is not violated. However, the presence of back-action heating does not necessarily preclude an overall optical cooling effect on the mechanical oscillator. Indeed such a cooling mechanism can arise when a non-zero detuning ($\Delta \neq 0$) is introduced, and it is based on dynamical back-action. The essential idea is that, when the optical cavity is detuned, the mechanical position is imprinted on the amplitude of the optical field which then back-acts through radiation pressure upon the mechanical oscillator. Since the cavity also induces a delay in the optical response, this dynamical back-action is retarded, with a component of the optical force being proportional to the velocity of the mechanical oscillator. Depending on the sign of this component, it either damps/cools or amplifies/heats the mechanical motion [99, 111].
An alternative approach to understanding optomechanical cooling, is via an energy level diagram, as shown in Fig.(8). Here we observe that downwards going phonon number transitions are resonantly enhanced when the optical driving tone is red detuned, while upwards going transitions are enhanced by blue detuning. We will see that these two operations can be thought of, respectively, as beam splitting and down-conversion operations between the light and mechanical oscillator, with the former allowing cooling while the latter can be used to generate optomechanical entanglement.
Furthermore, we mention that optomechanical coupling between a moving mirror and the radiation pressure of light first appeared in the context of interferometric gravitational wave experiments. The pioneering work of V.Braginsky [112] predicted that the radiation pressure of light, confined within an interferometer (or resonator), gives rise to the effect of dynamic back-action. The resulting phenomena, which are the mechanical amplification and optomechanical back-action cooling, represent two sides of the same underlying "dynamic back-action" mechanism. In the following analysis of this mechanism, we attend to the same notation and derivation of the work done in [42, 97, 25, 111].

6.1 Red detuning: optomechanical cooling of mechanical motion

The optical field can be thought of as a thermal bath for the mechanical oscillator in a cavity optomechanical system, with radiation pressure shot noise introducing a random driving force. We know, from the quantum fluctuation-dissipation theorem, that the temperature of a quantum oscillator, that is linearly forced by a bath, is governed by the ratio of bath power spectral densities [35]

$$\frac{S_{FF}(\omega_m)}{S_{FF}(-\omega_m)} = \exp\left\{\frac{\hbar\omega_m}{k_B T}\right\}. \tag{6.1.1}$$

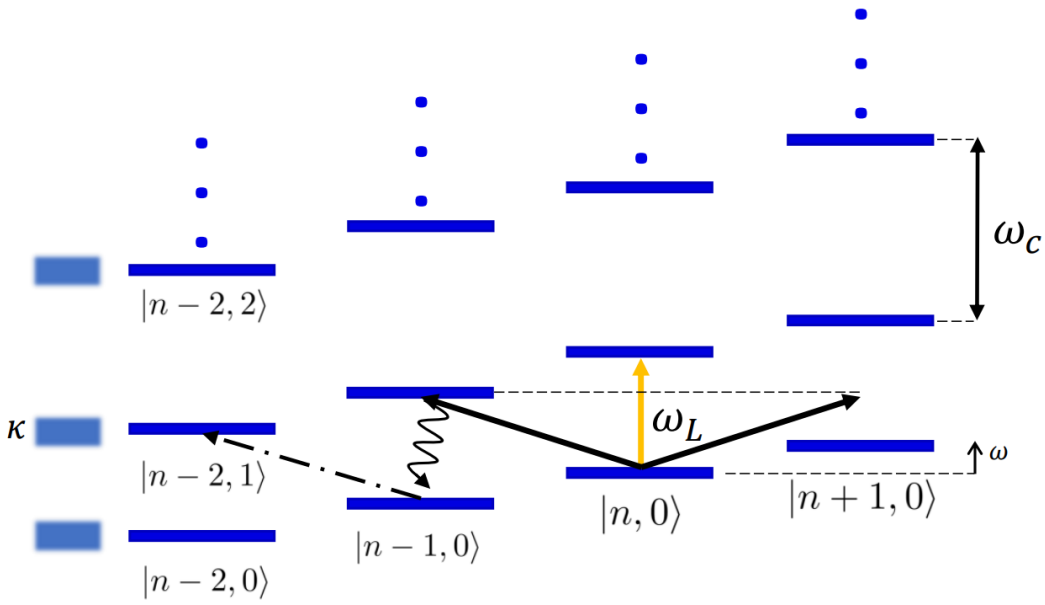

Figure 8: Energy level diagram for (optical) cooling of mechanical motion. $|n,m\rangle$: n-phonon, m-photon state. ω_c: cavity resonance frequency, ω_L: laser resonance frequency. Three processes can be distinguished. First, a photon can be absorbed by the cavity leaving the states unchanged (carrier transitions). Second, the photon can create a phonon (corresponding to absorption on the upper motional sideband). Third, the photon leads to the annihilation of a phonon (corresponding to a photon being absorbed by the lower motional sideband). Appropriate red detuning of the laser can lead to effective suppression of the first two processes and efficient cooling.

This relationship provides an elegant approach to determining the effect of the optical field on the temperature of the oscillator, as first observed in [113].
To understand the effect of the optical field on the temperature of the mechanical oscillator, it is useful to consider first the zero dissipation case of the mechanical oscillator ($\gamma \to 0$), or where, at least, the heating from the optical field dominates the heating from the mechanical bath [6]. In this case, the optical force makes the only significant contribution. We can find the optical force $\hat{F}_c$ in a cavity optomechanical system in the linearised regime by taking the derivative of the optomechanical Hamiltonian to $\hat{q}$. Here, we use the non-linearised Hamiltonian of Eq.(5.3.3) to obtain the force

$$\hat{F}_c(t) = \frac{\partial \hat{H}}{\partial \hat{q}} = \hbar g_0 a^\dagger a.$$

The power spectral density of this force can be found from its autocorrelation function, which is given by

$$\begin{aligned}\langle \hat{F}_c(t+\tau)\hat{F}_c(t)\rangle_{t=0} &= \hbar^2 g_0^2 \langle a^\dagger(t+\tau)a^\dagger(t+\tau)a^\dagger(t)a(t)\rangle_{t=0} \\ &\approx \frac{\hbar^2 g^2}{x_{\rm zp}^2}\left[\alpha^2 + n_c + 2\langle \hat{X}(t+\tau)\hat{X}(t)\rangle_{t=0}\right],\end{aligned}$$

[6] That is, in the regime where radiation pressure shot noise dominates mechanical thermal noise.

where we have made the substitution $a \to \alpha + a$ to displace away the coherent amplitude of the cavity field, linearised the resulting expression by neglecting the term that does not contain the coherent amplitude α, substituted $\alpha g_0/x_{\rm zp} = g/x_{\rm xp}$, and used the relation $\langle a^\dagger(t)a(t)\rangle = n_c$ with n_c being the thermal occupancy of the displaced optical field. As usual, $\hat{X}$ is the amplitude quadrature of the cavity field.
We have to specify that, for an optical field in thermal equilibrium with its environment, n_c is essentially zero. Here we retain the optical occupancy explicitly, motivated both by the aim of clarifying the effect of a non-zero optical bath temperature and by the fact that, in realistic experiments, technical noise often raises the optical occupancy above its equilibrium value.
Therefore, using Eq.(2.2.4)

$$S_{\mathcal{O}\mathcal{O}}(\omega) = \int_{-\infty}^{\infty} d\tau e^{i\omega\tau} \left\langle \hat{\mathcal{O}}^\dagger(t+\tau)\hat{\mathcal{O}}(t) \right\rangle_{t=0} = \int_{-\infty}^{\infty} d\omega' \left\langle \hat{\mathcal{O}}^\dagger(-\omega)\hat{\mathcal{O}}(\omega') \right\rangle$$

the optical force power spectral density can then be directly calculated as

$$\begin{aligned} S_{F_cF_c}(\omega) &= \int_{-\infty}^{\infty} d\tau e^{i\omega\tau} \left\langle \hat{F_c}^\dagger(t+\tau)\hat{F}_c(t) \right\rangle_{t=0} \\ &= \int_{-\infty}^{\infty} d\tau e^{i\omega\tau} \frac{\hbar^2 g^2}{x_{\rm zp}^2} \left[\alpha^2 + n_c + 2\langle \hat{X}(t+\tau)\hat{X}(t)\rangle_{t=0} \right] \\ &= \frac{\hbar^2 g^2}{x_{\rm zp}^2}[(\alpha^2 + 2n_c)\delta(\omega) + 2S_{XX}(\omega)]. \end{aligned}$$

Using again Eq.(2.2.4) the power spectral density of the cavity field can be expressed in terms of frequency domain annihilation and creation operators as

$$\begin{aligned} S_{XX}(\omega) &= \int_{-\infty}^{\infty} d\omega' \langle \hat{X}^\dagger(-\omega)\hat{X}(\omega')\rangle \\ &= \frac{1}{2}\int_{-\infty}^{\infty} d\omega' \langle (a(\omega)a^\dagger(-\omega))(a^\dagger(-\omega')a(\omega'))\rangle. \end{aligned} \tag{6.1.2}$$

To find an analytical expression for this power spectral density, we must determine $a(\omega)$ and $a^\dagger(\omega)$. To do this we use the Hamiltonian of Eq.(5.3.4) in the rotating wave quantum Langevin equation. We simplify the problem by making one substantial approximation, that is the cavity optical field is not affected by the motion of the mechanical oscillator (i.e. setting $g_0 = 0$). This may seem like an unreasonable approximation, however, it is appropriate as long as the optical cavity decay rate κ is sufficiently large to remove the fluctuations introduced to the optical field by the interaction with the mechanical oscillator. We will consider the case where this is not true in the next section, where we find that the approximation is reasonable as long as κ is large enough that the optomechanical system is not operating within the strong coupling regime.
Returning to our problem, setting $g_0 = 0$ and taking the Fourier transform of the equation of motion for the cavity field, we find

$$a(\omega) = \frac{\sqrt{\kappa}}{\kappa/2 + i(\Delta - \omega)} a_{\rm in}(\omega) = \chi_c(\omega) a_{\rm in}(\omega),$$

where, in the same way as the mechanical susceptibility $\chi(\omega)$, we define the cavity susceptibility

$$\chi_c(\omega) = \frac{\sqrt{\kappa}}{\kappa/2 - i(\Delta + \omega)}.$$

Substituting these equations into Eq.(6.1.2) and using the correlation relations of the cavity field, which are valid for our model since we have done the RWA, we then find that

$$S_{XX}(\omega) = \frac{1}{2}[n_c|\chi_c(-\omega)|^2 + (n_c+1)|\chi_c(\omega)|^2].$$

Note that this spectral density is asymmetric in frequency. As discussed in Chapter 2, this is a key sign that the bath is acting to heat or cool the mechanical oscillator. Neglecting the coherent driving term at $\omega = 0$, which acts only to statically displace the mechanical oscillator, we can now establish an analytical expression for the optical force power spectral density:

$$S_{F_cF_c}(\omega) = \frac{\hbar^2 g^2}{x_{\mathrm{zp}}^2}[n_c|\chi_c(-\omega)|^2 + (n_c+1)|\chi_c(\omega)|^2].$$

At this point, using again the quantum fluctuation-dissipation theorem, one can determine the mechanical occupancy n_m and the optically induced mechanical decay rate γ_{opt} as follows:

$$\begin{aligned}
\gamma_{\mathrm{opt}} &= \frac{x_{\mathrm{zp}}^2}{\hbar}\Big(S_{F_cF_c}(\omega_m) - S_{F_cF_c}(-\omega_m)\Big) = g^2\Big[|\chi_{\mathrm{c}}(\omega_m)|^2 - |\chi_{\mathrm{c}}(-\omega_m)|^2\Big] \\
n_m &= \frac{S_{F_cF_c}(-\omega_m)}{S_{F_cF_c}(\omega_m) - S_{F_cF_c}(-\omega_m)} = \frac{g^2}{\gamma_{\mathrm{opt}}}\Big[n_c|\chi_{\mathrm{c}}(\omega_m)|^2 + (n_c+1)|\chi_{\mathrm{c}}(-\omega_m)|^2\Big] \\
&= \frac{n_c|\chi_{\mathrm{c}}(\omega_m)|^2 + |\chi_{\mathrm{c}}(-\omega_m)|^2}{|\chi_{\mathrm{c}}(\omega_m)|^2 - |\chi_{\mathrm{c}}(-\omega_m)|^2}.
\end{aligned}$$

To understand these relations, it is worthwhile to consider three specific scenarios:

- If the optical driving field is on resonance ($\Delta = 0$), $|\chi_{\mathrm{c}}(\omega)| = |\chi_{\mathrm{c}}(-\omega)|$, so that the optically induced rate $\gamma_{\mathrm{opt}} = 0$ and $n_b = \infty$. As already seen, in this regime the optical field causes heating and does not affect the mechanical damping rate.

- If the optical field is blue detuned ($\Delta > 0$), each photon impinging on the optical cavity carries more energy than a cavity photon. To enter the cavity, a scattering process must occur whereby the mechanical oscillator takes up some of the photons' energy (see Fig.(8)). As a result, the optical field coherently adds energy to the mechanical oscillator, providing gain (or negative damping) to its motion.

- If the optical field is red detuned ($\Delta < 0$), we have to take into account the reverse situation to that discussed above, with each incident optical photon carrying less energy than a cavity photon. As a result, scattering processes cause net optical damping of the mechanical oscillator, which then reaches a finite positive equilibrium occupancy.

It can be seen that the maximum damping/amplification occurs near detunings equal to $\Delta = \mp\omega_m$, indeed in these cases the scattering process that transfers energy between the optical field and the mechanical oscillator is resonant. Taking this special resonant case while driving on the red (cooling) side of the optical resonance ($\Delta = -\omega_m$), we find

$$\gamma_{\mathrm{opt}} = \frac{4g^2}{\kappa}\left[1 + \left(\frac{\kappa}{4\omega_m}\right)^2\right]^{-1} \tag{6.1.3}$$

$$n_m = n_c + \left(\frac{\kappa}{4\omega_m}\right)^2(2n_c+1) \tag{6.1.4}$$

This is exactly the scenario we will consider in Section 7.1.2, where we will show that with this detuning, the state of the optical field and mechanical oscillator swap at the rate of 2g.
Furthermore, we find that this results in the cooling of the mechanical oscillator. Indeed observing Eq.(6.1.4), in the resolved sideband regime ($\kappa \ll \omega_m$), we recognize that the mechanical oscillator equilibrates to the occupancy of the optical field ($n_m = n_c$), with additional heating introduced as the resolved sideband factor decreases. On the other hand, if light is shot-noise limited ($n_c = 0$), this additional heating introduces the fundamental limit [113, 114]

$$n_m = \left(\frac{\kappa}{4\omega_m}\right)^2 \tag{6.1.5}$$

on the mechanical occupancy. Thus, we see that the presence of the cavity causes the field to act like a non-zero temperature bath for the mechanical oscillator.
Nevertheless, in most scenarios, it is not realistic to neglect the coupling of the mechanical oscillator to its mechanical bath. In general, if the oscillator is coupled to two independent baths (called A and B), the total force power spectral density is simply

$$S_{FF}(\omega) = S_{FF}^{A}(\omega) + S_{FF}^{B}(\omega)$$

and so (using again FDT) the equilibrium phonon occupancy of the oscillator is then the weighted mean

$$\begin{aligned} n_m &= \left(\frac{x_{\mathrm{zp}}}{\hbar}\right)^2 \left[\frac{S_{FF}^{A}(-\omega_m) + S_{FF}^{B}(-\omega_m)}{\gamma_A + \gamma_B}\right] \\ &= \frac{\gamma_A n_b^A + \gamma_B n_b^B}{\gamma_A + \gamma_B} \end{aligned} \tag{6.1.6}$$

where n_b^A and n_b^B, and γ_A and γ_B, are the phonon occupancies and damping rates, respectively, that would be obtained if the baths were individually coupled to the oscillator, as previously defined. If we substitute the optical and mechanical parameters into Eq.(6.1.6), it is then possible to analytically determine the equilibrium mechanical occupancy in the presence of both optical and mechanical baths, remembering that the result is only valid outside of the optomechanical strong coupling limit (specifically in the regime where $\kappa \ll g$).
Summarizing these considerations, we have seen that net optical heating occurs for $\Delta > 0$, while net cooling of the mechanical oscillators occurs for $\Delta < 0$, and is strongly peaked near $\Delta = -\omega_m$. In this resonant cooling regime, if the optical field is treated as $n_c = 0$, we find that the mechanical occupancy is

$$n_m = n_b + \frac{(\kappa/4\omega_m)^2(n_b + C)}{1 + C + (\kappa/4\omega_m)^2}$$

where n_b is the mechanical bath occupancy. Furthermore, in the limit where the resolved sideband factor $(\kappa/\omega_m)^2 \ll \{n_b/(n_b + C), 1 + C\}$, this can be approximated as (see Sec.6.1.1)

$$n_m = \frac{n_b}{1 + C}, \tag{6.1.7}$$

while in the alternative limit that the optomechanical cooperativity C dominates all other terms, the mechanical occupancy reaches the fundamental limit set by optical radiation pressure heating given in Eq.(6.1.5). Generally when $n_m < 1$ we speak of being "close to the ground state". With this definition, we see that in the first of the above limit the ground state can be approached for $C > n_b + 1$.

6.1.1 Resolved sideband regime

In this section, we use a quantum Langevin approach to include the ideal resolved sideband regime $\kappa \ll \omega_m$. In the resolved sideband regime the interaction term in the Hamiltonian in Eq.(5.3.3) may then be simplified by making a rotating wave approximation that neglects the fast oscillating terms (ab and $a^\dagger b^\dagger$). A way to justify this assumption is by considering the optomechanical energy level diagram in Fig.(8). It is clear that the scattering processes described by ab and $a^\dagger b^\dagger$ are off-resonance and therefore suppressed if $\kappa \ll \omega_m$. With this approximation, the Hamiltonian becomes

$$\hat{H} = \hbar\omega_m a^\dagger a + \hbar\omega_m b^\dagger b + \hbar g(a^\dagger b + a b^\dagger).$$

This is a beam splitter Hamiltonian that acts to swap excitations between the mechanical oscillator and the optical field. We can solve the QLE in the Fourier space, to find equations of motion for both a and b, valid within RWA:

$$a\left(-i\omega + \frac{\kappa}{2}\right) = \sqrt{\kappa}a_{\text{in}} + igb$$
$$b\left(\frac{\gamma}{2} - i\omega\right) = \sqrt{\gamma}b_{\text{in}} + iga$$

If we define the cavity and the mechanical susceptibilities as $\chi_c = \left(\frac{\kappa}{2} - i\omega\right)^{-1}$, $\chi_m = \left(\frac{\gamma}{2} - i\omega\right)^{-1}$ we can write a unique linear matrix equation

$$\begin{pmatrix} \chi_c^{-1} & -ig \\ -ig & \chi_m^{-1} \end{pmatrix} \begin{pmatrix} a \\ b \end{pmatrix} = \begin{pmatrix} \sqrt{\kappa}a_{\text{in}} \\ \sqrt{\gamma}b_{\text{in}} \end{pmatrix}$$

which solutions are

$$a(\omega) = \frac{\chi_c}{1 + g^2\chi_c\chi_m}\sqrt{\kappa}a_{\text{in}} + \frac{\chi_c\chi_m ig}{1 + g^2\chi_c\chi_m}\sqrt{\gamma}b_{\text{in}} \tag{6.1.1.1}$$
$$b(\omega) = \frac{\chi_m}{1 + g^2\chi_c\chi_m}\sqrt{\gamma}b_{\text{in}} + \frac{\chi_c\chi_m ig}{1 + g^2\chi_c\chi_m}\sqrt{\kappa}a_{\text{in}} \tag{6.1.1.2}$$

At this point, we can manipulate Eq.(6.1.1.2) considering the limit case where $\kappa \gg \gamma$. In this way, for the mechanical mode, we obtain

$$b(\omega) = \sqrt{\gamma}\chi_{eff}b_{\text{in}} + ig\chi_{eff}\chi_c\sqrt{\kappa}a_{\text{in}},$$

in which we have defined $\chi_{eff} = \frac{1}{\frac{\gamma}{2} - i\omega + \frac{2g^2}{\kappa}}$. Furthermore, upon calling first $\frac{\gamma}{2} + \frac{2g^2}{\kappa} = \frac{\gamma_{eff}}{2}$, we can proceed to compute the mechanical occupancy:

$$n_m = \int_{-\infty}^{\infty} \frac{d\omega}{2\pi}\langle b^\dagger_{-\omega} b_\omega\rangle = \frac{\gamma}{\gamma_{eff}}n_b + \frac{(4g^2/\kappa)}{\gamma_{eff}}n_c \tag{6.1.1.3}$$

Hence, in the usual limit where the optical bath occupancy is much lower than the mechanical bath occupancy ($n_c \ll n_b$), the optomechanical coupling results in cooling and we exactly recover the same expression as (6.1.7). Indeed Eq.(6.1.1.3) is telling us that the occupancy in our mechanical oscillator strictly depends on the ratio $\frac{\gamma}{\gamma_{eff}}$, meaning that it is cooling down due to red detuning dynamics.

A selection of cooling experiments in the optical domain was performed in 2006 in different works by Heidmann, Schliesser and Aspelmeyer [115, 116, 117]. While cooling via radiation-pressure in resolved sideband regime was achieved by Schliesser [118], Park [119] and Teufel [120] in 2008. However, we mention that the first experimental attempts of cooling by radiation-pressure dynamical were carried out by Braginsky and Manukin in 1970 [101], and also by Ashkin in 1978 [8].
Furthermore, resolved sideband cooling experiments that approached the ground state ($n_m < 1$) were first achieved in 2011, using a photonic-phononic crystal architecture [121] by Chan et al. and using a superconducting electromechanical system by Teufel et al [122].

6.1.2 Normal-mode splitting

As we mentioned in Sec.5.5, in the strong coupling regime $g \gg \{\gamma, \kappa\}$ we can observe normal mode splitting, i.e. the state of the optical field and mechanical oscillator swap at the rate 2g. In this regime, we can just consider again the linearized Hamiltonian

$$\hat{H} = -\hbar\Delta a^\dagger a + \hbar\omega_m b^\dagger b + \hbar g(a + a^\dagger)(b + b^\dagger).$$

We already know that in red-detuned regime, where $\Delta = -\omega_m$, we can employ the RWA obtaining the beam-splitter Hamiltonian $\hat{H} = \hbar g(a^\dagger b + a b^\dagger)$. This Hamiltonian is then easily diagonalized, with the eigenmodes representing excitations between the mechanical oscillations and the driven cavity mode, around the strong coherent amplitude. Their eigenfrequencies are

$$\omega_\pm = \frac{\omega_m - \Delta}{2} \pm \sqrt{g^2 + \left(\frac{\omega_m + \Delta}{2}\right)^2},$$

and right at $\Delta = -\omega_m$, one a splitting of $\omega_+ - \omega_- = 2g$ between the two excitation branches. At this point, the eigenmodes are symmetric and antisymmetric superpositions of light and mechanics, with new annihilation operators $(\hat{a} \pm \hat{b}/\sqrt{2})$. On the other hand, far from resonance, one recovers the two bare frequencies $-\Delta$ and ω_m, and the excitations become again of purely optical and mechanical nature, respectively. Of course, this picture cannot be observed in the opposite case, namely $g \ll \kappa$ where the two peaks at $\omega_\pm$ merge, as shown in Fig.(9). In this spirit, one can address the cooling problem in the strong coupling regime. To do it, we have to rewrite the linearized equations of motion for the cavity and the mechanical mode, in the regime $\Delta = -\omega_m$, and solve them for the complex eigenvalues $\omega_\pm$. We prefer leaving the mathematical derivation to [25]. What it turns out is that we end up with Eq.(6.1.4), already introduced in Sec.6.1., showing us that cooling becomes less efficient when one approaches the strong-coupling regime.
The peak splitting in the strong-coupling regime, and the resulting modification to cooling, was predicted by Marquardt & Girvin in 2007 [113]. It was also studied in 2008 in a collection of different works by Kippenberg, Wilson-Rae, Rossi & Vitali and Marquardt [123, 124, 125, 126, 127, 128]. In addition, the first experimental observation was made by Aspelmeyer in 2009 [129]. Nowadays, there are cooling schemes that follow a different strategy, for example using an incoherent thermal source [130] or a coherent mechanical resonator [131]. In the latter case, Schliesser et *al.* [131] realize an ultracoherent electromechanical system based on a soft-clamped silicon nitride membrane, which was capacitively coupled to a microwave mode, strong enough to enable ground-state-cooling of the mechanics (they reached the value of $n_m = 0.76 \pm 0.16$). On the other hand, Naseem [130] propose a scheme for simultaneous cooling of multiple mechanical resonators to their quantum ground-state. As opposed to standard laser cooling schemes, where coherence renders the motion of a resonator to its ground-state, they consider an incoherent

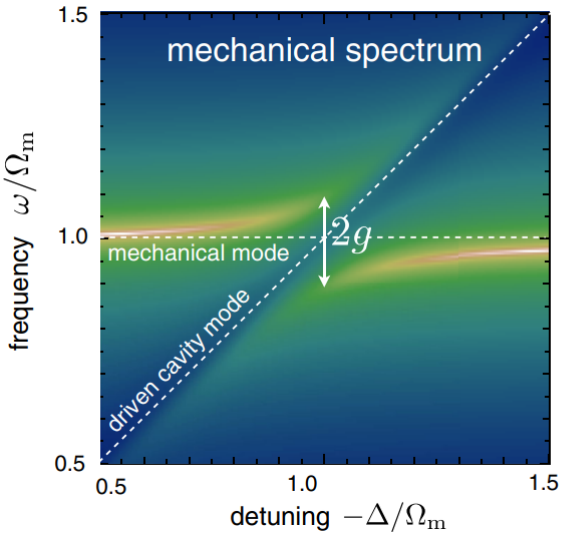

Figure 9: Mechanical frequency spectrum as a function of laser detuning, for a strongly coupled optomechanical system. An avoided crossing, with a splitting of size $2g$, appears when the negative detuning equals the mechanical resonance frequency (Credit from Aspelmeyer et *al.* Physical Review 2014). [25]

thermal source to achieve the same aim. They use a complementary approach, namely "cooling by heating", where an incoherent thermal drive removes energy from the quantum system only to dump it in another bath at a lower temperature.

6.2 Blue Detuning: linear amplification and entanglement

In the previous section, we have seen how red detuning implies cooling of the mechanical motion. Analogously, we now aim to describe the opposite case, where $\Delta > 0$ provides a gain to the mechanical oscillator motion. As seen in Chapter 2, this gain is directly linked to a mechanism of linear amplification. We study here in detail this regime, following the analysis made by Lehnert in 2008 [132] and especially by Massel et al. in 2011 [40]. We focus on these two works because they offer us the opportunity to shape our analysis in the microwaves domain, and not in the optical one anymore.
Let's recall the blue-detuned Hamiltonian obtained in Sec.5.4:

$$\hat{H} = g(a^\dagger b^\dagger + ab).$$

As usual, we can derive and solve the QLE for the cavity and the mechanical degrees of freedom. In this case, we would like to consider a slightly different situation than before, but very useful later on. In general, the field a_{in} represents an input field to the optical cavity, and is often coherently populated $\alpha_{\text{in}} \equiv \langle a_{\text{in}} \rangle \neq 0$. However, the dissipation from the cavity occurs through several channels, including an experimentally accessible channel which we call *input port*, and other loss channels due, for instance, to absorption, and scattering, which we treat as loss port. In practice, it is important to account separately for these two different types of channels. This can be done via the substitution

$$\kappa a_{\text{in}} \longrightarrow \sqrt{\kappa_i} a_{\text{in}}^I + \sqrt{\kappa_e} a_{\text{in}}^E,$$

where κ_i and κ_e are the dissipation rates through the input and loss ports, respectively, with the total dissipation rate $\kappa = \kappa_i + \kappa_e$, and in the substitution $a^I_{\rm in}$ and $a^E_{\rm in}$ are the fields entering through each port. Typically, for an optical cavity at room temperature, the field entering through the loss port can be well treated as a vacuum state so that $\langle a^E_{\rm in}\rangle = 0$.
In this way, leaving the calculation to [40], we obtain an expression for the output cavity field in the Fourier space

$$a_{\rm out}(\omega) = M(\omega)a_{\rm in}(\omega) + L(\omega)a^\dagger_{\rm in} + M_I(\omega)a^I_{\rm in}(\omega) + L_I(\omega)a^{I\dagger}_{\rm in}(\omega) + Q(\omega)\xi(\omega)$$

where $a^I_{\rm in}(\omega)$ and $\xi(\omega)$ represent the noise introduced by the internal losses of the cavity and the mechanical bath, while M and L are the amplitude gains for the input signal, and M_I, L_I, Q those for the input noise. Without writing explicitly these expressions [40], one can show that the key role in the amplification is played by the factor

$$\Gamma(\omega) = \frac{\omega_m^2 - \omega^2 - i\gamma\omega}{\omega_{\rm eff}^2 - \omega^2 - i\gamma_{\rm eff}\omega} \ ,$$

which depends on the effective resonant frequency and the effective damping coefficient, respectively $\omega_{\rm eff}$ and $\gamma_{\rm eff}$, induced by the coupling of the mechanical resonator with the cavity. At resonance $\omega = \omega_m$, a decrease of $\gamma_{\rm eff} \to 0$ leads to $\Gamma \gg 1$, and since $M(\omega), L(\omega) \propto \Gamma$ we obtain an amplification of the input signal. Furthermore, the amplifier equations can be written in terms of the quadrature fields (dropping here the added-noise terms)

$$\begin{aligned} X_{\rm out} &= (|M| + |L|)X_{\rm in} \\ Y_{\rm out} &= (|M| - |L|)Y_{\rm in} \ , \end{aligned}$$

which generates the expression of the power gains [41]

$$\begin{aligned} G_X &= (|M| + |L|)^2 \\ G_Y &= (|M| - |L|)^2. \end{aligned}$$

Such microwave amplification mechanisms, where the interaction of a micro-mechanical device with radiation pressure can be used to amplify weak electrical signals, have been extensively studied in the past years. From a theoretical point of view, this set-up represents one of the simplest realizations of a quantum amplifier that could potentially operate at the noise limit set by the Heisenberg uncertainty principle. Furthermore, in Chapter 7 we will see a case of microwave input amplification in a two-mode cavity optomechanical system [133].

6.2.1 Entanglement between a cavity and mechanical oscillator

We now want to investigate optomechanical entanglement between the cavity field and the mechanical oscillator. Starting from the linearized optomechanical Hamiltonian

$$\hat{H} = -\hbar\Delta a^\dagger a + \hbar\omega_m b^\dagger b + \hbar g(a + a^\dagger)(b + b^\dagger),$$

if the cavity is blue detuned, namely $\Delta = \omega_m$, one can apply the same procedure of Sec.5.4 for the QLE, using the rotating wave approximation to obtain Eqs. (5.4.13, 5.4.14), and simplifying the interaction to a down-conversion process (which is known to generate bipartite entanglement).
At this point, the covariance matrix (CM) of the Gaussian state of the bipartite system, can be obtained as (with the technique of Chapter 4)

$$\boldsymbol{\sigma} = \begin{pmatrix} \sigma_{11} & 0 & 0 & \sigma_{14} \\ 0 & \sigma_{11} & \sigma_{14} & 0 \\ 0 & \sigma_{14} & \sigma_{33} & 0 \\ \sigma_{14} & 0 & 0 & \sigma_{33} \end{pmatrix} \ ,$$

where

$$\sigma_{11} = n_m + \frac{1}{2} + \frac{g^2\kappa(n_m+1)}{(\gamma+2\kappa)(2\gamma\kappa+g^2/2)}$$
$$\sigma_{14} = \frac{1}{2} + \frac{g^2\gamma(n_m/2+1/2)}{(\gamma+2\kappa)(2\gamma\kappa+g/2)}$$
$$\sigma_{33} = \frac{g\gamma\kappa(\sqrt{2}n_m+\sqrt{2})}{(\gamma+2\kappa)(2\gamma\kappa+g/2)}.$$

However, one can show that in the RWA limit the amount of achievable optomechanical entanglement is seriously limited by the condition $g < \sqrt{\kappa\gamma}$. Since one needs a small mechanical dissipation rate γ_m to see quantum effects, this means a very low maximum value for g. The logarithmic negativity $E_{\mathcal{N}}$, that quantify our entanglement, is an increasing function of the effective optomechanical coupling[7] g and therefore the above condition puts a strong upper bound also on $E_{\mathcal{N}}$. It is possible to prove that the following bound on $E_{\mathcal{N}}$ exists

$$E_{\mathcal{N}} \leq \ln\left[\frac{1+(g/\sqrt{\kappa\gamma})}{1+n_m}\right],$$

showing that $E_{\mathcal{N}} \leq \ln 2$ (see Eq.(4.2.1.6)) and above all that entanglement is extremely fragile with respect to temperature in the RWA limit because, due to the above condition, $E_{\mathcal{N}}$ vanishes as soon as $n_m \geq 1$. Entanglement between mechanical motion and cavity fields was both observed and predicted in optical and microwave domains, as by Genes in 2008 [134] (optical), and Palomaki in 2013 [24] (microwave).

6.3 Mechanical squeezing

Previously, we have seen how different phenomena, such as cooling, amplification, and entanglement, can occur in optomechanical systems. However, there is another phenomenon, that we have introduced in Chapter 3, which can be observed under certain conditions.
In this last section, we aim to address the mechanical squeezing problem in optomechanical systems. We would like to follow here two particular works in our discussion, i.e. Schwab et al. in 2015 [135], and Massel et al. in the same year [136].
We know that in the quantum ground state, the mechanical oscillator has position fluctuations divided equally between its two quadratures, $\hat{X}_1$ and $\hat{X}_2$. Additionally, the ground-state fluctuations minimize the uncertainty relation given by the quadratures' commutator

$$\langle\Delta\hat{X}_1^2\rangle\langle\Delta\hat{X}_2^2\rangle \geq \frac{1}{4}|\langle[\hat{X}_1,\hat{X}_2]\rangle|^2 = x_{\rm zp}^4,$$

where $x_{\rm zp} = \sqrt{\hbar/2m\omega_m}$ is the amplitude of the zero-point fluctuations. Given this uncertainty relation, it is possible to squeeze the zero-point noise such that fluctuations in one quadrature are reduced below the zero-point level at the expense of increasing noise in the orthogonal quadrature. Now, in the usual optomechanical setup, the scheme consists of applying two pump tones to an optical (or microwave) cavity coupled to a mechanical resonator. The pumps are detuned from the cavity frequency ω_c by the mechanical frequency $\pm\omega_m$, with the red-detuned pump at a higher power than the blue-detuned pump, as in Fig.(10). The squeezing effect of the drives

[7] We can note this from the definition of logarithmic negativity [76] $E_{\mathcal{N}} = \max[0, -\ln 2\nu^-]$ where we have $\nu^- \equiv \frac{1}{\sqrt{2}}\left[\Delta(\boldsymbol{\sigma}) - [\Delta(\boldsymbol{\sigma})^2 - 4\det\boldsymbol{\sigma}]^{1/2}\right]^{1/2}$, with $\Delta(\boldsymbol{\sigma}) = \det\boldsymbol{\alpha} + \det\boldsymbol{\beta} + 2\det\boldsymbol{\gamma}$ and $\boldsymbol{\sigma}$ the 2x2 block CM.

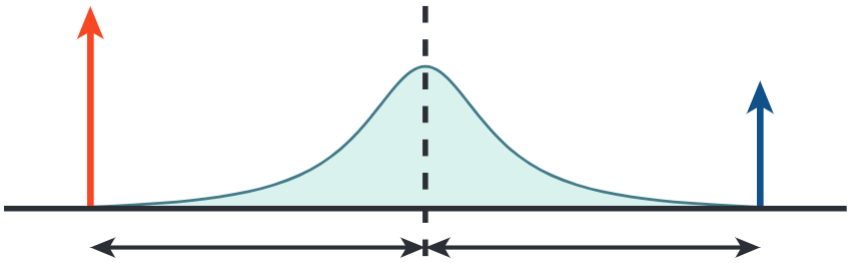

Figure 10: Sketch showing frequencies of squeezing drive tones relative to the cavity frequency.

can be understood as damping of both quadratures by the excess red-detuned power, similar to that of sideband cooling, but with less back-action noise added to $\hat{X}_1$ than the zero-point noise associated with the damping. Here, we take the cavity (mechanics) to be coupled to a bath with thermal occupation n_c (n_m) at a rate κ (γ). For optical systems, n_c is usually indistinguishable from 0, but for microwave systems, a non-zero n_c is commonly observed at high pump powers. We also define the pumps as $\omega_\pm = \omega_c \pm \omega_m$, and the optomechanical coupling rates for the blue and red pumps as $G_\pm$, with the effective optomechanical coupling rate $\mathcal{G} = \sqrt{G_-^2 - G_+^2}$. The presence of the pumps at $\omega_\pm$ generates (coherent) intracavity photon occupations $n_p^\pm$, which are proportional to both the pump power applied at the input of the system, and to the pump power measured at the output. This notation will also hold throughout Chapter 7.
In this way, the linearized interaction Hamiltonian is given by

$$\hat{H} = -\hbar a^\dagger (G_+ b^\dagger + G_- b + G_+ b e^{-2i\omega_m t} + G_- b^\dagger e^{2i\omega_m t}) + \text{h.c.}$$

In the so-called good-cavity limit ($\omega_m \gg \kappa$), and when $\kappa \gg \gamma$, the quadrature fluctuations are then given by (Appendix B)

$$\langle \Delta \hat{X}_{1,2}^2 \rangle = x_{\text{xp}}^2 \left[\frac{\gamma}{\kappa} \frac{(4\mathcal{G}^2 + \kappa)}{(4\mathcal{G}^2 + \gamma\kappa)} (2n_m + 1) \frac{4(G_- \mp G_+)^2}{(4\mathcal{G}^2 + \gamma\kappa)} (2n_c + 1) \right].$$

For both $\Delta \hat{X}_1^2$ and $\Delta \hat{X}_2^2$, the first term is proportional to $2n_m + 1$ and has a prefactor that is less than 1 for all $\mathcal{G} > 0$. This term represents the damping of both quadratures due to the red-detuned power. The second term is proportional to $2n_c + 1$ and is due to the backaction from the cavity field. We see that the back-action is reduced for $\Delta \hat{X}_1^2$ and increased $\Delta \hat{X}_2^2$. It is thanks to this reduction that we can reduce $\Delta \hat{X}_1^2$ below x_{zp}^2.
Although a squeezed thermal state always has a positive Wigner function, when the fluctuations in one quadrature are reduced below the zero-point level, the squeezed state no longer has a well-behaved P representation, i.e. it cannot be represented as a mixture of coherent states [137]. For this reason, a quantum squeezed state is considered a non-classical state. The bath occupations and the quadrature variances are plotted in Fig.(11). We find that, at the lowest point, we are squeezed to $\langle \Delta \hat{X}_1^2 \rangle / x_{\text{zp}}^2 = 0.797 \pm 0.034$, below the zero-point fluctuations [135].
Analogously, also Pirkkalainen et *al.* [136] in their work found squeezing of one quadrature amplitude of 1.1 ± 0.4 dB, below the standard quantum limit. In their work, they obtained a first realization of squeezing of motional state of a macroscopic body, designed as a micromechanical resonator measuring 15 microns in diameter. To achieve this result, Pirkkalainen used the idea of dissipative squeezing [138], where the system is allowed to cool towards a squeezed low-energy state. This scheme does not rely on any explicit measurement, instead it uses a dissipative

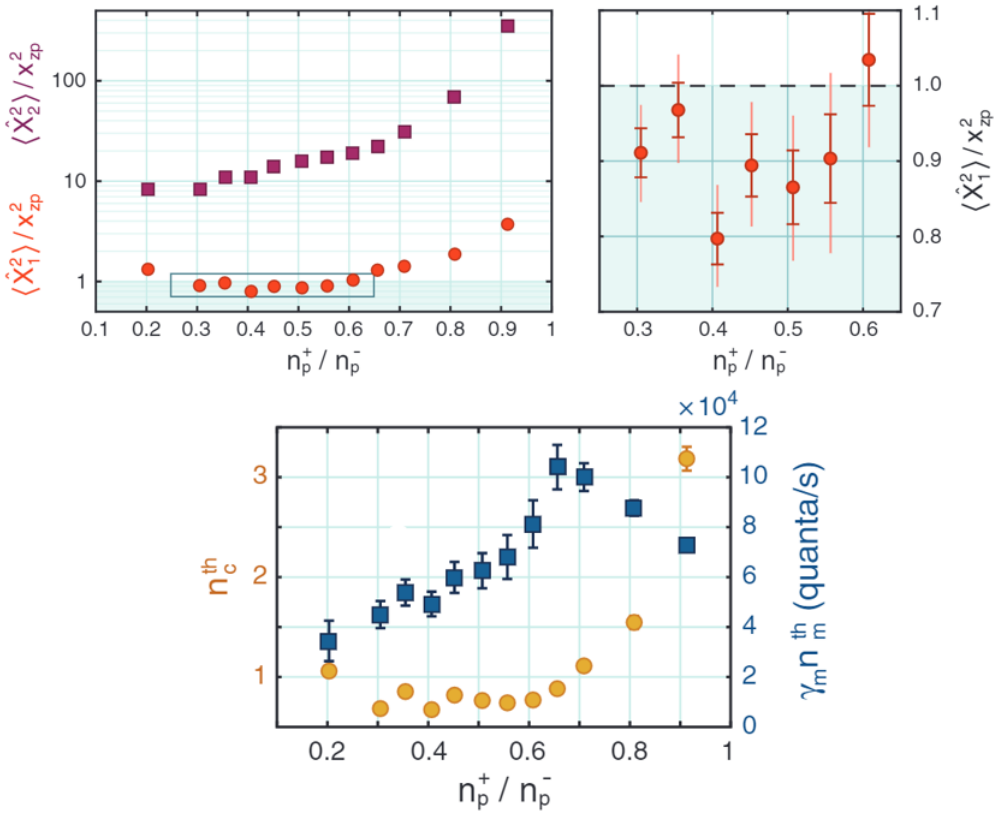

Figure 11: (a-Left) Calculated quadrature noise for $\langle \Delta \hat{X}_1^2 \rangle$ (red circles) and $\langle \Delta \hat{X}_2^2 \rangle$ (purple squares). The shaded region indicates squeezing. (a-Right) Close-up of the boxed area showing data with $\hat{X}_1$ fluctuations below the zero-point level. The lowest point has $\langle \Delta \hat{X}_1^2 \rangle / x_{\rm zp}^2 = 0.797 \pm 0.034$. (b) Values of n_c (yellow circles) and γn_m (blue squares) obtained from Bayesian analysis of the spectra (Credit from Schawb et *al.* 2015 [135]).

mechanism with an optomechanical cavity, driven on the red and blue mechanical sideband with different laser amplitudes, acting as an engineered reservoir which only couples to a single mechanical quadrature. It can equivalently be viewed as a coherent feedback process, obtained by perturbing the quantum measurement of a single quadrature. This method has the great advantage of being able to create unconditional squeezing in the steady-state, being in contrast to many other plausible methods of squeezing [139, 140, 141].

7 Two modes optomechanical systems

Up to now we almost exclusively considered one cavity mode coupled to one mechanical mode. This is the "minimal model" of cavity optomechanics, captured by the Hamiltonian (5.3.3). In this chapter, we are going to deal with two mode optomechanical systems, namely two cavity mode coupled with one mechanical oscillator, or two mechanical resonators coupled with one cavity mode. We use the mathematical formalism of two-mode squeezed states (TMSS), and two-mode coherent states (TMCS), introduced by Caves & Schumaker [142, 143] (see also Sec.3.3.1).
In the following, we thus discuss some scenarios and features where it becomes crucial to go beyond the minimal model. To do it, we first rely on the work done by Massel et al. in 2016 [133].
Our setup consists of two electromagnetic cavities with different resonant frequencies, simultaneously coupled to a single mechanical resonator. In the presence of appropriately external pump tones (as shown in Fig.12), the mechanical resonator mediates the interaction between the cavities, enabling entanglement between these two. Moreover, as shown in [133], this scheme

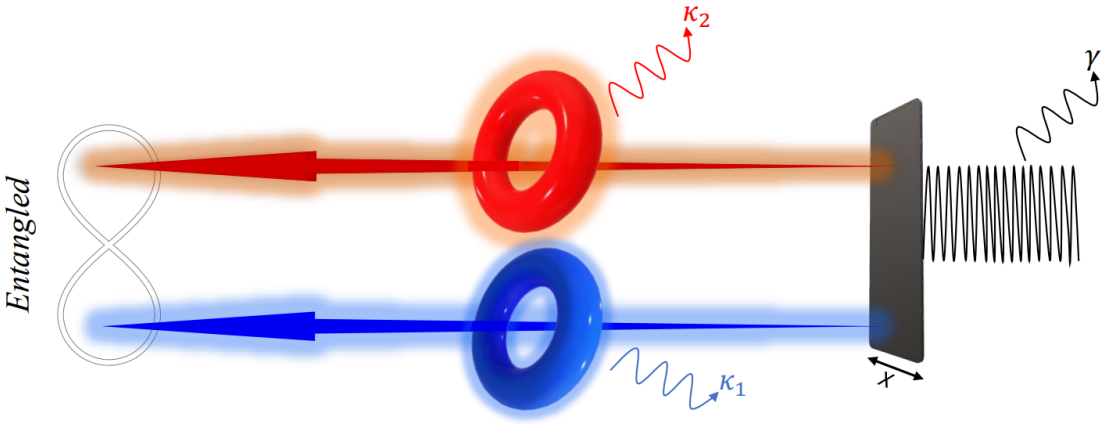

Figure 12: Schematic representation of the setup. Two microwave cavities with a shared mechanical oscillator generate two entangled output fields. X indicates the mechanical displacement, γ denotes the mechanical loss rate and $\kappa_{1,2}$ the cavity loss rates.

supports amplification, namely, a signal incident in one cavity can irradiate out from the other cavity, and be amplified until it reaches the SQL. The two-mode amplifier is created by injecting two pump tones, one at the blue mechanical sideband of cavity 1 (ω_{P_+}), and the other at the red sideband of cavity 2 (ω_{P_-}). Thus, the Hamiltonian describing the optomechanical interaction can be written as

$$\hat{H} = \omega_1 a^\dagger a + \omega_2 c^\dagger c + \omega_m b^\dagger b + (g_1 a^\dagger a + g_2 c^\dagger c)(b^\dagger + b), \tag{7.1}$$

for simplicity, we set $\hbar = 1$. Here, a and c represent the cavity modes for cavity 1 and 2 with resonant frequencies ω_1 and ω_2, while $b(b^\dagger)$ is the lowering (raising) operator associated with the mechanical resonator, with resonant frequency ω_m. The coupling between the cavities and the mechanics is described in terms of radiation pressure interaction with coupling constants g_1 and g_2. We follow [144] and consider below the experimental situation where the pump frequencies satisfy $\omega_{P_-} = \omega_2 - \omega_m$ and $\omega_{P_+} = \omega_1 + \omega_m$, as shown in Fig.13. In the rotating frame with respect to cavity frequencies, the first quantum corrections are described by $\hat{H} = \hat{H}_0 + \hat{H}_I$, where

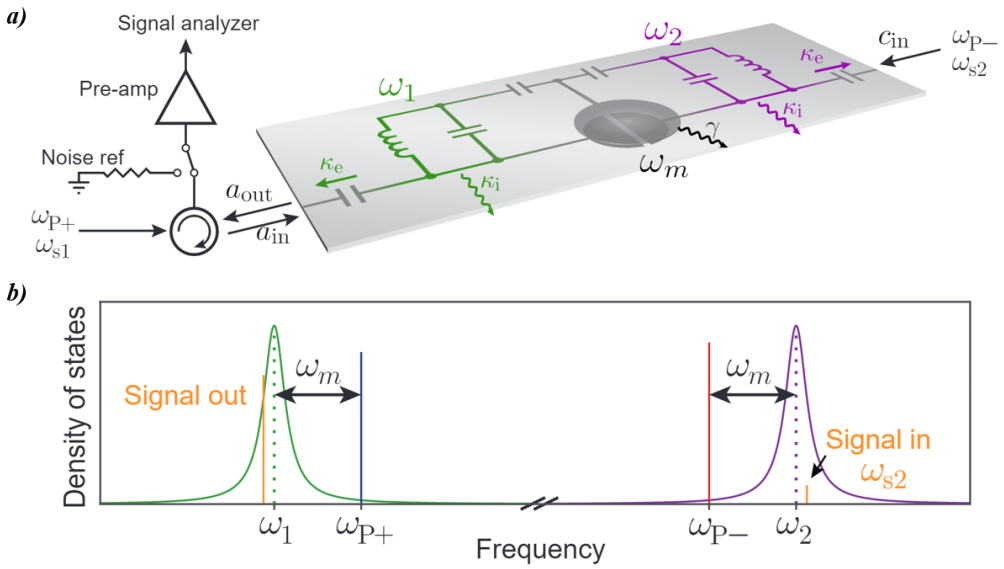

Figure 13: Experimental setup. **a)** Schematic of the device, showing the two microwave cavities (ω_1, ω_2) both coupled to a central mechanical drum resonator (ω_m). Signals (ω_{s1}, ω_{s2}) and pumps (ω_{P_+}, ω_{P_-}) are fed to the cavities as shown. The output of cavity 1 is measured with a signal analyzer. **b)** Representation of the cavity modes and pump frequencies used to realize a two-port amplifier. As an example, an input signal with frequency ω_{s2} is injected to cavity 2, with the amplified output emerging from cavity 1. Credit from Ockeloen-Korppi et *al.* Physical Review X 2016 [133].

the uncoupled Hamiltonian is $\hat{H}_0 = \omega_m(b^\dagger b + c^\dagger c - a^\dagger a)$. Retaining only the resonant terms in the remaining linearized interaction yields the coupling Hamiltonian

$$\hat{H}_I = (G_- c^\dagger + G_+ a)b + h.c.,$$

where $G_- = g_2\sqrt{n_2}$, $G_+ = g_1\sqrt{n_1}$, and n_2 and n_1 are the photon numbers for the red-detuned and blue-detuned pumping tones for cavity 2 and 1, respectively. Applying the *two-mode squeezing operator*

$$S(\xi) = \exp\{\xi c^\dagger a^\dagger - \xi c a\},$$

to the cavity operators

$$\eta_A = S^\dagger(\xi) a S(\xi) = \cosh\xi a + \sinh\xi c^\dagger$$
$$\eta_C = S^\dagger(\xi) c S(\xi) = \cosh\xi c + \sinh\xi a^\dagger,$$

the Hamiltonian H_I can be recast as the usual beam-splitter Hamiltonian

$$\hat{H}_I = \mathcal{G}(\eta_C b^\dagger + \eta_C^\dagger b),$$

where we have defined

$$\cosh\xi = G_-/\mathcal{G}, \quad \sinh\xi = G_+/\mathcal{G}, \quad \text{with } \mathcal{G}^2 = G_-^2 - G_+^2,$$

with $G_- > G_+$. Note how η_A is a mechanically dark mode (i.e. it does not couple to the mechanics). Assuming the standard dissipation mechanism for the cavities and the mechanics, with dissipation coefficients given by κ (equal for both cavities) and γ, the quantum Langevin equations for η_A and η_C can be solved to give [40, 144]

$$\eta_A = \chi_c\sqrt{\kappa}\cosh\xi a_{\rm in} + \chi_c^*\sqrt{\kappa}\sinh\xi c_{\rm in}^\dagger$$
$$\eta_C = \frac{\chi_m^{-1}}{\chi_m^{-1}\chi_c^{-1}+\mathcal{G}^2}\sqrt{\kappa}\eta_C - \frac{i\mathcal{G}\sqrt{\gamma}}{\chi_m^{-1}\chi_c^{-1}+\mathcal{G}^2}b_{\rm in},$$

where $\chi_m = [\gamma/2 - i\omega]^{-1}$ and $\chi_c = [\kappa/2 - i\omega]^{-1}$ are the bare mechanical and cavity susceptibilities in the rotating frame. Transforming η_A and η_B back to a and c,

$$a = S(\xi)\eta_A S^\dagger(\xi) = \cosh\xi\eta_A - \sinh\xi\eta_C^\dagger$$
$$c = S(\xi)\eta_C S^\dagger(\xi) = \cosh\xi\eta_C - \sinh\xi\eta_A^\dagger,$$

and, taking into account the input-output relations for the cavity fields [145],

$$a_{\rm out} + a_{\rm in} = \sqrt{\kappa_e}a$$
$$c_{\rm out} + c_{\rm in} = \sqrt{\kappa_e}c$$

we can write the expression for the output fields a and c. It reads

$$\begin{aligned} a_{\rm out} &= (-\kappa_e\mathcal{A}_{aa} - 1)a_{\rm in} - \kappa_e\mathcal{A}_{ac}c_{\rm in}^\dagger - \sqrt{k_i k_e}\mathcal{A}_{aa}a_{I,\rm in} \\ &- \sqrt{k_i k_e}\mathcal{A}_{ac}c_{I,\rm in}^\dagger + i\sqrt{\gamma\kappa_e}\frac{G_+}{(\chi_c\chi_m)^{-1}+\mathcal{G}^2}b_{\rm in}^\dagger \end{aligned} \tag{7.2}$$

$$\begin{aligned} c_{\rm out} &= (\kappa_e\mathcal{A}_{cc} - 1)c_{\rm in} + \kappa_e\mathcal{A}_{ca}a_{\rm in}^\dagger + \sqrt{k_i k_e}\mathcal{A}_{cc}c_{I,\rm in} \\ &+ \sqrt{k_i k_e}\mathcal{A}_{ca}a_{I,\rm in}^\dagger - i\sqrt{\gamma\kappa_e}\frac{G_-}{(\chi_c\chi_m)^{-1}+\mathcal{G}^2}b_{\rm in} \end{aligned} \tag{7.3}$$

where

$$\mathcal{A}_{aa} = (\chi_c^e\sinh^2\xi - \chi_c\cosh^2\xi)^*$$
$$\mathcal{A}_{cc} = \chi_c^e\cosh^2\xi - \chi_c\sinh^2\xi$$
$$\mathcal{A}_{ca} = \mathcal{A}_{ac}^* = (\chi_c^e - \chi_c)\cosh\xi\sinh\xi$$

and $\chi_c^e = \chi_c(1 + \mathcal{G}^2\chi_c\chi_m)^{-1}$ represents the effective cavity response in the presence of the two-tone optomechanical drive. In Eqs.(7.2, 7.3), we have explicitly included the possibility of internal cavity losses (and noise) for both cavities by introducing the operators $a_{I,\rm in}$, $c_{I,\rm in}$, and $\sqrt{\kappa} = \sqrt{\kappa_e} + \sqrt{\kappa_i}$ (see Chapter 6). Finally, from the latter equations, one can write the explicit amplification form for the output field of cavity 1

$$a_{\rm out} = A_d a_{\rm in} + A_x c_{\rm in}^\dagger + F,$$

with

$$A_d = -\kappa_e\mathcal{A}_{aa} - 1$$
$$A_x = -\kappa_e\mathcal{A}_{ac},$$

and similar for $c_{\rm out}$ of cavity 2. Here, A_d is the direct gain of signals $a_{\rm in}$ incident on cavity 1, and A_x is the cross gain of signals incident on cavity 2. Operator $\hat{F}$ describes the added noise due

to the internal modes of the device (as seen in Chapter 2). Maximum amplification is achieved in the strong pumping regime $4G_-^2 \gg \gamma\kappa$, with the further assumption $G_+ \simeq G_-$ (the term -1 in Eq.(7.2) can be neglected). In this case, the direct and cross gains are approximately equal

$$|A_d|^2 \approx |A_x|^2 \approx \left| 2\frac{\kappa_e}{\kappa} \frac{4G_-^2/\kappa}{\gamma_{\text{eff}}} \right|,$$

where $\gamma_{\text{eff}} = \gamma + 4\mathcal{G}^2/\kappa$ is the effective damping of the mechanical oscillator. Similar to optomechanical amplifiers powered by a single blue-detuned pump [40], the amplification bandwidth is associated with the effective mechanical damping γ_{eff}. Moreover, the gain-bandwidth $G = |A_d|\gamma_{\text{eff}}$ is determined by G_-, and is not fundamentally limited. The direct gain is plotted in Fig.14.

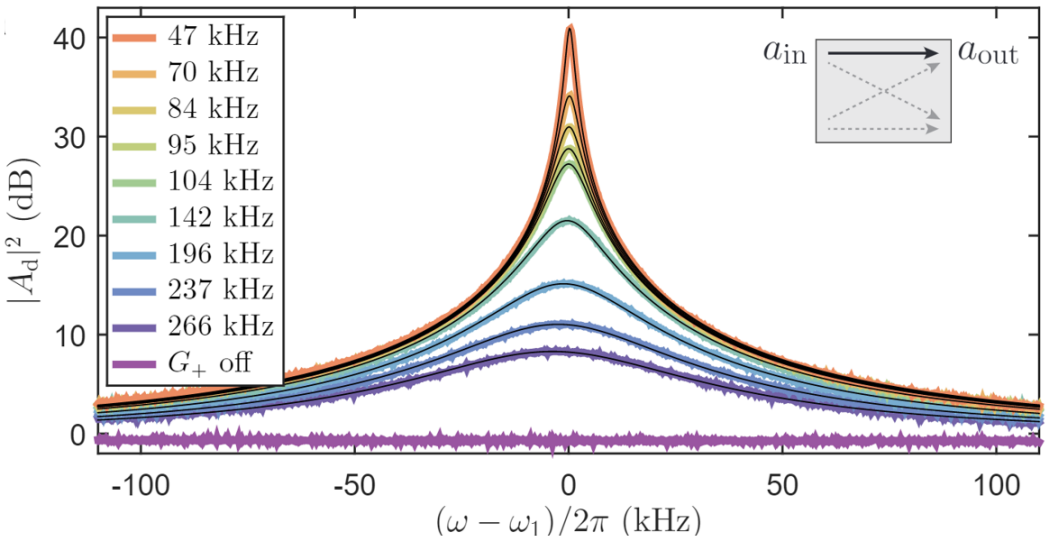

Figure 14: Two-mode amplifier performance. Direct gain $|A_d|^2$ versus signal frequency for fixed G_- and various values of G_+ (colored lines, legend shows $\mathcal{G}/2\pi$) together with theory fits (black lines). Credit from Ockeloen-Korppi et *al.* Physical Review X 2016 [133].

7.1 Two modes squeezing and entanglement

In this section, we would like to use the previous optomechanical model to search for entanglement between the two cavities interacting with the mechanical resonator. This type of analysis was first conducted by Clerk and Wang in 2013 [144], where they considered the possibility of entanglement via reservoir engineering, and, more recently, by Fink et al. in 2019 [146], where they didn't use any additional reservoir but the two cavities were simply coupled with one mechanical oscillator in the microwave domain. What they did is analyzed hereafter.
Let us take into account again Hamiltonian (7.1):

$$\hat{H} = \hbar\omega_1 a^\dagger a + \hbar\omega_2 c^\dagger c + \hbar\omega_m b^\dagger b + \hbar(g_1 a^\dagger a + g_2 c^\dagger c)(b^\dagger + b),$$

where, in the rotating frame, retaining only the resonant terms in the linearized interaction yield the coupling Hamiltonian

$$\hat{H}_I = \hbar G_+(ab + b^\dagger a^\dagger) + \hbar G_-(cb^\dagger + bc^\dagger),$$

with usual $G_+ = g_1\sqrt{n_1}$ and $G_- = g_2\sqrt{n_2}$ for cavities 1 and 2, respectively. The full quantum treatment of the system can be given in terms of the quantum Langevin equations in which we add to the Heisenberg equations the quantum noise acting on the mechanical resonator ($b_{\rm in}$ with damping rate γ), as well as the cavities' input fluctuations ($a_{\rm ex}$ and $c_{\rm ex}$, with rates $\kappa_{\rm ex}$, plus the intrinsic losses of the resonator modes ($a_{I,{\rm in}}$ and $c_{I,{\rm in}}$, with loss rates $\kappa_{\rm in}$). These noises have the following correlation functions

$$\begin{aligned}
\langle a_{\rm ex}(t)a^\dagger_{\rm ex}(t')\rangle &= \langle a^\dagger_{\rm ex}(t)a_{\rm ex}(t')\rangle + \delta(t-t') = (n_a^T+1)\delta(t-t')\\
\langle a_{\rm I,in}(t)a^\dagger_{\rm I,in}(t')\rangle &= \langle a^\dagger_{\rm I,in}(t)a_{\rm I,in}(t')\rangle + \delta(t-t') = (n_a^{\rm in}+1)\delta(t-t')\\
\langle b_{\rm in}(t)b^\dagger_{\rm in}(t')\rangle &= \langle b^\dagger_{\rm in}(t)b_{\rm in}(t')\rangle + \delta(t-t') = (n_m+1)\delta(t-t'),
\end{aligned}$$

where $n_a^T, n_a^{\rm in}, n_m$ are the Planck-law thermal occupancies of each bath. Analogously the same holds for $c_{\rm ex}$ and $c_{\rm I,in}$, yielding to n_c and $n_c^{\rm in}$. Therefore, the resulting Langevin equations are

$$\begin{aligned}
\dot{a} &= -\frac{\kappa}{2}a - iG_+b + \sqrt{\kappa_{\rm ex}}a_{\rm ex} + \sqrt{\kappa_{\rm in}}a_{\rm I,in}\\
\dot{c} &= -\frac{\kappa}{2}c - iG_-b^\dagger + \sqrt{\kappa_{\rm ex}}c_{\rm ex} + \sqrt{\kappa_{\rm in}}c_{\rm I,in}\\
\dot{b} &= -\frac{\gamma}{2}b - iG_+a^\dagger - iG_-c + \sqrt{\gamma}b_{\rm in}.
\end{aligned}$$

At this point, one can solve the above equations in the Fourier domain to obtain the microwave variables, however, we prefer leaving this discussion to [146]. Instead, to quantify entanglement, let us first determine the covariance matrix $\boldsymbol{\sigma}$ (CM) of our system in the frequency domain, which can be expressed as [144]

$$\sigma_{i,j} = \frac{1}{2}\langle u_i u_j + u_j u_i\rangle,$$

where

$$\boldsymbol{u} = [X_1, Y_1.X_2, Y_2]^T,$$

is the vector of quadratures

$$\begin{aligned}
X_1 &= (a + a^\dagger)/\sqrt{2}\\
Y_1 &= (a - a^\dagger)/i\sqrt{2}\\
X_2 &= (c + c^\dagger)/\sqrt{2}\\
Y_2 &= (c - c^\dagger)/i\sqrt{2}.
\end{aligned}$$

Now, by substituting the solutions of equations of motion into the corresponding input-output formula for the variables, i.e., $a_{\rm out} = \sqrt{k_{\rm ex}}a - a_{\rm ex}$ (similarly for $c_{\rm out}$), we obtain the CM for the quadratures of the outputs

$$\boldsymbol{\sigma}(\omega) = \begin{pmatrix} \sigma_{11} & 0 & \sigma_{13} & 0\\ 0 & \sigma_{11} & 0 & -\sigma_{13}\\ \sigma_{13} & 0 & \sigma_{33} & 0\\ 0 & -\sigma_{13} & 0 & \sigma_{33}\end{pmatrix}, \tag{7.1.1}$$

note that Eq.(7.1.1) is the typical CM of a two-mode squeezed thermal state, where the elements of the CM can be written in terms of photon numbers n_i, squeezing angle φ and squeezing parameter ξ, reads

$$\sigma_{11} = \frac{(1+n_1+n_2)\cosh 2\xi + (n_1-n_2)}{2}$$
$$\sigma_{33} = \frac{(1+n_1+n_2)\cosh 2\xi - (n_1-n_2)}{2}$$
$$\sigma_{13} = \frac{(1+n_1+n_2)\sinh 2\xi \cos\varphi}{2},$$

when $n_i = 0$ the Gaussian state is called two-mode squeezed vacuum. Squeezing in the two-mode squeezed thermal state can be determined by the following expression [74, 147]

$$S(\varphi) = \sigma_{11} + \sigma_{33} - 2\sigma_{13} = \frac{1}{2}(1+n_1+n_2)(\cosh 2\xi - \sinh 2\xi \cos\varphi),$$

which for $\varphi = 0$ and $n_i = 0$ gives the maximum squeezing $S(0) = e^{-2\xi/2}$. Furthermore, the degree of two-mode squeezing is best visualized using the quasi-probability Wigner function

$$W(\psi) = \frac{\exp\{-\frac{1}{2}(\psi\boldsymbol{\sigma}^{-1}\psi^\dagger)\}}{\pi^2\sqrt{\det\boldsymbol{\sigma}}}$$

with the state vector $\psi = (X_1, P_1, X_2, P_2)$. Fig.(15) shows the Wigner function of the squeezed

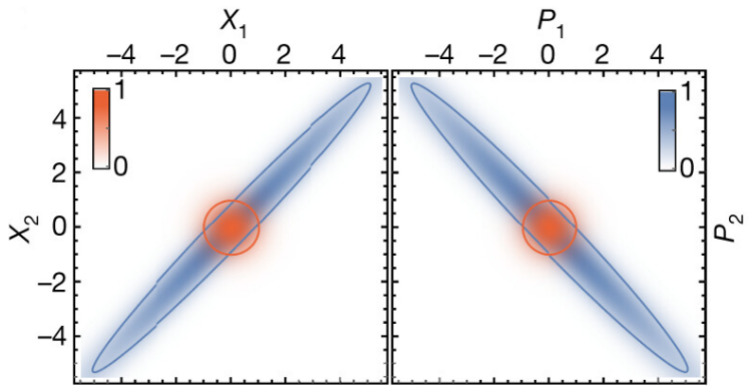

Figure 15: Wigner function of the squeezed state (blue) compared with the ideal vacuum state (red) for two non-local quadrature pairs, where the other two quadratures are integrated out. Solid lines indicate a drop by $1/e$ of the maximum value. Credit from Fink et *al.* Nature 2019 [146].

state (blue) compared with the ideal vacuum state $\boldsymbol{\sigma}_{\text{vac}} = \text{I}/2$ in red (I is the identity matrix) for two quadrature pairs, while the other two quadratures are integrated out. The $\{X_1, X_2\}$ and $\{P_1, P_2\}$ projections clearly show cross-quadrature two-mode squeezing below the quantum limit in the diagonal directions.
Finally, to verify the existence of entanglement between the two output modes we can either use the Duan criterion [81], or the log-Negativiy [76]. We already know that $E_{\mathcal{N}} = \max[0, -\ln 2\nu^-]$,

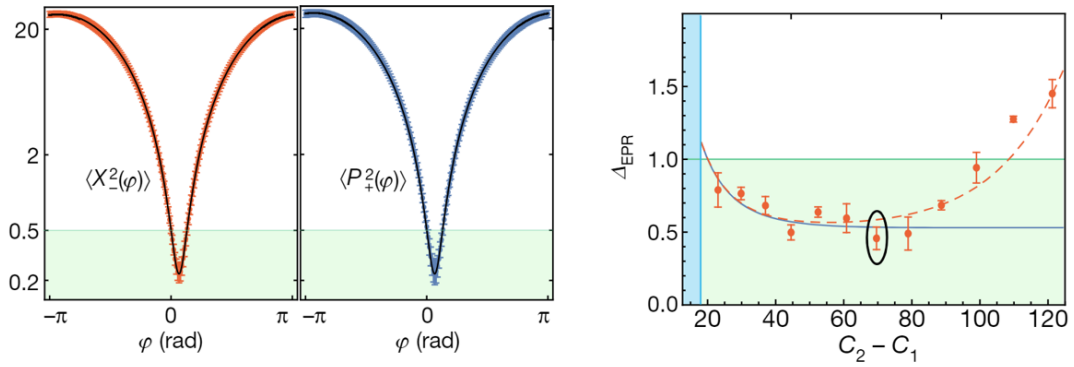

Figure 16: (Left) Measured variance of the EPR basis states as a function of the detector angle φ of channel 1. The green area shows the region of vacuum squeezing. (Right) The measured Duan non-separability measure Δ_{EPR} as a function of cooperativity difference, $C_- - C_+$. Theoretical values are shown without (solid) and with (dashed) pump noise. The green area indicates the region of entangled states and the blue area shows the unstable region where the theory breaks down and the measured squeezing values exceed the range of the plot. Credit from Fink et *al.* Nature 2019 [146].

where ν^- is the smallest partially-transposed symplectic eigenvalue of the covariance matrix $\boldsymbol{\sigma}$, given by

$$\nu^- \equiv \frac{1}{\sqrt{2}}\left[\Delta(\boldsymbol{\sigma}) - [\Delta(\boldsymbol{\sigma})^2 - 4\det\boldsymbol{\sigma}]^{1/2}\right]^{1/2},$$

with

$$\Delta(\boldsymbol{\sigma}) = \det\boldsymbol{\alpha} + \det\boldsymbol{\beta} + 2\det\boldsymbol{\gamma}.$$

Substituting the expression for the CM we can obtain

$$\nu^- = \frac{1}{\sqrt{2}}\left[\sigma_{11}^2 + \sigma_{33}^2 + 2\sigma_{13}^2 - \sqrt{(\sigma_{11}^2 - \sigma_{33}^2)^2 + 4\sigma_{13}^2(\sigma_{11} + \sigma_{33})^2}\right]^{1/2}.$$

On the other hand, using the Duan bound criterion the two-mode Gaussian state is entangled if $\Delta_{\mathrm{EPR}} \equiv \langle \hat{X}_-^2(\varphi)\rangle + \langle \hat{P}_+^2(\varphi)\rangle < 1$, and it is exactly in a vacuum state for $\Delta_{\mathrm{EPR}} = 1$. The EPR operator pair are defined as follow:

$$\hat{X}_- = \frac{1}{\sqrt{2}}(\hat{X}_2 - \hat{X}_1)$$
$$\hat{P}_+ = \frac{1}{\sqrt{2}}(\hat{P}_2 + \hat{P}_1),$$

consequently

$$\langle \hat{X}_-^2(\varphi)\rangle = \frac{\sigma_{11} + \sigma_{33} - 2\sigma_{13}}{2}$$
$$\langle \hat{P}_+^2(\varphi)\rangle = \frac{\sigma_{11} + \sigma_{33} + 2\sigma_{13}}{2}$$

The measured variance of the EPR basis states $\hat{u}(\varphi)$ and $\hat{v}(\varphi)$ as a function of the angle φ is shown in Fig.(16). We also show the results obtained in [146], where they reported measurements of Δ_{EPR} for the optimal angle φ as a function of the calculated difference between the red and blue cooperativities, $C_- - C_+$ (where $C_\mp = 4G_\mp^2/\kappa\gamma$).

7.1.1 Two mechanical oscillators coupled with one cavity mode

In the previous section, we have seen how it is possible to generate entanglement between cavity fields, while they are simultaneously coupled to a mechanical oscillator. Therefore, we want now to describe the other case around, where two movable mirrors (massive mechanical oscillators) are incorporated into a resonant optical cavity, and radiation pressure forces inside the cavity can be tailored so that the motion of the mirrors becomes highly correlated and even entangled. There exist several proposals for this kind of system, for example, in [148, 149, 150, 151]. To describe this system, we initially assume for simplicity that the two oscillators have equal radiation-pressure coupling strengths, g and that the pump tones are applied at the red- and blue-sideband frequencies $\omega_- = \omega_c - \omega_1$ and $\omega_+ = \omega_c + \omega_2$, respectively. As in the previous section, ω_c is the cavity's frequency, while ω_j is the j-th oscillator's frequency. Moreover, throughout the following we will indicate the two mechanical modes with the notation b_1 and b_2, while the cavity one with a. Details of the theoretical model, including non-idealities, are discussed in the Supplementary material of the paper by Ockeloen-Korppi et *al.* [88]. The pump tones enhance the radiation-pressure interaction, yielding an effective optomechanical coupling rate $G_\pm = g\alpha_\pm$, where $\alpha_\pm$ are the field amplitudes induced in the resonator by the pump $\omega_\pm$. Now, it is useful to introduce the mechanical Bogoliubov modes, which are obtained by a two-mode squeezing transformation (see Chapter 5) on the original mechanical annihilation operators, i.e.

$$\hat{\beta}_1 = b_1 \cosh\xi + b_2^\dagger \sinh\xi$$
$$\hat{\beta}_2 = b_2 \cosh\xi + b_1^\dagger \sinh\xi$$

where ξ is the *two-mode squeezing parameter*, given by $\tanh\xi = G_+/G_-$. By defining $\Omega = (\omega_2 - \omega_1)/2$ and working in a rotating frame (at frequency $\omega_c + \Omega$ for the cavity and $(\omega_2 + \omega_1)/2$ for each mechanical oscillator), the linearized optomechanical Hamiltonian becomes

$$\hat{H} = -\Omega a^\dagger a + \Omega(\beta_2^\dagger\beta_2 - \beta_1^\dagger\beta_1) + \mathcal{G}[a^\dagger(\beta_1 + \beta_2) + a(\beta_1^\dagger + \beta_2^\dagger)], \tag{7.1.1.1}$$

with $\mathcal{G} = \sqrt{G_-^2 - G_+^2}$. Hamiltonian (7.1.1.1) describes the cavity cooling of the Bogoliubov modes towards their ground state, which corresponds to a two-mode squeezed state of the bi-partite mechanical system. Now, if we introduce a second oscillator, we can rewrite the four collective quadrature operators as

$$\hat{X}_\pm = \frac{1}{\sqrt{2}}(\hat{X}_2 \pm \hat{X}_1)$$
$$\hat{P}_\pm = \frac{1}{\sqrt{2}}(\hat{P}_2 \pm \hat{P}_1),$$

where

$$\hat{X}_j = \frac{\hat{b}_j + \hat{b}_j^\dagger}{\sqrt{2}}$$
$$\hat{P}_j = \frac{-i(\hat{b}_j - \hat{b}_j^\dagger)}{\sqrt{2}}$$

are the individual mechanical oscillator quadrature operators, for $j = 1, 2$. Equivalently to the previous section, here the Duan bound [81] ensures that a state is entangled if $\Delta_{\mathrm{EPR}} = \langle \hat{X}_+^2 \rangle + \langle \hat{P}_-^2 \rangle < 1$.
What Ockeloen-Korppi did in their work [88], is to use a single driven cavity mode both to prepare a correlated state of two mechanical oscillators and to directly measure fluctuations in the $\hat{X}_+$ collective quadrature, and inferred those in $\hat{P}_-$. Their device was designed with the two oscillators separated by $600\mu m$ having no direct coupling, and with resonance frequencies $\omega_1/(2\pi) \approx 10$ Mhz and $\omega_2/(2\pi) \approx 11.3$ MHz. The microwave cavity, with a frequency of $\omega_c/(2\pi) \approx 5.5$ GHz, had separate input and output ports. All the input signals were applied through a port having coupling rate of $\kappa_E^{\mathrm{in}}/(2\pi) \approx 60$ kHz, whereas the output was strongly coupled at $\kappa_E^{\mathrm{out}}/(2\pi) \approx 1.13$ MHz. They also included internal losses of the cavity with a rate of $\kappa_I/(2\pi) \approx 190$ kHz, and the sum of all the loss channels gave a total rate of $\kappa/(2\pi) \approx 1.38$ MHz. In this way, for the mechanical oscillators quadrature fluctuations they founded $\langle \hat{X}_+^2 \rangle \approx 0.41 \pm 0.04$, and $\langle \hat{P}_-^2 \rangle \approx 0.42 \pm 0.08$. Therefore, this shows that the system is in an entangled state with $\langle \hat{X}_+^2 \rangle + \langle \hat{P}_-^2 \rangle \approx 0.83 \pm 0.13 < 1$ of the (center of mass) motion of two mechanical oscillators.
In Fig.17 is displayed the Duan quantity for entanglement as a function of the probe tone phase ϕ, and as a function of the strength of the red-detuned pump tone. This is because, in the main experiment, they have used two pairs of tones, namely, the pump and probe tones. The pump tones are used to create entanglement, while the probe tones enable the measurement of the collective quadrature operators of the mechanical state. The ability to control the relative phase ϕ of the two probe tones allowed them to infer the variance of a general collective quadrature $\hat{X}_+^{\phi} = \hat{X}_+ \cos\phi + \hat{P}_+ \sin\phi$.

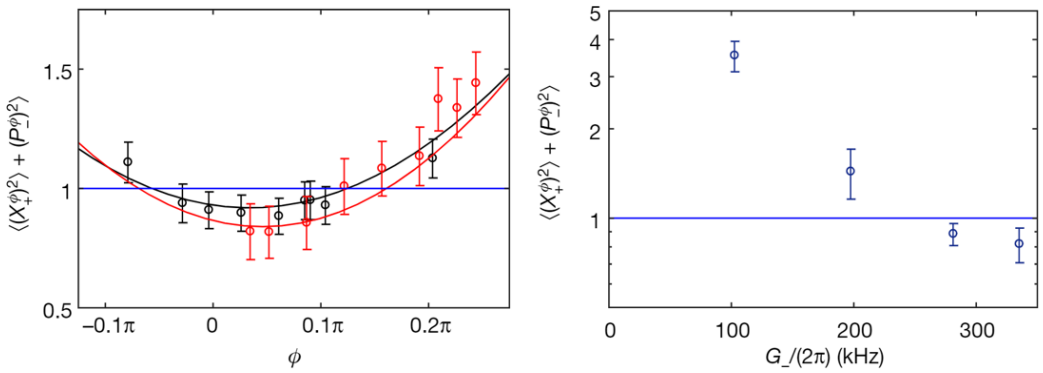

Figure 17: Fluctuations of collective quadratures. (Left) The Duan quantity for entanglement as a function of the probe tone phase φ. (Right) The Duan quantity for the optimal value of φ, as a function of the strength of the red-detuned pump tone. The black and red solid lines are theoretical fits to the corresponding datasets, obtained using the bath temperatures determined by the pump spectra. The blue horizontal line marks the quantum zero-point fluctuations level. The error bars denote statistical confidence of two standard deviations. Credit from Ockeloen-Korppi et *al.* Nature 2018 [88].

Moreover, we know that an oscillator is squeezed if the fluctuations of either of the quadrature-amplitude operators $\hat{X}_1$ and $\hat{P}_1$ is smaller than the quantum zero-point fluctuation level. This is exactly our case, as shown in Fig.18, where the sum of the $\hat{X}$ quadratures, and the difference

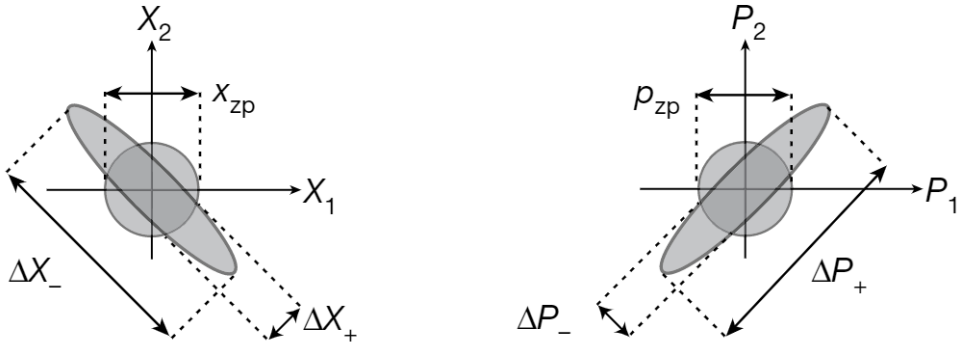

Figure 18: Correlations in two-mode squeezing, shown in terms of fluctuations (shaded) of the quadrature amplitudes. Left, the sum of the $\hat{X}$ quadratures of the two oscillators fluctuates less than the zero-point level $x_{\rm zp}$. Right, the difference between $\hat{P}$ quadratures is similarly localized below the zero-point fluctuation level $p_{\rm zp}$.

between the $\hat{P}$ quadratures, of the two oscillators fluctuates less than the zero-point level $x_{\rm zp}$.

8 Conclusions

Quantum entanglement in optomechanical systems plays a vital role in the progress of quantum science and technology, such as exploring fundamental physics and quantum information processing. Although the physical laws of quantum mechanics do not specifically limit the size of objects that carry the entangled states, the experimental preparation and detection of quantum entanglement in the macro world still face great challenges. Fortunately, with the practical advances in recent years, several pioneering works have demonstrated non-local correlation and entanglement among mechanical oscillators or between electromagnetic fields mediated by a mechanical oscillator.

In this thesis, we have analyzed the main features of optomechanical systems, starting from the basic interaction between light and matter, and concluding with the study of the entanglement properties between various mechanical or cavity modes. We have also given a perspective of the mathematical foundations with which these phenomena are described; providing a theoretical overview of how open quantum systems are defined, how Gaussian states (including continuous variables states) are used, and in particular how entanglement measurements are performed. We have thus formally introduced as criteria for the separability of Gaussian states the Peres–Horodecki criterion, and we also have demonstrated the Duan bound violation, the one that we have used throughout our analysis.

During the discussion of the properties of optomechanical systems, we have seen how we can amplify a signal of an output cavity field a_{out} (relying on the amplification theory explained by Caves [41], and on the results obtained by Ockeloen-Korppi et *al* [40]), and on the other hand how it is possible to cool down the motion of the mechanical mode down to its ground state (exploiting the works done by Teufel et *al* [122], and by Schliesser et *al* [118]). As we have noticed, both results actually depend on the choice we make on the Δ detuning (blue or red respectively) performed on our system. In this sense, we have further explored which are the consequences of the optomechanical interaction according to the regimes of parameters we have worked on.

In our case, for example, resolved sideband, large cooperativity, and strong coupling regime, were the three situations analyzed which allowed us to implement Rotating Wave Approximation techniques (to cool the mechanical motion down to its ground state), and to achieve normal mode splitting. In this way, in the last chapters, we have set together all these requirements in order to analyze two modes optomechanical systems, going into details of two-mode squeezing and two-mode (mechanical/cavity) entanglement.

Therefore, we now expect that the research landscape will increasingly focus on refining the applications of optomechanical devices in quantum technologies, on the one hand, and on understanding fundamental phenomena such as those above, on the other. Cross-fertilization between these two branches will probably remain a hallmark of the field, bringing new insight and advances to materials science, nano and micro-structure fabrication, and fundamental quantum science, to investigate among other topics the emergence of new physics. There is nothing in quantum mechanics to suggest that there is any limit to how large and complex a device can be before it fails to be described by quantum mechanics. Of course it will not be easy to develop the technology to control the quantum probability amplitudes of such systems. One thing will always remain the case: no matter how large and how complex a quantum system becomes, its quantum character will be revealed by comparing classical stochastic control signals with classical stochastic measurement records. The classical-quantum border will remain, but where we will put it will be a function of our engineering capability alone.

A Inseparability Criterion for CV Systems: Duan bound violation

This appendix is mostly based on the derivation in the paper by Duan [81],so its role is to provide some additional information that can help to better understand the proof of the Duan bound criterion.
The inseparability criterion for continuous variables systems states that a quantum state ρ of two modes 1 and 2 is separable if and only if it can be expressed in the following form:

$$\rho = \sum_i p_i \rho_{i,1} \otimes \rho_{i,2}, \tag{A.1}$$

where $\rho_{i,1}$ and $\rho_{i,2}$ are assumed to be normalized states of the modes 1, and $p_i \geq 0$ to satisfy $\sum_i p_i = 1$. We have seen that an entangled continuous variable state can be expressed as a co-eigenstate of a pair of EPR-type operators [60], such as $\hat{x}_1 + \hat{x}_2$ and $\hat{p}_1 - \hat{p}_2$. In this way, for maximally entangled states the total variance of these two operators reduces to zero. In fact, if we consider the following type of EPR-like operator:

$$\hat{u} = |a|\hat{x}_1 + \frac{1}{a}|\hat{x}_2| \tag{A.2}$$

$$\hat{v} = |a|\hat{p}_1 + \frac{1}{a}|\hat{p}_2|, \tag{A.3}$$

for a (nonzero) arbitrary real number, the Duan bound criterion ensures that for any separable quantum state the total variance of a pair of EPR-like operators satisfies the inequality

$$\langle(\Delta\hat{u})^2\rangle_\rho + \langle(\Delta\hat{p})^2\rangle_\rho \geq a^2 + \frac{1}{a^2}. \tag{A.4}$$

Proof. We can directly compute the total variance of the $\hat{u}$ and $\hat{v}$ operators using the relation (A.1) of the density operator ρ, and get the following result

$$\begin{aligned}
&\langle(\Delta\hat{u})^2\rangle_\rho + \langle(\Delta\hat{p})^2\rangle_\rho = \sum_i p_i(\langle\hat{u}^2\rangle_i + \langle\hat{v}^2\rangle_i) - \langle\hat{u}^2\rangle_\rho - \langle\hat{v}^2\rangle_\rho \\
&= \sum_i p_i\left(a^2\langle\hat{x}_1^2\rangle_i + \frac{1}{a^2}\langle\hat{x}_2^2\rangle_i + a^2\langle\hat{p}_1^2\rangle_i + \frac{1}{a^2}\langle\hat{p}_1^2\rangle_i\right) \\
&+ 2\frac{a}{|a|}\left(\sum_i p_i\langle\hat{x}_1\rangle_i\langle\hat{x}_2\rangle_i - \sum_i p_i\langle\hat{p}_1\rangle_i\langle\hat{p}_2\rangle_i\right) - \langle\hat{u}^2\rangle_\rho - \langle\hat{v}^2\rangle_\rho \\
&\sum_i p_i\left(a^2\langle(\Delta\hat{x}_1)^2\rangle_i + \frac{1}{a^2}\langle(\Delta\hat{x}_1)^2\rangle_i + a^2\langle(\Delta\hat{p}_1)^2\rangle_i + \frac{1}{a^2}\langle(\Delta\hat{p}_2)^2\rangle_i\right) \\
&+ \sum_i p_i\langle\hat{u}\rangle_i - \left(\sum_i p_i\langle\hat{u}\rangle_i\right)^2 + \sum_i p_i\langle\hat{v}\rangle_i - \left(\sum_i p_i\langle\hat{v}\rangle_i\right)^2.
\end{aligned} \tag{A.5}$$

In the former equation, the symbol $\langle\cdots\rangle_i$ denotes the average over the product density operator $\rho_{i,1}\otimes\rho_{i,2}$. Therefore, it follows from the uncertainty relation that $\langle(\Delta\hat{x}_j)^2\rangle_i + \langle(\Delta\hat{p}_j)^2\rangle_i geq|[\hat{x}_j, \hat{p}_j]| = 1$ for $j = 1, 2$, and by applying the Cauchy-Schwarz inequality $\left(\sum_i p_i\right)\left(\sum_i p_i\langle\hat{u}_i^2\rangle\right) \geq \left(\sum_i p_i|\langle\hat{u}_i^\rangle|\right)^2$, we ensure that the last line of Eq.(A.5) is bounded from below by zero. Hence, the total variance of the two EPR-like operators is bounded from below by $a^2 + \frac{1}{a^1}$ for any separable state. This completes the proof of the criterion.

B Interaction phenomena between light and matter: one-mode mechanical squeezing

In this appendix we would like to give an extensive derivation of the quadrature squeezing result obtained in Section 6.3.
To derive the mechanical quadrature spectrum, we shall consider the so-called good-cavity limit ($\omega_m \gg \kappa$), including also the case of $\kappa \gg \gamma$. In this sense, it is convenient to define the vectors

$$\begin{aligned}\boldsymbol{V} &= \left(\hat{a}, \hat{a}^\dagger, \hat{b}, \hat{b}^\dagger\right)^T \\ \boldsymbol{V}_{\rm in} &= \left(\hat{a}_{\rm in}, \hat{a}^\dagger_{\rm in}, \hat{b}_{\rm in}, \hat{b}^\dagger_{\rm in}\right)^T \\ \boldsymbol{W} &= \left(\sqrt{\kappa}, \sqrt{\kappa}, \sqrt{\gamma}, \sqrt{\gamma}\right).\end{aligned} \tag{B.1}$$

We then find the following solution to the quantum Langevin equations in frequency space:

$$\hat{\boldsymbol{V}}[\omega] = \boldsymbol{\chi}[\omega] \cdot \boldsymbol{W} \cdot \hat{\boldsymbol{V}}_{\rm in},$$

where

$$\boldsymbol{\chi}[\omega] = \begin{pmatrix} \frac{\kappa}{2} - i(\omega+\Delta) & 0 & -iG_- & -iG_+ \\ 0 & \frac{\kappa}{2} - i(\omega-\Delta) & iG_+ & iG_- \\ -iG_- & -iG_+ & \frac{\gamma}{2} - i(\omega+\Delta) & 0 \\ iG_+ & iG_- & 0 & \frac{\kappa}{2} - i(\omega-\Delta) \end{pmatrix}^{-1}. \tag{B.2}$$

Now, we can compute the output cavity spectrum through $\hat{a}_{\rm out}(\omega)$ using the input-output relation $\hat{a}_{\rm out}(\omega) = \hat{a}_{\rm in}(\omega) - \sqrt{\kappa}\hat{a}(\omega)$. This yields

$$\hat{a}_{\rm out}(\omega) = \hat{a}_{\rm in}(\omega) - \kappa\Big(\boldsymbol{\chi}[\omega]\Big)_{11}\hat{a}_{\rm in} - \kappa\Big(\boldsymbol{\chi}[\omega]\Big)_{12}\hat{a}^\dagger_{\rm in} - \kappa\gamma\Big(\boldsymbol{\chi}[\omega]\Big)_{13}\hat{b}_{\rm in} - \kappa\gamma\Big(\boldsymbol{\chi}[\omega]\Big)_{14}\hat{b}^\dagger_{\rm in}. \tag{B.3}$$

In this way, the symmetric power spectral density is given by

$$\bar{S}[\omega] = \frac{1}{2}\int dt \Big\langle \Big\{\hat{a}^\dagger_{\rm out}(0), \hat{a}_{\rm out}(t)\Big\}\Big\rangle e^{i\omega t} = \frac{1}{2} + S[\omega] \tag{B.4}$$

with

$$\begin{aligned} S[\omega] &= \frac{1}{2}\int dt \Big\langle \hat{a}^\dagger_{\rm out}(0), \hat{a}_{\rm out}(t)\Big\rangle e^{i\omega t} \\ &= \kappa^2\Big|\boldsymbol{\chi}[\omega]_{11}\Big|^2 n_c + \kappa^2\Big|\boldsymbol{\chi}[\omega]_{12}\Big|^2(n_c+1) + \kappa\gamma\Big|\boldsymbol{\chi}[\omega]_{13}\Big|^2 n_m + \kappa\gamma\Big|\boldsymbol{\chi}[\omega]_{14}\Big|^2(n_m+1). \end{aligned}$$

Thus, for $\Delta = 0$ and $\mathcal{G}^2 := G_-^2 - G_+^2$, the mechanical quadrature spectra are considerably simplified as

$$\begin{aligned} \bar{S}_{X_{1,2}}[\omega] &= \frac{1}{2}\int dt \Big\langle \Big\{\hat{X}_{1,2}(t), \hat{X}_{1,2}(0)\Big\}\Big\rangle e^{i\omega t} \\ &= 4x_{\rm zp}^2 \frac{4\kappa(G_- \mp G_+)^2(n_c+1/2) + \gamma(\kappa^2+4\omega^2)(n_m+1/2)}{(4\mathcal{G}^2+\gamma\kappa)^2 + 4\omega^2(\gamma^2+\kappa^2-8\mathcal{G}^2) + 16\omega^4}. \end{aligned} \tag{B.5}$$

The mechanical quadrature fluctuations are obtained by integrating the mechanical quadrature spectra

$$\begin{aligned}\left\langle \hat{X}_{1,2}^2 \right\rangle &= \int \frac{d\omega}{2\pi} \bar{S}_{X_{1,2}}(\omega) \\ &= x_{\mathrm{zp}}^2 \frac{4\kappa(G_- \mp G_+)^2(2n_c+1) + \gamma[4\mathcal{G}^2 + \kappa(\kappa+\gamma)](2n_m+1)}{(\kappa+\gamma)(4\mathcal{G}^2+\gamma\kappa)},\end{aligned} \tag{B.6}$$

and therefore we have recovered the expression of Section 6.3.

References

[1] Kepler, J. De cometis libelli tres (typis andreae apergiri) (1619).

[2] Lebedev, P. Untersuchungen ber die druckkrfte des lichtes. *Annalen der Physik* **311**, 433458 (1901).

[3] Nichols, E. F. & Hull, G. F. A preliminary communication on the pressure of heat and light radiation. *Physical Review (Series I)* **13**, 307 (1901).

[4] Einstein, A. *Eine neue bestimmung der moleküldimensionen.* Ph.D. thesis, ETH Zurich (1905).

[5] Einstein, A. Über die entwicklung unserer anschauungen über das wesen und die konstitution der strahlung. *Physikalische Blätter* **25**, 386–391 (1969).

[6] Hanbury Brown, R. & Twiss, R. The question of correlation between photons in coherent light rays. *Nature* **178**, 1447–1448 (1956).

[7] Glauber, R. J. The Quantum Theory of Optical Coherence. *Physical Review* **130**, 2529–2539 (1963).

[8] Ashkin, A. Trapping of Atoms by Resonance Radiation Pressure. *Physical Review Letters* **40**, 729–732 (1978).

[9] Hänsch, T. W. & Schawlow, A. L. Cooling of gases by laser radiation. *Optics Communications* **13**, 68–69 (1975).

[10] Wineland, D. J., Drullinger, R. E. & Walls, F. L. Radiation-pressure cooling of bound resonant absorbers. *Physical Review Letters* **40**, 1639 (1978).

[11] Stenholm, S. The semiclassical theory of laser cooling. *Reviews of Modern Physics* **58**, 699–739 (1986).

[12] Metcalf, H. J. & Straten, P. v. d. Evaporative cooling. In *Laser Cooling and Trapping* (Springer, 1999).

[13] Fabre, C. *et al.* Quantum-noise reduction using a cavity with a movable mirror. *Physical Review A* **49**, 1337–1343 (1994).

[14] Mancini, S. & Tombesi, P. Quantum noise reduction by radiation pressure. *Physical Review A* **49**, 4055–4065 (1994).

[15] Bose, S., Jacobs, K. & Knight, P. L. Preparation of nonclassical states in cavities with a moving mirror. *Physical Review A* **56**, 4175–4186 (1997).

[16] Mancini, S., Man'ko, V. I. & Tombesi, P. Ponderomotive control of quantum macroscopic coherence. *Physical Review A* **55**, 3042–3050 (1997).

[17] Mancini, S., Vitali, D. & Tombesi, P. Optomechanical Cooling of a Macroscopic Oscillator by Homodyne Feedback. *Physical Review Letters* **80**, 688–691 (1998).

[18] Hechenblaikner, G., Gangl, M., Horak, P. & Ritsch, H. Cooling an atom in a weakly driven high-q cavity. *Physical Review A* **58**, 3030 (1998).

[19] Vuletić, V. & Chu, S. Laser cooling of atoms, ions, or molecules by coherent scattering. *Physical Review Letters* **84**, 3787 (2000).

[20] Cohadon, P.-F., Heidmann, A. & Pinard, M. Cooling of a mirror by radiation pressure. *Physical Review Letters* **83**, 3174 (1999).

[21] Zurek, W. H. From quantum to classical. *Phys Today* **37** (1991).

[22] Leggett, T. Quantum theory: weird and wonderful. *Physics World* **12**, 73 (1989).

[23] Martinis, J. M., Devoret, M. H. & Clarke, J. Experimental tests for the quantum behavior of a macroscopic degree of freedom: The phase difference across a josephson junction. *Physical Review B* **35**, 4682 (1987).

[24] Palomaki, T. A., Teufel, J. D., Simmonds, R. W. & Lehnert, K. W. Entangling Mechanical Motion with Microwave Fields. *Science* **342**, 710–713 (2013).

[25] Aspelmeyer, M., Kippenberg, T. J. & Marquardt, F. Cavity optomechanics. *Reviews of Modern Physics* **86**, 1391–1452 (2014).

[26] Whittle, C. *et al.* Approaching the motional ground state of a 10-kg object. *Science* **372**, 1333–1336 (2021).

[27] Barzanjeh, S., Abdi, M., Milburn, G. J., Tombesi, P. & Vitali, D. Reversible optical-to-microwave quantum interface. *Physical Review Letters* **109**, 130503 (2012).

[28] Mirhosseini, M., Sipahigil, A., Kalaee, M. & Painter, O. Superconducting qubit to optical photon transduction. *Nature* **588**, 599–603 (2020).

[29] Fiaschi, N. *et al.* Optomechanical quantum teleportation. *Nature Photonics* **15**, 817–821 (2021).

[30] Davies, E. B. & Davies, E. *Quantum theory of open systems* (Academic Press, 1976).

[31] Alicki, R. & Lendi, K. *Quantum dynamical semigroups and applications*, vol. 717 (Springer, 2007).

[32] Breuer, H.-P., Petruccione, F. *et al. The theory of open quantum systems* (Oxford University Press on Demand, 2002).

[33] Breuer, H.-P., Laine, E.-M., Piilo, J. & Vacchini, B. Colloquium: Non-Markovian dynamics in open quantum systems. *Reviews of Modern Physics* **88**, 021002 (2016).

[34] Gardiner, C. & Zoller, P. *Quantum Noise: A Handbook of Markovian and Non-Markovian Quantum Stochastics Methods with Applications to Quantum Optics.* Springer Series in Synergetics (2004).

[35] Walls, D. & Milburn, G. *Quantum Optics.* Springer (2008).

[36] Gardiner, C. W. & Collett, M. J. Input and output in damped quantum systems: Quantum stochastic differential equations and the master equation. *Physical Review A* **31**, 3761–3774 (1985).

[37] Clerk, A. A., Devoret, M. H., Girvin, S. M., Marquardt, F. & Schoelkopf, R. J. Introduction to quantum noise, measurement, and amplification. *Reviews of Modern Physics* **82**, 1155–1208 (2010).

[38] Giovannetti, V. & Vitali, D. Phase-noise measurement in a cavity with a movable mirror undergoing quantum Brownian motion. *Physical Review A* **63**, 023812 (2001).

[39] Zoller, P. & Gardiner, C. W. Quantum Noise in Quantum Optics: the Stochastic Schrödinger Equation. *Elsevier Science Publishers B.V* (1997).

[40] Massel, F. *et al.* Microwave amplification with nanomechanical resonators. *Nature* **480**, 351–354 (2011).

[41] Caves, C. M. Quantum limits on noise in linear amplifiers. *Physical Review D* **26**, 1817–1839 (1982).

[42] P.Bowen, W. & Milburn, G. J. *Quantum Optomechanics*. CRC Press (2016).

[43] Zhang, W.-M., Feng, D. H. & Gilmore, R. Coherent states: Theory and some applications. *Reviews of Modern Physics* **62**, 867–927 (1990).

[44] Schrödinger, E. Der stetige übergang von der mikro-zur makromechanik. *Naturwissenschaften* **14**, 664–666 (1926).

[45] Glauber, R. J. Coherent and Incoherent States of the Radiation Field. *Physical Review* **131**, 2766–2788 (1963).

[46] Sudarshan, E. Equivalence of semiclassical and quantum mechanical descriptions of statistical light beams. *Physical Review Letters* **10**, 277 (1963).

[47] Klauder, J. R. Continuous-representation theory. i. postulates of continuous-representation theory. *Journal of Mathematical Physics* **4**, 1055–1058 (1963).

[48] Klauder, J. R. Continuous-representation theory. ii. generalized relation between quantum and classical dynamics. *Journal of Mathematical Physics* **4**, 1058–1073 (1963).

[49] Perelomov, A. M. Coherent states for arbitrary lie group. *Communications in Mathematical Physics* **26**, 222–236 (1972).

[50] Gilmore, R. Geometry of symmetrized states. *Annals of Physics* **74**, 391–463 (1972).

[51] Penna, V. Coherent states approach to quantum system. *Doctoral Course Notes* (March, 2021).

[52] Caves, C. M. Quantum-mechanical noise in an interferometer. *Physical Review D* **23**, 1693–1708 (1981).

[53] Yuen, H. P. Two-photon coherent states of the radiation field. *Physical Review A* **13**, 2226 (1976).

[54] Hollenhorst, J. N. Quantum limits on resonant-mass gravitational-radiation detectors. *Physical Review D* **19**, 1669 (1979).

[55] Caves, C. M. & Schumaker, B. L. New formalism for two-photon quantum optics. i. quadrature phases and squeezed states. *Physical Review A* **31**, 3068 (1985).

[56] Schumaker, B. L. & Caves, C. M. New formalism for two-photon quantum optics. ii. mathematical foundation and compact notation. *Physical Review A* **31**, 3093 (1985).

[57] Grishchuk, L. & Sidorov, Y. V. Squeezed quantum states of relic gravitons and primordial density fluctuations. *Physical Review D* **42**, 3413 (1990).

[58] Kiefer, C. Hawking radiation from decoherence. *Classical and Quantum Gravity* **18**, L151 (2001).

[59] Hawking, S. W. Particle creation by black holes. In *Euclidean quantum gravity*, 167–188 (World Scientific, 1975).

[60] Einstein, A., Podolsky, B. & Rosen, N. Can Quantum-Mechanical Description of Physical Reality Be Considered Complete? *Physical Review* **47**, 777–780 (1935).

[61] Yuen, H. & Shapiro, J. Optical communication with two-photon coherent states–part iii: Quantum measurements realizable with photoemissive detectors. *IEEE Transactions on Information Theory* **26**, 78–92 (1980).

[62] Werner, R. F. Quantum states with einstein-podolsky-rosen correlations admitting a hidden-variable model. *Physical Review A* **40**, 4277 (1989).

[63] Popescu, S. Bell's inequalities versus teleportation: What is nonlocality? *Physical review letters* **72**, 797 (1994).

[64] Horodecki, P. Separability criterion and inseparable mixed states with positive partial transposition. *Physics Letters A* **232**, 333–339 (1997).

[65] Vedral, V. & Plenio, M. B. Entanglement measures and purification procedures. *Physical Review A* **57**, 1619–1633 (1998).

[66] Horodecki, M., Horodecki, P. & Horodecki, R. Mixed-state entanglement and distillation: Is there a "bound" entanglement in nature? *Physical Review Letters* **80**, 5239 (1998).

[67] J.S.Bell. *Speakable and Unspeakable in Quantum Mechanics: Collected Papers on Quantum Philosophy*. Cambridge University Press (1987).

[68] Aspect, A. Quantum [Un]speakables, From Bell to Quantum Information. *Springer* 119–153 (2002).

[69] Bennett, C. H., DiVincenzo, D. P., Smolin, J. A. & Wootters, W. K. Mixed-state entanglement and quantum error correction. *Physical Review A* **54**, 3824–3851 (1996).

[70] Vedral, V., Plenio, M. B., Rippin, M. A. & Knight, P. L. Quantifying Entanglement. *Physical Review Letters* **78**, 2275–2279 (1997).

[71] Peres, A. Separability Criterion for Density Matrices. *Physical Review Letters* **77**, 1413–1415 (1996).

[72] Horodecki, M., Horodecki, P. & Horodecki, R. Separability of mixed states: necessary and sufficient condition. *Physical Review A* **223**, 1–8 (1996).

[73] Popescu, S. & Rohrlich, D. Thermodynamics and the measure of entanglement. *Physical Review A* **56**, R3319–R3321 (1997).

[74] Adesso, G. & Illuminati, F. Entanglement in continuous-variable systems: recent advances and current perspectives. *Journal of Physics A: Mathematical and Theoretical* **40**, 7821 (2007).

[75] Simon, R. Peres-Horodecki Separability Criterion for Continuous Variable Systems. *Physical Review Letters* **84**, 2726–2729 (2000).

[76] Adesso, G., Serafini, A. & Illuminati, F. Extremal entanglement and mixedness in continuous variable systems. *Physical Review A* **70**, 022318 (2004).

[77] Życzkowski, K., Horodecki, P., Sanpera, A. & Lewenstein, M. Volume of the set of separable states. *Physical Review A* **58**, 883 (1998).

[78] Vidal, G. & Werner, R. F. Computable measure of entanglement. *Physical Review A* **65**, 032314 (2002).

[79] Eisert, J., Simon, C. & Plenio, M. B. On the quantification of entanglement in infinite-dimensional quantum systems. *Journal of Physics A: Mathematical and General* **35**, 3911 (2002).

[80] Serafini, A., Illuminati, F. & De Siena, S. Symplectic invariants, entropic measures and correlations of gaussian states. *Journal of Physics B: Atomic, Molecular and Optical Physics* **37**, L21 (2003).

[81] Duan, L.-M., Giedke, G., Cirac, J. I. & Zoller, P. Inseparability Criterion for Continuous Variable Systems. *Physical Review Letters* **84**, 2722–2725 (2000).

[82] Braunstein, S. L. & Kimble, H. J. Teleportation of continuous quantum variables. *Physical Review Letters* **80**, 869 (1998).

[83] Braunstein, S. L. Quantum error correction for communication with linear optics. *Nature* **394**, 47–49 (1998).

[84] Furusawa, A. *et al.* Unconditional quantum teleportation. *science* **282**, 706–709 (1998).

[85] Zhang, J., Peng, K. & Braunstein, S. L. Quantum-state transfer from light to macroscopic oscillators. *Physical Review A* **68**, 013808 (2003).

[86] Vitali, D. *et al.* Optomechanical Entanglement between a Movable Mirror and a Cavity Field. *Physical Review Letters* **98**, 030405 (2007).

[87] Vitali, D., Tombesi, P., Woolley, M. J., Doherty, A. C. & Milburn, G. J. Entangling a nanomechanical resonator and a superconducting microwave cavity. *Physical Review A* **76**, 042336 (2007).

[88] Ockeloen-Korppi, C. F. *et al.* Stabilized entanglement of massive mechanical oscillators. *Nature* **556**, 478–482 (2018).

[89] Aspect, A., Dalibard, J. & Roger, G. Experimental test of bell's inequalities using time-varying analyzers. *Physical review letters* **49**, 1804 (1982).

[90] Rowe, M. A. *et al.* Experimental violation of a bell's inequality with efficient detection. *Nature* **409**, 791–794 (2001).

[91] Hensen, B. *et al.* Loophole-free bell inequality violation using electron spins separated by 1.3 kilometres. *Nature* **526**, 682–686 (2015).

[92] Giustina, M. *et al.* A significant-loophole-free test of bell's theorem with entangled photons. In *Quantum Information Science and Technology III*, vol. 10442, 19–27 (SPIE, 2017).

[93] Bohr, N. Can quantum-mechanical description of physical reality be considered complete? *Physical review* **48**, 696 (1935).

[94] Matsko, A., Zubova, E. & Vyatchanin, S. The value of the force of radiative friction. *Optics communications* **131**, 107–113 (1996).

[95] Karrai, K., Favero, I. & Metzger, C. Doppler optomechanics of a photonic crystal. *Physical review letters* **100**, 240801 (2008).

[96] Mertz, J., Marti, O. & Mlynek, J. Regulation of a microcantilever response by force feedback. *Applied Physics Letters* **62**, 2344–2346 (1993).

[97] Milburn, G. & Woolley, M. An Introduction to Quantum Optomechanics. *Acta Physica Slovaca. Reviews and Tutorials* **61** (2011).

[98] Dorsel, A., McCullen, J. D., Meystre, P., Vignes, E. & Walther, H. Optical bistability and mirror confinement induced by radiation pressure. *Physical Review Letters* **51**, 1550 (1983).

[99] Braginski, V. & Manukin, A. Ponderomotive effects of electromagnetic radiation. *Sov. Phys. JETP* **25**, 653–655 (1967).

[100] Dykman, M. Heating and cooling of local and quasilocal vibrations by a nonresonance field. *Sov. Phys. Solid State* **20**, 1306–1311 (1978).

[101] Braginskiĭ, V. Investigation of Dissipative Ponderomotive Effects of Electromagnetic Radiation. *Soviet Journal of Experimental and Theoretical Physics, Vol.31.* (1970).

[102] Braginsky, V. B. & Khalili, F. Y. *Quantum Measurement.* Cambridge University Press (1992).

[103] Ozawa. Measurement breaking the standard quantum limit for free-mass position. *Physical review letters* **60**, 385–388 (1988).

[104] Yuen, H. P. Contractive States and the Standard Quantum Limit for Monitoring Free-Mass Positions. *Physical Review Letters* **51**, 719–722 (1983).

[105] Braginskii, V. B. & Vorontsov, Y. I. Quantum-mechanical limitations in macroscopic experiments and modern experimental technique. *Uspekhi Fizicheskih Nauk* **114**, 41 (1974).

[106] Caves, C. M. Quantum-Mechanical Radiation-Pressure Fluctuations in an Interferometer. *Physical Review Letters* **45**, 75–79 (1980).

[107] Caves. Defense of the standard quantum limit for free-mass position. *Physical review letters* **54**, 2465–2468 (1985).

[108] Carmichael, H. Spectrum of squeezing and photocurrent shot noise: a normally ordered treatment. *JOSA B* **4**, 1588–1603 (1987).

[109] Murch, K. W., Moore, K. L., Gupta, S. & Stamper-Kurn, D. M. Observation of quantum-measurement backaction with an ultracold atomic gas. *Nature Physics* **4**, 561–564 (2008).

[110] Purdy, T. P., Peterson, R. W. & Regal, C. Observation of radiation pressure shot noise on a macroscopic object. *Science* **339**, 801–804 (2013).

[111] Kippenberg, T. J. & Vahala, K. J. Cavity opto-mechanics. *Optics express* **15**, 17172–17205 (2007).

[112] Braginskii, V. B. & Manukin, A. B. Measurement of weak forces in physics experiments. *Chicago* (1977).

[113] Marquardt, F., Chen, J. P., Clerk, A. A. & Girvin, S. M. Quantum Theory of Cavity-Assisted Sideband Cooling of Mechanical Motion. *Physical Review Letters* **99**, 093902 (2007).

[114] Wilson-Rae, I., Nooshi, N., Zwerger, W. & Kippenberg, T. J. Theory of Ground State Cooling of a Mechanical Oscillator Using Dynamical Backaction. *Physical Review Letters* **99**, 093901 (2007).

[115] Arcizet, O., Cohadon, P.-F., Briant, T., Pinard, M. & Heidmann, A. Radiation-pressure cooling and optomechanical instability of a micromirror. *Nature* **444**, 71–74 (2006).

[116] Schliesser, A., Del'Haye, P., Nooshi, N., Vahala, K. J. & Kippenberg, T. J. Radiation Pressure Cooling of a Micromechanical Oscillator Using Dynamical Backaction. *Physical Review Letters* **97**, 243905 (2006).

[117] Gigan, S. *et al.* Self-cooling of a micromirror by radiation pressure. *Nature* **444**, 67–70 (2006).

[118] Schliesser, A., Rivière, R., Anetsberger, G., Arcizet, O. & Kippenberg, T. J. Resolved-sideband cooling of a micromechanical oscillator. *Nature Physics* **4**, 415–419 (2008).

[119] Park, Y.-S. & Wang, H. Resolved-sideband and cryogenic cooling of an optomechanical resonator. *Nature Physics* **5**, 489–493 (2009).

[120] Teufel, J. D., Harlow, J. W., Regal, C. A. & Lehnert, K. W. Dynamical Backaction of Microwave Fields on a Nanomechanical Oscillator. *Physical Review Letters* **101**, 197203 (2008).

[121] Chan, J. *et al.* Laser cooling of a nanomechanical oscillator into its quantum ground state. *Nature* **478**, 89–92 (2011).

[122] Teufel, J. D. *et al.* Sideband cooling of micromechanical motion to the quantum ground state. *Nature* **475**, 359–363 (2011).

[123] Dobrindt, J. M., Wilson-Rae, I. & Kippenberg, T. J. Parametric Normal-Mode Splitting in Cavity Optomechanics. *Physical Review Letters* **101**, 263602 (2008).

[124] Wilson-Rae, I., Nooshi, N., Dobrindt, J., Kippenberg, T. J. & Zwerger, W. Cavity-assisted backaction cooling of mechanical resonators. *New Journal of Physics* **10**, 095007 (2008).

[125] Rossi, M. *et al.* Normal-Mode Splitting in a Weakly Coupled Optomechanical System. *Physical Review Letters* **120**, 073601 (2018).

[126] Marquardt, F., Clerk, A. & Girvin, S. Quantum theory of optomechanical cooling. *Journal of Modern Optics* **55**, 3329–3338 (2008).

[127] Bhattacherjee, A. B. Cavity quantum optomechanics of ultracold atoms in an optical lattice: Normal-mode splitting. *Physical Review A* **80**, 043607 (2009).

[128] Teufel, J. D. *et al.* Circuit cavity electromechanics in the strong-coupling regime. *Nature* **471**, 204–208 (2011).

[129] Gröblacher, S., Hammerer, K., Vanner, M. R. & Aspelmeyer, M. Observation of strong coupling between a micromechanical resonator and an optical cavity field. *Nature* **460**, 724–727 (2009).

[130] Naseem, M. T. & Müstecaplıoğlu, Ö. E. Ground-state cooling of mechanical resonators by quantum reservoir engineering. *Communications Physics* **4**, 1–10 (2021).

[131] Seis, Y. *et al.* Ground state cooling of an ultracoherent electromechanical system. *Nature Communications* **13**, 1507 (2022).

[132] Castellanos-Beltran, M. A., Irwin, K. D., Hilton, G. C., Vale, L. R. & Lehnert, K. W. Amplification and squeezing of quantum noise with a tunable Josephson metamaterial. *Nature Physics* **4**, 929–931 (2008).

[133] Ockeloen-Korppi, C. F. *et al.* Low-Noise Amplification and Frequency Conversion with a Multiport Microwave Optomechanical Device. *Physical Review X* **6**, 041024 (2016).

[134] Genes, C., Mari, A., Tombesi, P. & Vitali, D. Robust entanglement of a micromechanical resonator with output optical fields. *Physical Review A* **78**, 032316 (2008).

[135] Wollman, E. E. *et al.* Quantum squeezing of motion in a mechanical resonator. *Science* **349**, 952–955 (2015).

[136] Pirkkalainen, J.-M., Damskägg, E., Brandt, M., Sillanpää, M. A. & Massel, F. Squeezing of Quantum Noise of Motion in a Micromechanical Resonator. *Physical Review Letters* **115**, 243601 (2015).

[137] Kim, M., De Oliveira, F. & Knight, P. Properties of squeezed number states and squeezed thermal states. *Physical Review A* **40**, 2494 (1989).

[138] Kronwald, A., Marquardt, F. & Clerk, A. A. Arbitrarily large steady-state bosonic squeezing via dissipation. *Physical Review A* **88**, 063833 (2013).

[139] Woolley, M., Doherty, A., Milburn, G. & Schwab, K. Nanomechanical squeezing with detection via a microwave cavity. *Physical Review A* **78**, 062303 (2008).

[140] Clerk, A. A., Marquardt, F. & Jacobs, K. Back-action evasion and squeezing of a mechanical resonator using a cavity detector. *New Journal of Physics* **10**, 095010 (2008).

[141] Szorkovszky, A., Doherty, A. C., Harris, G. I. & Bowen, W. P. Mechanical squeezing via parametric amplification and weak measurement. *Physical review letters* **107**, 213603 (2011).

[142] Schumaker, B. L. & Caves, C. M. New formalism for two-photon quantum optics. II. Mathematical foundation and compact notation. *Physical Review A* **31**, 3093–3111 (1985).

[143] Caves, C. M. & Schumaker, B. L. New formalism for two-photon quantum optics. I. Quadrature phases and squeezed states. *Physical Review A* **31**, 3068–3092 (1985).

[144] Wang, Y.-D. & Clerk, A. A. Reservoir-Engineered Entanglement in Optomechanical Systems. *Physical Review Letters* **110**, 253601 (2013).

[145] Ford, G. W., Lewis, J. T. & O'Connell, R. Quantum langevin equation. *Physical Review A* **37**, 4419 (1988).

[146] Barzanjeh, S. *et al.* Stationary entangled radiation from micromechanical motion. *Nature* **570**, 480–483 (2019).

[147] Barzanjeh, S., Abdi, M., Milburn, G. J., Tombesi, P. & Vitali, D. Reversible Optical-to-Microwave Quantum Interface. *Physical Review Letters* **109**, 130503 (2011).

[148] Mancini, S., Giovannetti, V., Vitali, D. & Tombesi, P. Entangling macroscopic oscillators exploiting radiation pressure. *Physical review letters* **88**, 120401 (2002).

[149] Woolley, M. J. & Clerk, A. A. Two-mode back-action-evading measurements in cavity optomechanics. *Physical Review A* (2013).

[150] Tan, H., Li, G. & Meystre, P. Dissipation-driven two-mode mechanical squeezed states in optomechanical systems. *Physical Review A* **87**, 033829 (2013).

[151] Ockeloen-Korppi, C. *et al.* Quantum backaction evading measurement of collective mechanical modes. *Physical review letters* **117**, 140401 (2016).